BOREAS An international journal of Quaternary research

The last Eurasian ice sheets – a chronological database and time-slice reconstruction, DATED-1

ANNA L. C. HUGHES, RICHARD GYLLENCREUTZ, ØYSTEIN S. LOHNE, JAN MANGERUD AND JOHN INGE SVENDSEN

BOREAS

Hughes, A. L. C., Gyllencreutz, R., Lohne, Ø. S., Mangerud, J., Svendsen, J. I.: The last Eurasian ice sheets – a chronological database and time-slice reconstruction, DATED-1. *Boreas*. 10.1111/bor.12142. ISSN 0300-9483.

We present a new time-slice reconstruction of the Eurasian ice sheets (British–Irish, Svalbard–Barents–Kara Seas and Scandinavian) documenting the spatial evolution of these interconnected ice sheets every 1000 years from 25 to 10 ka, and at four selected time periods back to 40 ka. The time-slice maps of ice-sheet extent are based on a new Geographical Information System (GIS) database, where we have collected published numerical dates constraining the timing of ice-sheet advance and retreat, and additionally geomorphological and geological evidence contained within the existing literature. We integrate all uncertainty estimates into three ice-margin lines for each time-slice; a most-credible line, derived from our assessment of all available evidence, with bounding maximum and minimum limits allowed by existing data. This approach was motivated by the demands of glaciological, isostatic and climate modelling and to clearly display limitations in knowledge. The timing of advance and retreat were both remarkably spatially variable across the ice-sheet area. According to our compilation the westernmost limit along the British–Irish and Norwegian continental shelf was reached up to 7000 years earlier (at *c.* 27–26 ka) than the eastern limit on the Russian Plain (at *c.* 20–19 ka). The Eurasian ice sheet complex as a whole attained its maximum extent (5.5 Mkm^2) and volume (~24 m Sea Level Equivalent) at *c.* 21 ka. Our continental-scale approach highlights instances of conflicting evidence and gaps in the ice-sheet chronology where uncertainties remain large and should be a focus for future research. Largest uncertainties coincide with locations presently below sea level and where contradicting evidence exists. This first version of the database and time-slices (DATED-1) has a census date of 1 January 2013 and both are available to download via the Bjerknes Climate Data Centre and PANGAEA (www.bcdc.no; http://doi.pangaea.de/10.1594/PANGAEA.848117).

Anna L. C. Hughes (anna.hughes@uib.no), Øystein S. Lohne, Jan Mangerud and John Inge Svendsen, Department of Earth Science, University of Bergen and Bjerknes Centre for Climate Research, P.O. Box 7803, N-5020 Bergen, Norway; Richard Gyllencreutz, Department of Geological Sciences, Stockholm University, 10691 Stockholm, Sweden; *received 12th May 2015, accepted 5th August 2015.*

Geologists require summaries of accumulated evidence from field data and chronological dates to put new observations in context and formulate (or re-consider) hypotheses and palaeoglaciological interpretations. Numerical-glaciological, isostatic and palaeoclimatic models all require empirical constraints on past ice-sheet extent as either inputs or for testing outputs. Here we present new empirically-based reconstructions of the growth and decay of the interconnected Eurasian ice sheets (EurIS) comprising the Scandinavian, Svalbard, Barents Sea, Kara Sea and British–Irish ice sheets, for the period 40–10 ka, i.e. during the build-up to and deglaciation from the Last Glacial Maximum (LGM). As such, this is the first geological reconstruction of the last deglaciation of the entire EurIS to document the underlying chronological data since Andersen's (1981) monumental paper. The work presented was additionally inspired by the more recent compilation of chronological information and retreat-pattern reconstruction conducted for the last Laurentide Ice Sheet (Dyke *et al.* 2002).

Our motivation is twofold; first to depict the evolution of the ice-sheet complex in its entirety as a coherent and easily accessible summary of, and test for, regional field geology; both to identify gaps to be filled and conflicts within the existing evidence that require further investigation. Second, to provide an empirically based reconstruction of changes in the ice-sheet extent through time, suitable as boundary conditions for numerical ice sheet, isostatic and climatic models (e.g. Tarasov *et al.* 2012) or alternatively for testing and validating such models. For such purposes the ice-sheet scale is essential, whereas by nature glacial-geological evidence, collected over decades through diligent efforts of numerous field scientists, typically is highly detailed and often restricted by national boundaries. Assembling such information in a format that satisfies the requirements of numerical modelling and adequately reflects the nuances of the geological data, and archiving it for future use is therefore a nontrivial task. In 2005 we set up a project to establish a comprehensive database of available dates and geomorphological observations that could be used to undertake this task; Database of the Eurasian Deglaciation, DATED (Gyllencreutz *et al.* 2007). This ambitious undertaking has been in progress over the last decade.

In this paper we present and document the first version of the results, 'DATED-1'. The results include a chronological database and a series of maps of time-slice reconstructions of the ice-sheet extent during the last 40 ka. We introduce some new procedures for ice-

DOI 10.1111/bor.12142

margin compilations from geological evidence compared to other former ice-sheet reconstructions (e.g. Kleman *et al.* 1997; Boulton *et al.* 2001; Svendsen *et al.* 2004; Clark *et al.* 2012), namely to integrate all accountable uncertainties (e.g. in dating results, stratigraphy, moraine correlations) and present them collectively in terms of uncertainty in the ice-margin position. For each time-slice we present maximum and minimum ice-limit positions in addition to the limits that we conclude to be the most-probable or credible ice extension. Both the compiled underlying chronological data and our time-slice reconstructions are made available for scrutiny as Supporting Information (Tables S1-5, Data S1, S2) and at the Bjerknes Centre Data Centre/PANGAEA (http://doi.pangaea.de/10.1594/PANGAEA.848117). The DATED-1 database has a census date of 1 January 2013 and it is our intention that the dataset and reconstructions will be updated and revised as new information becomes available. In the Discussion we make additional reference to some post-census literature where relevant.

The Eurasian ice sheets

Various names and abbreviations have been used for the interconnected complex of ice sheets located on the northeastern edge of the North Atlantic during repeated glacial cycles, which we refer to collectively as the Eurasian ice sheets (EurIS) (Fig. 1). The largest component was the Scandinavian or Fennoscandian Ice Sheet. We use the former name and abbreviation (Scandinavian Ice Sheet, SIS), taking the name from the nucleus of the ice sheet, the Scandinavian Mountains (Mangerud 2008). To the west, ice covering the British Isles was at times connected to the SIS across the North Sea and formed the smallest component of the combined EurIS. This ice sheet is commonly referred to as the British–Irish or British Isles (or occasionally Celtic) Ice Sheet; here we use the former name and abbreviation (British–Irish Ice Sheet, BIIS). The ice sheets north of Scandinavia are often divided into three main parts and named based on location. Three names are commonly used both alone and in different combinations, partly reflecting real changes in the centre of ice mass over time; Svalbard, Barents Sea and Kara Sea ice sheets. We refer to this ice mass collectively as the Svalbard–Barents–Kara Ice Sheet (SBKIS).

The SIS and BIIS were predominantly terrestrially based although the westernmost sector of the SIS and up to a third of the BIIS were grounded below present-day sea level in fjords and on the continental shelf. In comparison the SBKIS was predominantly marine-based for much of the last glacial cycle. At maximum extension, over half (~6000 km) of the combined EurIS margin terminated at the continental-shelf edge and a similarly long terrestrial margin (~4000 km) stretched across the Russian and northern European plains. Parts of this margin terminated into large proglacial lakes dammed by the ice sheet (e.g. Lunkka *et al.* 2001; Jakobsson *et al.* 2007).

The ultimate limit reached by ice during the last 40 ka has been carefully defined on the basis of till deposits, stratigraphy, moraines and other ice-contact landforms at sites across the region (Ehlers & Gibbard 2004; Ehlers *et al.* 2011; Fig. 1). Although often referred to as the Last Glacial Maximum (LGM) ice extent, the timing of ice extension to this limit occurred at different times for sectors of the individual ice sheets and across the ice-sheet complex as a whole (Svendsen *et al.* 2004; Böse *et al.* 2012; Clark *et al.* 2012). Therefore, the line as depicted on Fig. 1 does not represent a synchronous ice-sheet margin. In this paper we use the last (most-recent) peak in global ice volume as the definition for the LGM (23–21 ka, Clark *et al.* 2009), which may or may not coincide with the timing of the maximum achieved ice extent for different sectors of the EurIS margin.

Geological reconstructions of the entire EurIS complex have been published (e.g. Andersen 1981; Svendsen *et al.* 2004) but more frequently reconstructions of individual ice sheets (e.g. Kleman *et al.* 1997; Boulton *et al.* 2001; Saarnisto & Lunkka 2004; Clark *et al.* 2012) or ice-sheet sectors (e.g. Saarnisto & Saarinen 2001; Houmark-Nielsen & Kjær 2003; Kalm 2012; Larsen *et al.* 2014) have been undertaken. Much of the most recent work has been facilitated by the increasing use and quality of remote sensing imagery, digital elevation models, and high-resolution multibeam and seismic bathymetry data for landform mapping (e.g. Clark 1997; Ottesen *et al.* 2007; Greenwood & Clark 2008; Hughes *et al.* 2010; Winsborrow *et al.* 2010). Some such reconstructions grounded in regional mapping of glacial geomorphology have focussed on ice sheet-scale retreat-pattern dynamics (e.g. Boulton *et al.* 2001; Clark *et al.* 2012) and ice-flow path evolution (e.g. Kleman *et al.* 1997; Greenwood & Clark 2009a,b; Hughes *et al.* 2014) (Fig. 2). However, high-resolution studies of discrete sectors or individual ice lobes from detailed field observations of sediments and geomorphology remain the main lines of evidence for reconstructing former ice-sheet behaviour.

Geological reconstructions have been supplemented by isostatic and numerical glaciological models that have varied in terms of geographic and temporal scope, as well as mathematical and physical complexity and resolution (e.g. Boulton *et al.* 1995; Holmlund & Fastook 1995; Payne & Baldwin 1999; Siegert *et al.* 2001; Arnold *et al.* 2002; Forsström *et al.* 2003; van den Berg *et al.* 2008; Hubbard *et al.* 2009; Lambeck *et al.* 2010; Clason *et al.* 2014).

Fig. 1. Map of northern Eurasia showing maximum extent of ice cover during the last glacial period (white lines over Greenland, Iceland and Eurasia taken from Funder *et al.* (2011), Geirsdóttir (2011) and Svendsen *et al.* (2004) respectively, with small modifications over Britain and Ireland after Sejrup *et al.* (2005)). Dashed white lines mark approximate boundaries of the three Eurasian ice sheets: SBKIS = Svalbard–Barents–Kara Ice Sheet; SIS = Scandinavian Ice Sheet; BIIS = British–Irish Ice Sheet. Trough-mouth fans that line the continental-shelf edge are shown in orange. In this and subsequent figures, topography and bathymetry is from the GEBCO Digital Atlas published by the British Oceanographic Data Centre on behalf of IOC and IHO (2003), land-sea distribution is as defined by present-day coastlines and sea level, and present-day ice extent over Greenland and Iceland is shown in white.

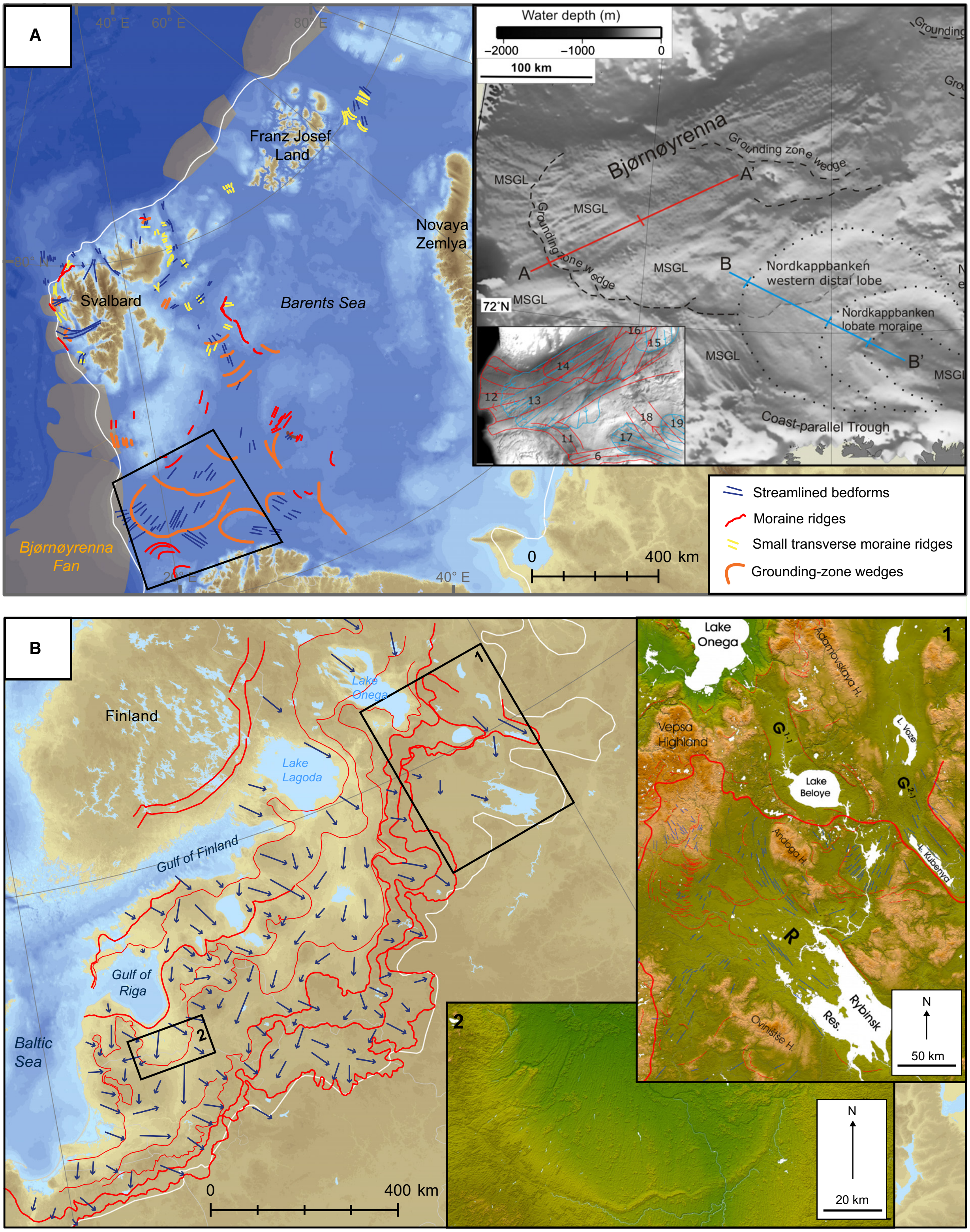

Fig. 2. Examples of landform evidence used to assist reconstruction and interpolation of lines across regions with poor chronological control. A. Sub-marine glacial landforms of the Barents Sea (redrafted from compilation by Jakobsson *et al.* 2014). Inset map shows detail of moraines, lineations and flowsets identified along Bjørnøyrenna and north of Norway (reproduced from Winsborrow *et al.* 2010). B. Mapped moraines (red) and summary lineation directions (blue) in the eastern European Plain as mapped by Kalm (2012). White lines delineate maximum extent of ice cover during MIS 2 as in Fig. 1. Inset maps show detail of moraines overlain on digital surface model (reproduced from Kalm 2012).

Methods and procedures

Compilation of dates

Dates relevant to the advance and retreat of ice during the last glacial cycle, including those giving insights into the vertical extent of ice, were compiled from the published literature (journal articles, books, theses, geological survey reports and maps). We attempt to include all relevant dates from within the geographic area shown in Fig. 1 and in order to reduce redundancy in the dataset do not include confirmatory ages considerably younger (in practice ~1–5 ka, depending on location) than the earliest date for deglaciation at a site. For some stratigraphical sites (e.g. lake cores) we include some younger dates that support the reliability of the earliest deglaciation dates. We include a small number of ages beyond the ultimate last glacial limit that constrain this position. Marine cores located beyond the continental-shelf edge document the timing of delivery of ice-rafted debris and deposition of glacial material to trough-mouth fans and the deep ocean, and therefore provide an additional indirect guide to the extent of ice on the adjacent continental shelf. We use the timing of ice-rafted debris and trough-mouth fan deposits to assist in placing the ice margin where direct on-shelf evidence and dates are sparse.

The DATED database version 1 (DATED-1) has a census date of 1 January 2013. Dates published after this date will be included in subsequent versions. Despite our best efforts, we expect that some dates have been missed and appeal to the wider Quaternary community to contact us with missing information and corrections of included data so that we may update and improve future versions of the database.

Each date was entered into an Excel spreadsheet, which was used to create an ArcGIS point shapefile (.shp) for incorporation with a Geographic Information System (GIS). Each date is attributed to the source publication and fully documented with information relevant to its interpretation in terms of ice advance and retreat (Table 1). For dates obtained from compilations or review articles, citation is made to both the review article or compilation and the original

Table 1. Metadata recorded for each date, included in both the database table (Table S1) and shapefile attributes (DATED1_database.shp; Data S1, S2). These metadata form the basis for our quality control assessment and palaeoglaciological classifications of each date.

DATED ID	Unique database identification number
Location	Country/sea, region, site name, DATED site number Latitude and longitude co-ordinates: °N, °E (WGS84) Comment on precision of location if not reported from original source, e.g. taken from map
Sample characteristics	Site type: marine core, lake core, bog core, section, surface, borehole Elevation (m a.s.l.) Sample depth (m), if applicable
Dated material	Sample field number and/or Laboratory ID number Class of dated material: TPM (terrestrial plant macrofossils, including wood), organic (peat, detritus, bulk, mixed, aquatic macrofossils), bone (including teeth, antlers, tusks), shell (molluscs and mollusc fragments), foram (single species and mixed), sand, boulder, bedrock, speleothem Detailed description of dated material: free text Organic material type: terrestrial (T), marine (M)
Stratigraphic context or setting	Detailed notes on stratigraphic setting: free text Glacial context class: *advance, margin, deglacial, ice free, exposure time (cumulative)*
Dating method	Radiocarbon (^{14}C, ^{14}C AMS, ^{14}C Conv.), thermal luminescence (TL), optically stimulated luminescence (OSL), infrared stimulated luminescence (IRSL), electron spin resonance (ESR), terrestrial cosmogenic nuclide (TCN^{10}Be, TCN^{26}Al, TCN^{36}Cl), U series
Quality control	Reliability of the age: 1 = reliable; 2 = possibly reliable; 3 = unlikely to be reliable (see Table 2 for criteria)
Ages	Uncalibrated radiocarbon age and error (as reported, without correction for marine reservoir effect) TCN age and error (as reported in source) Calibrated/calendar age and error (reported to 1 SD). Radiocarbon ages calibrated to INTCAL13 or MARINE13 (Reimer *et al.* 2013) as appropriate (on basis of type of organic material: T/M). ^{10}Be and ^{26}Al TCN ages recalculated using 'Arctic' production rate (Young *et al.* 2013) and Lal/Stone scaling (Lal 1991; Stone 2000). Necessary information to recalculate ^{10}Be and ^{26}Al TCN ages using different production rates additionally collated and recorded in Table S3 Comments on calibration (e.g. beyond calibration curve limit)
Comments	Any additional pertinent comments (e.g. reliability of date)
Citation information	Source reference (author, year) Compilation reference (author, year) Database reference (for ages also included in other datasets, e.g. BRITICE (Hughes *et al.* 2011))

source. Several previously or contemporaneously collated datasets were generously provided by other members of the Quaternary community (Görsdorf & Kaiser 2001; Kalm 2005, 2006; Tornivaara 2007; Wohlfarth 2009; Hughes *et al.* 2011; Hormes *et al.* 2013) and these compilations are also credited where applicable. Dates from these compilations were fully merged into the DATED-1 database, returning to the original sources where necessary to populate columns in the table. The shapefile retains all metadata (columns) from the spreadsheet within the associated attribute table as fields. In many instances geographical co-ordinates were missing from the original (source) publications. Where maps were provided in the original publication co-ordinates were either derived by geo-correcting scanned or digital versions of the figures, or by identifying the site on Google Earth to derive the co-ordinates. Where neither co-ordinates nor map locations were given, the co-ordinate information was derived using the site name and Google Earth mapping software; dates for which the location information is likely to be imprecise are flagged.

Calibration of radiocarbon ages

To maintain consistency within the dataset as a whole we recalibrated all dates using INTCAL13 and MARINE13 calibration curves (Reimer *et al.* 2013) and the OxCal v4.2 radiocarbon calibration software. OxCal (in common with the alternative Calib and Clam calibration software programs) returns calibrated ages as ranges at 68 or 95% probability. Occasionally, due to the nonlinear nature of the calibration curves, more than one range is returned accompanied by a probability estimate for each range. For ease of comparison with the rest of the dataset, we use the midpoint ± half of the total range at 68% probability to represent the calendar age and associated uncertainty. Calibrated ranges at 95% are additionally included as Supporting Information (Table S2). Minimum radiocarbon ages were calibrated using the reported >age and a nominal associated error of 1 year and are flagged as minimum ages in the database table. In this paper we report all ages in calibrated or calendar years, unless otherwise specified. For reference the conventional radiocarbon ages are reported in Table S1.

For simplicity in our recalibrations we have used a ΔR value of 0 for marine samples, corresponding to a marine reservoir age correction of *c.* 400 years across the dataset, which spans both a large geographic area and several thousand years. This is close to the mean for pre-bomb samples from the region (Mangerud *et al.* 2006) and also for the deglacial period, although reservoir ages were as high as 600 years during the Younger Dryas (Bondevik *et al.* 2006). Some ages from marine samples were originally reported with corrections. For example, some laboratories previously corrected for isotopic fractionation in marine molluscs to 0‰ PDB $\delta^{13}C$; in our table this applies to dates from the laboratories at Trondheim (T-), Copenhagen (K-) and Stockholm (St-). This process 'builds-in' a correction for a marine reservoir age of approximately 410 years compared with standard calculations in which isotopic fractionation is corrected to −25‰ PDB $\delta^{13}C$ (Mangerud 1972). In Trondheim this was done up to sample T-3000; thereafter standard calculations were used but a reservoir age of 440 years was subtracted (Mangerud & Gulliksen 1975) when reporting the age. All affected ages have been 're-corrected' in the database and are reported as conventional radiocarbon years uncorrected for marine reservoir ages, as defined by Stuiver & Polach (1977). Ages may therefore differ from the original publications where a correction was applied.

Recalculation of terrestrial cosmogenic exposure ages

There is presently debate over which production rate and scaling factors are appropriate when converting terrestrial cosmogenic nuclide (TCN) concentrations into calendar ages. Latest research indicates a lower production rate for ^{10}Be for high-latitude locations than the previously implemented globally averaged value (e.g. Balco *et al.* 2009; Fenton *et al.* 2011; Briner *et al.* 2012; Goehring *et al.* 2012; Young *et al.* 2013; Heyman 2014; Stroeven *et al.* 2015). For consistency across the dataset we recalculated all ^{10}Be and ^{26}Al ages with the CRONUS-EARTH online calculator v2.2 (Balco *et al.* 2008) using the 'Arctic' production rate calibration dataset of Young *et al.* (2013) and report values using 'St' scaling (Lal 1991; Stone 2000), which gives a reference production rate of 3.96 ± 0.15 atoms g^{-1} a^{-1} for ^{10}Be. Authors were contacted to supply any additional information that this required if not reported in the original sources. The additional data are included in Table S3 to facilitate future recalculation. In the main table, we include the calendar age as reported in the original source (where original references give multiple age estimates based on alternative scaling schemes, we list the 'preferred' age of the original authors) and our recalculation. We chose the 'Arctic' production rate because this dataset includes several sites from Norway (Fenton *et al.* 2011; Goehring *et al.* 2012) located in the centre of our study area. It also compares favourably with an updated global reference rate for ^{10}Be calculated by Heyman (2014) to assess a compilation of dates from the Tibetan Plateau to the east (3.99 ± 0.22 atoms g^{-1} a^{-1}, 'St' scaling), and a new reference production rate that includes a site in southern Sweden (3.95 ± 0.10 atoms g^{-1} a^{-1}, 'St' scaling) (Stroeven *et al.* 2015). Using solely production rate calibration sites in western Norway (Goehring *et al.* 2012) the calculated ages are ~4% younger. There is not an equivalent production rate for

^{26}Al; therefore, we used the reference ^{26}Al production rate calculated from the 'Arctic' ^{10}Be rate (26.55±1.01 atoms g^{-1} a^{-1}, 'St' scaling). In the absence of a simple system for recalculating ^{36}Cl derived ages, these ages remain as given in the original sources.

For simplicity no corrections were made for post-exposure uplift, erosion, submergence or vegetation/snow cover. Post-exposure erosion and delayed exposure owing to temporary submergence following deglaciation or snow/vegetation/soil cover will all serve to reduce the total nuclide accumulation in a sample and therefore lead to anomalously young ages if not corrected. For an applied erosion rate of 1 mm ka^{-1} (André 2002) we calculate a <2% increase for ages 10–25 ka and 2.5–4% increase for ages 25–50 ka and thus negligible at our target 1000-year resolution. Typical changes owing to snow and vegetation cover depend on the setting of sampled material and are likely to be below 4%, but in some cases may be larger (Fenton *et al.* 2011). Postglacial emergence of Fennoscandia exhibits a radial pattern decreasing from a maximum total emergence of 310 m on the western coast of the Bothnian Sea (Berglund 2004) decreasing towards the ultimate limit of the former SIS. Although changes in atmospheric depth (and therefore pressure) due to postglacial uplift could be significant in some locations, e.g. close to the centre of the former SIS, relative sea-level records show that for most sites the majority of isostatic rebound following deglaciation was achieved within a few thousand years and before the start of the Holocene (Larsen *et al.* 2012). For simplicity therefore we do not correct for post-exposure uplift. From sites in Norway, Goehring *et al.* (2008) observed age increases as a result of postglacial uplift of 5–10%, but noted that this predominantly affected older (>18 ka) and high-elevation (>1600 m) sites. Finally, we do not attempt to correct for any effect of ice-sheet proximity on atmospheric pressure, which could potentially lead to an overestimation of ages at locations experiencing strong katabatic winds from the adjacent ice sheet (Staiger *et al.* 2007). We expect that this effect would only be significant for boulders that remain close (within 10s km) to the ice-sheet margin for several thousand years. In contrast to the other factors that may have changed over time, this effect generates anomalously old ages.

Varve records – The Swedish Time Scale

We additionally incorporate the deglaciation pattern inferred from clay-varve records of the 'Swedish Time Scale' (e.g. De Geer 1935; Cato 1985; Strömberg 1985, 1989, 1990, 2005; Wohlfarth *et al.* 1995) digitized from Fredén (2009) in our reconstruction and correlation of ice-sheet retreat from the Baltic Sea and across Sweden and Finland. To correct for potential gaps in the 13 300-year sequence of clay-varves, 900 years have been added to varve ages younger than 10 300 varve years ago, based on correlation between the Swedish Time Scale and the GRIP $\delta^{18}O$ record and the new Greenland ice-core chronology GICC05 (Andrén *et al.* 1999; Rasmussen *et al.* 2006).

Consistency and quality control of dates

Our calibration choices for both radiocarbon and TCN dates were pragmatic considering the large area under consideration (~6.3 Mkm^2), the long time-span of data accumulation (over 50 years) and volume of dates (over 5000). Ages derived using luminescence techniques are not recalculated. In general luminescence dates are clearly reported in the literature with all necessary background data for a reassessment of their quality (e.g. dose rates). Calibrated radiocarbon ages are reported as years BP (i.e. before 1950). Luminescence and TCN ages are reported relative to the year of sampling/analysis following standard convention. We do not impose a consistent datum across dates derived from different methods as the maximum deviation between datums (and thus any additional uncertainty) is negligible in terms of our 1000-year time-slices and uncertainties due to other factors for the majority of dates.

The resulting database contains a large volume of information, acquired over a period of more than 50 years. All available dating techniques have developed and improved during this time, as well as what is considered to be a reliable age derived using each technique. Accurate interpretation of ages from all dating methods rests critically on careful consideration of the geological quality of each sample selected for dating and our ability to accurately decipher its individual history (e.g. of exposure, contamination, transport, redeposition, water content, etc.). For this reason we include key metadata for each date as reported by the original sources (Table 1) and report comments made by the original authors as to the data quality. Unfortunately for some dates (mainly older publications) some of this data are unreported, and so there are gaps within the DATED-1 table (Table S1). These data are the basis for our reliability assessment of each date, and palaeoglaciological classifications (see following section).

We assign each date contained within DATED-1 (including those derived from other regional collations supplied to us) a qualitative quality control (QC) or reliability rating according to a defined set of criteria dependent upon the dating technique (Table 2) to flag potentially problematic ages: 1 = all criteria are satisfied; the age is robust and reliable, 2 = some of the criteria are met but not all; the age is probably reliable, 3 = no criteria are met, age is unlikely to be reliable. We also take into account comments on reliability

Table 2. Age quality control criteria (based on Duller 2006, 2008; Thrasher *et al.* 2009; Wohlfarth 2009; Heyman *et al.* 2011; Alexanderson & Murray 2012; England *et al.* 2013; Reimer *et al.* 2013). Ages within DATED-1 are given a quality control (QC) rating based on the criteria specific to the dating method used. QC = 1, all criteria are satisfied; QC = 2, most of the criteria are satisfied; QC = 3 no (or few) criteria are satisfied.

Dating technique	Quality control criteria
Radiocarbon ^{14}C Conv (Conventional), ^{14}C AMS	Known and uncontaminated sample material; sediment-feeding marine mollusc (e.g. *Portlandia arctica*) receives lower rating Organic content >5% LOI Sample composition: Conv - bulk samples not acceptable; AMS - bulk sample acceptable if age <20 ka Within calibration range of INTCAL/MARINE13 Uncalibrated ^{14}C age determination provided with errors to enable recalibration using the latest calibration curves Multiple and/or stratigraphically consistent ages
Terrestrial cosmogenic nuclide TCN ^{10}Be, ^{26}Al, ^{36}Cl	Multiple (ideally three or more, but at least two) samples from the same feature/site Ages are internally consistent and clustered (reduced Chi-square value ~1) Observed spread in ages is similar to expected measurement uncertainty Geomorphological setting is accounted for: erosion, submergence, uplift Data necessary to recalculate ages (^{10}Be, ^{26}Al) using different production rates (Balco *et al.* 2008) No indication of isotopic inheritance, or if present expected/stated
Luminescence TL, OSL, IRSL	Quartz have a higher rating than feldspar-derived ages Single-grain or small aliquot Homogenous sample; preferably aeolian, fluvial, glacifluvial sediments that are likely to have received sufficient exposure. Sample setting considered and accounted for; e.g. water-content history Dose rate information and equivalent dose including errors described in source Multiple and/or stratigraphically consistent ages
Uranium series U-Series	Chemically precipitated calcium carbonate Multiple and/or stratigraphically consistent ages
All dating methods	Sample considered *in situ*, i.e. no postdepositional disturbance or reworking Specified error margins Precise ages: errors <10% of age Details of geological and stratigraphical setting given Considered by original authors to be reliable

made in the original source, if applicable. Dates flagged as outliers or as unreliable by the original authors (or by a later data compilation exercise such as by Wohlfarth (2009)) received the lowest rating (3). Dates with the lowest rating were not used in the ice-sheet reconstruction.

Palaeoglaciological interpretation and classification of dates

Each date is classified in terms of its role constraining either ice-sheet build-up or retreat on the basis of the stratigraphic context and setting. The classification system is similar to, but deviates slightly from that used by Hughes *et al.* (2011).

Advance: we recognize two types of samples that indicate an ice-front advance post-dating the obtained age; dated material incorporated within till and dated material from a unit stratigraphically below till. In many cases these ages also give a minimum age of a previous retreat, e.g. peat both underlying and overlying till, in which case they are classified as *Retreat/Advance*. In some cases a considerable period of time may have elapsed between ice cover and the obtained age.

Margin: dated material related to an ice-margin position, e.g. boulder from a moraine crest, shells from an ice-contact delta or from proximal glacimarine sediments.

Deglacial: dated material records most recent retreat from a location. The site possesses stratigraphic information specifically indicating ice-free conditions closely following ice cover, e.g. basal organic material in lake cores showing pioneer vegetation, shells in glacimarine sediments, an exposure age from an erratic boulder.

Ice free: dated material records ice-free conditions and potentially dates deglaciation and/or ice advance, but no sedimentary properties or stratigraphy indicate deposition close in time to glaciation; e.g. organic material lacking demonstrated pioneer vegetation and not lying directly above till. This category also includes dates lying beyond the maximum limit of the last glaciation that help to restrict ice extent, e.g. sites with continual organic sedimentation throughout MIS 2–3.

Cumulative exposure time: sample records cumulative length of exposure at sites that may have experienced multiple phases of exposure and burial beneath ice but where burial did not result in total removal of the accumulated nuclides from the previous period of exposure, i.e. glacial erosion was insufficient to reset the nuclide clock, e.g. samples in block fields or above a glacial trimline. This class applies exclusively to ages derived from *in situ* cosmogenic isotope analysis.

Ice-margin positions and ice sheet flow-pattern information

In addition to the database of numerical dates and metadata, we use landform evidence, especially published maps of end moraines and generally accepted correlations of ice-margin positions between individual moraines, to guide our reconstruction (Fig. 2; e.g. Jakobsson *et al.* 2014). Generalized flow patterns (e.g. Kleman *et al.* 1997) and identified ice-stream locations (e.g. Ottesen *et al.* 2007) are used to guide our interpretative decisions concerning the pattern of retreat and configuration of the ice sheets. These geomorphological signatures thus complement the numerical dates. Again these data are unevenly distributed in both space and time; we have reasonably good knowledge of the ice-divide configuration and evolution of flow patterns for the SIS (e.g. Kleman *et al.* 1997) and BIIS (e.g. Greenwood & Clark 2009b; Hughes *et al.* 2014) whereas by comparison the geometry of the SBKIS is virtually unknown to the east of the central Barents Sea (Bjarnadóttir *et al.* 2014). We use the timing of ice-rafted debris delivery to the deep ocean and glacigenic debris flow deposition at trough-mouth fans (e.g. Elliot *et al.* 2001) as supporting evidence for ice-margin proximity.

Reconstruction and representation of ice margins

Reconstruction of ice-extent time-slices progressed in an iterative fashion. We examined regional subsets of the dataset in turn, combining the chronological evidence with the available geomorphological information in a GIS setting. Topographic height and bathymetric depth data (from the General Bathymetric Chart of the Oceans, GEBCO) were used as a guide to connect lines across areas where no information was available. At some locations the resolution of both the chronological and landform data is very high, e.g. the Younger Dryas moraines of coastal Norway, whereas in other areas, e.g. for much of the continental shelf, there exist very few constraining dates or mapped moraine positions. The change from one time-slice to the next is not always documented by dates. In the absence of evidence to the contrary, during deglaciation we draw subsequent margins successively smaller (and successively larger during build-up towards the maximum limit); i.e. we assume simple linear expansion towards and retreat from the maximum limit. We emphasize that our goal is a continental-scale ice-sheet reconstruction in 1000-year timesteps that is useful for numerical modelling. We therefore attempt a spatial resolution that captures the broad spatial trends only and we do not resolve individual mountain glaciers or small ice caps (<500 km^2) that likely existed during both build-up and disintegration of the ice sheet. Before 25 ka, the evidence base becomes sparser, reflecting a decline in preservation potential of dateable material, and therefore we reconstruct only four selected time-slices between 40 and 25 ka to capture the general trend of ice-sheet evolution during this period.

Treatment of uncertainty

There are several sources of uncertainty in our reconstructions, both temporal and spatial, most obvious being the uncertainty in the individual age estimates. Significant uncertainty in the reconstructions derives simply from gaps in the record, both in the spatial and age distributions of the available evidence. We note for example that although we have more than 5000 dates in the database, only 1795 (~33%) are considered absolutely reliable (QC = 1). This is <100 per 1000 year time-slice if dates were evenly distributed in time, which of course they are not (Fig. 4). Note however that we only exclude 823 ages (~15%) on the basis of questionable reliability (QC = 3). Further uncertainty derives from calculation of sedimentation rates and correlation of moraines across geographic distance. Many instances of conflicting ages and earlier interpretations also occur, and we choose to express this discord as uncertainty where it is not possible to discount one of the conflicting pieces of information.

We evaluate and integrate all chronological, spatial and geological uncertainties and for each time-slice after 25 ka from this we reconstruct three ice-margin positions; maximum, minimum and most-credible. The most-credible line is the ice-margin position that we consider to be the most permissible based on the total sum of the available chronological and geomorphological evidence. The maximum and minimum lines express the total uncertainty in terms of distance from the most-credible line. Before 25 ka there is an increasing degree of uncertainty, which reflects the lower density of dates and larger errors associated with older dates. Although limited and patchy in distribution there does exist valuable information for some ice-sheet sectors for the period before 25 ka (e.g. Houmark-Nielsen 2010) and we combine this into four snapshots of the ice-sheet margins at 38–34, 32–30, 29–28 and 27 ka.

Area and volume calculations

The total area (in km^2) of each ice sheet for each time-slice was calculated using the geometry calculator

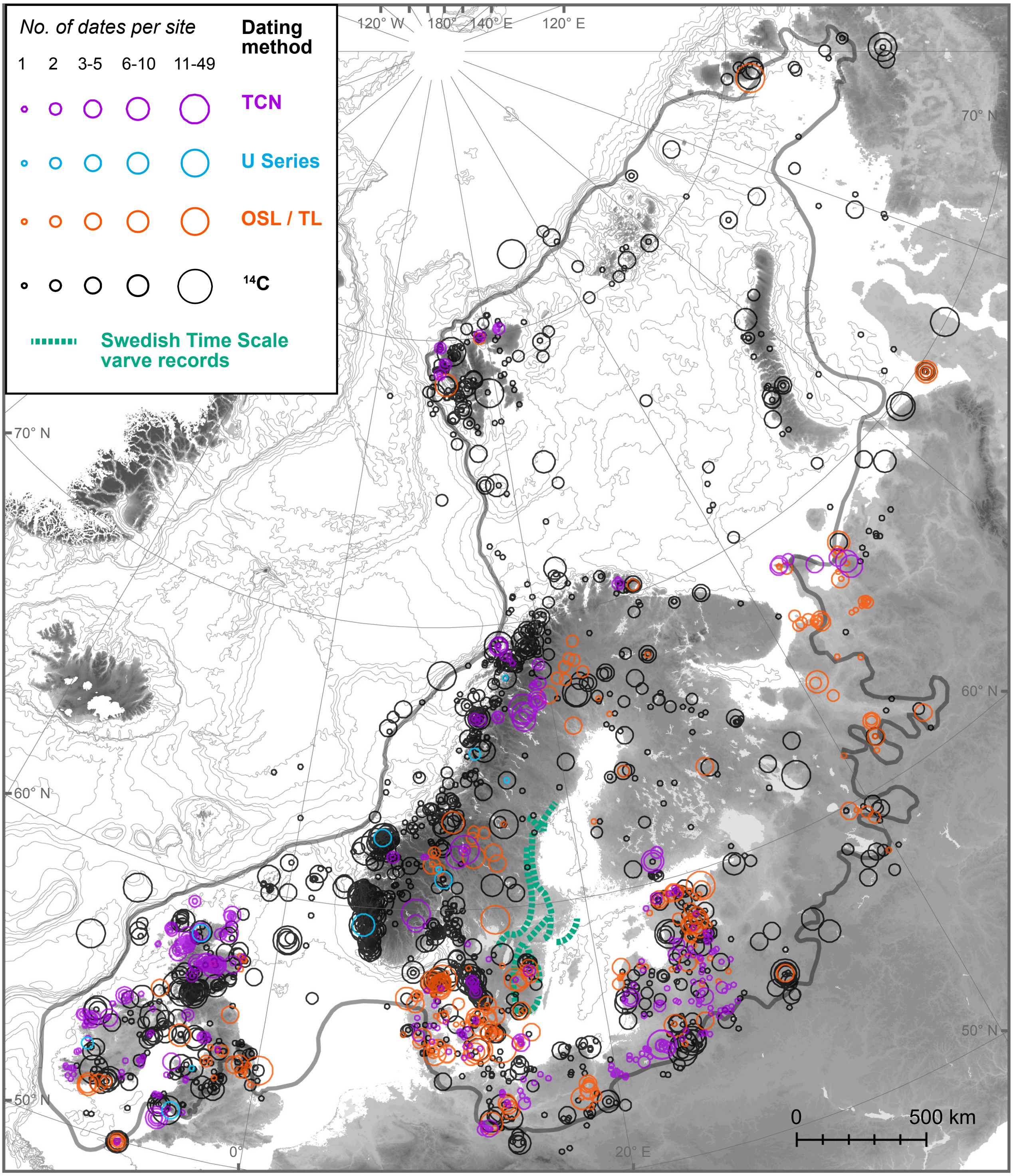

Fig. 3. Spatial distribution of all dates within the DATED-1 database. Proportional circles and colours show the number of dates from each dating method at each site (as defined by unique geographic co-ordinates). Approximate location where the deglacial Swedish varve chronology can be applied is also shown. Note the low density of information for the Barents and Kara seas, Baltic and North seas, the Irish, Scottish and Norwegian continental shelves, and across Finland and the Russian Plain. Dates were compiled from citations listed in Table S1 and at the end of this paper (references included as Supporting Information (Data S1)).

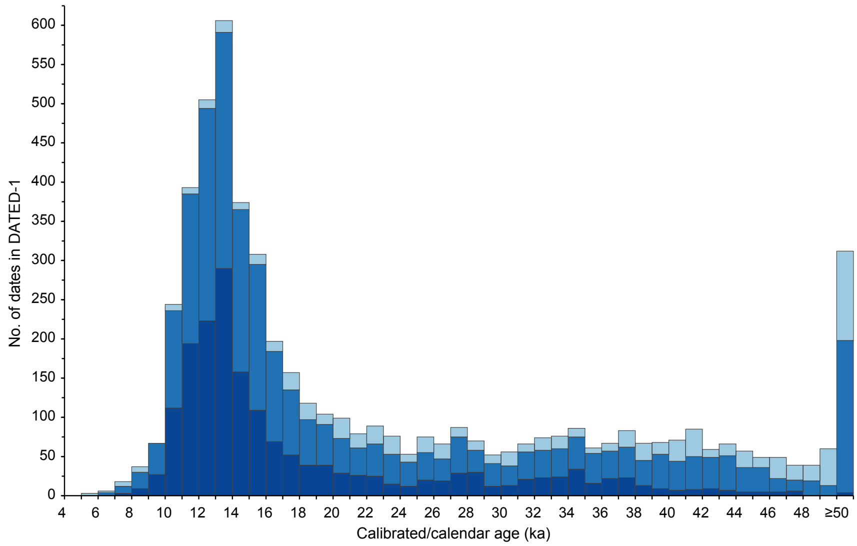

Fig. 4. Histogram of ages contained within the DATED-1 database, using a 1000-year bin size. Dates used in the reconstruction of ice-sheet time-slices, i.e. dates with a quality control rating of 1 (dark blue) or 2 (mid-blue). Excluded ages i.e. dates with a quality control rating of 3 (pale blue).

within ArcGIS 10.2, with all maps projected as North Pole Lambert Azimuthal Equal Area. To give estimates of the relative change of each ice-sheet component, we subdivided the total area into three geographical regions (Fig. 1). To give an estimate of total ice-sheet volume, the areas of each individual closed polygon(s) within each region were converted to volume using the relationship:

$$\log V = 1.23(\log A - 1) \quad (1)$$

where V = volume in km^3, and A = area in km^2. This relationship between ice-sheet area and volume is derived from a logarithmic linear regression of the area and volume of the six largest present-day ice sheets and ice caps (Paterson 1994). As the relationship is based on relatively few ice masses that exist under present-day climate conditions, it may tend to underestimate volume because colder temperatures of the last glacial cycle likely sustained ice sheets with steeper surface gradients. Conversely, for ice sheets resting on soft-beds and for a thinning and retreating ice sheet composed of many low gradient ice streams the equation will overestimate volume and our volume estimates likely become increasingly erroneous as deglaciation progressed, when the ice sheets thinned and started to develop more complex ice-flow structures with multiple divides.

To convert the volume estimates to eustatic sea-level equivalent (SLE) we use a global ocean surface area of 361.6 Mkm^2 and ice and seawater densities of 917 and 1028 kg m^{-3}, respectively, giving an ice-to-water density ratio of 0.892 and assume that seawater replaces ice grounded below sea level. We note that in terms of sea-level contribution our calculated volume is likely overestimated where ice is grounded below present-day sea level. For the SBKIS grounded ~210 m b.s.l. (average depth of the Barents Sea; Jakobsson (2002)) at its largest extent at ~21 ka, we estimate a maximum exaggeration of 1 m.

Results

The DATED-1 database

DATED-1 contains 5477 individual dates from 2505 discrete locations collated from over 900 published sources (Fig. 3, Table S1). The spatial distribution is uneven; the majority of dates are from coastal locations and at the outer margins of the ice sheets. Regions presently below sea level have the lowest densities of dates. Nearly 70% of the dates (3756) are

Fig. 5. Pre-25 ka DATED-1 time-slice reconstruction. Solid lines indicate limits where there is good evidence for an ice-margin position. Dashed lines indicate limits where evidence is sparse/non-existent and we have interpolated between evidence and/or sites. A. Ice extent during the Ålesund Interstadial, 38–34 ka. To represent the large degree of uncertainty for this time period, two possible ice extents are shown. A maximum (black dashed) line depicts a relatively substantial SIS contiguous over the Scandinavian Mountains, and a minimum (black dotted) line depicts ice retreated to the highest peaks in northern and western Norway. B. 32–30 ka. C. 29–28 ka. D. 27 ka. Small ice caps and glaciers (<500 km^2) are not shown. Maps are projected as North Pole Lambert Azimuthal Equal Area so that the area of map features is true everywhere, enabling accurate comparison and measurement.

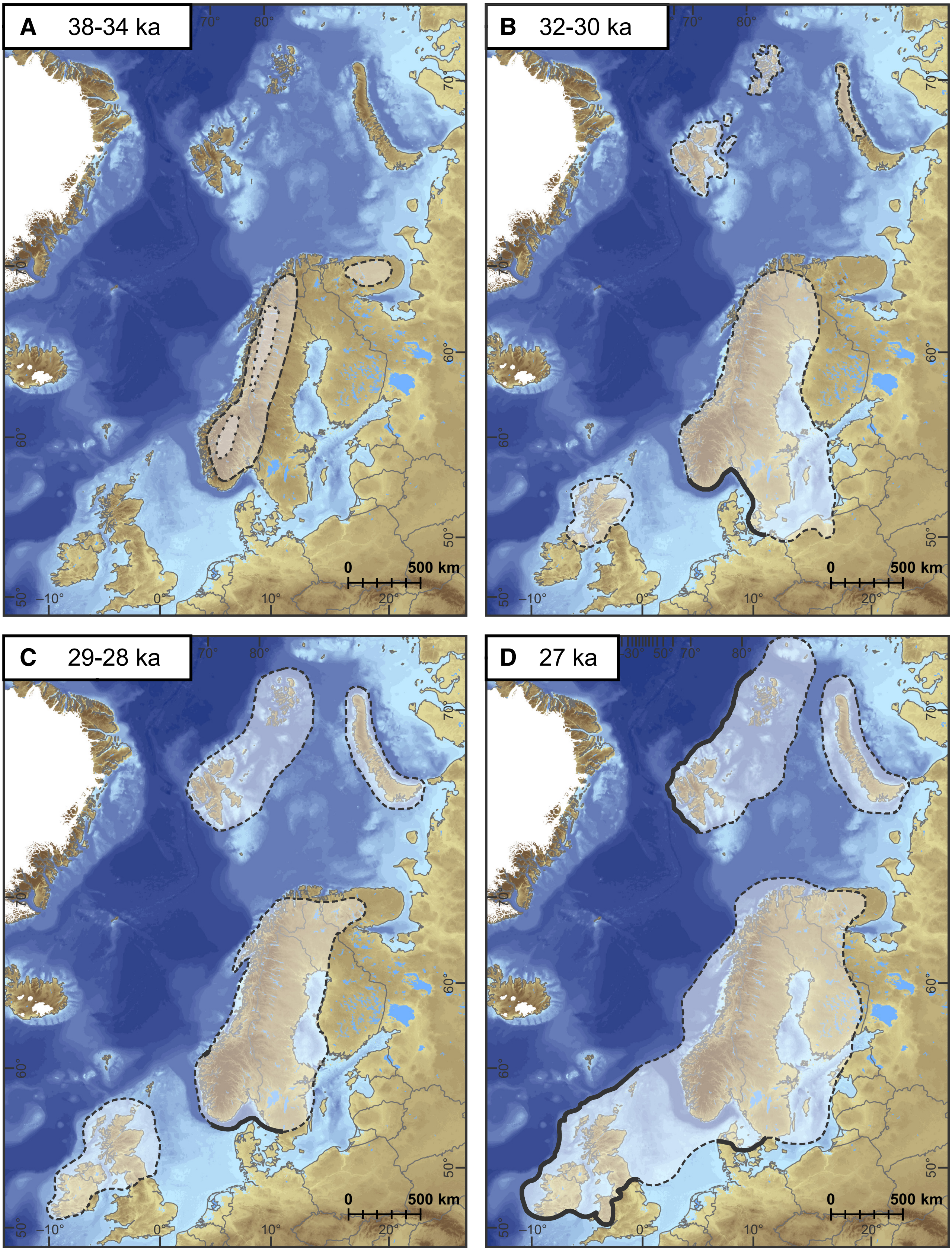
A 38-34 ka
B 32-30 ka
C 29-28 ka
D 27 ka
70°
80°
60°
50°
–10°
0°
10°
20°
0
500 km

derived from radiocarbon analysis, including 131 minimum ages (i.e. at the older limit of the radiocarbon method). There are slightly more terrestrial (2012) than marine radiocarbon ages (1744). The remainder of the database is comprised of dates from luminescence methods (14%; 787) and terrestrial cosmogenic nuclide (TCN) exposure techniques (17%; 904). There are a limited number of Uranium (U) Series ages (30; <1%). The spatial coverage of each dating method is variable (Fig. 3). The lower precision of luminescence and TCN dating, compared with radiocarbon, means that the ice-sheet margin will inevitably be less precise where we can rely on only these methods. For example the timing of the easternmost terrestrial limit on the Russian Plain is primarily informed by luminescence dating.

Half (2758) of the dates are younger than 17 ka, mainly reflecting the preservation bias of organic samples for radiocarbon dating (Fig. 4). There are a few ages older than 50 ka (312) included in the database, mainly from luminescence and TCN methods. Although much older than our chosen time frame of study, these ages either provide bounding ages in locations where no other evidence is available, or provide additional information relating to the style of glaciation such that it was prudent to retain them within the database. For example, 'artificially old' TCN ages that are thought to reflect inheritance due to insufficient erosion may indicate locations that were covered by cold-based ice during the last or even multiple successive glaciations (Fabel *et al.* 2002; Briner *et al.* 2006). 25% of TCN-derived ages (226) are thought to reflect inherited nuclides contained within the original samples (classified as *cumulative exposure time*).

Based on our quality-control criteria (Table 2) 1795 dates (33%) are considered reliable, 2859 (52%) raise some concern as to their reliability and 823 (15%) we regard as unlikely to be reliable and exclude from our reconstructions (Fig. 4). Of the total population of 5477 dates, 882 are classified as *advance*, 1301 as *deglacial*, 334 as defining both advance and retreat (i.e. where a date is both above and below till), 2366 as *ice free* and 368 as *margin*.

DATED-1 Ice-sheet time-slice maps

Our main result is a series of 20 maps of ice-sheet extent through time from 40–10 ka (Figs. 5, 6). Between 25 and 10 ka we delineate the ice-sheet margins every 1000 years, and show maximum and minimum lines in addition to our 'most-credible' line to represent uncertainty estimates as described above. Before 25 ka we present four reconstructions of the ice-sheet extent (38–34, 32–30, 29–28 and 27 ka) that capture the general timing of ice build-up between 40 and 25 ka. For these time-slices the ice margin is shown as solid lines in locations where there are good constraints for the position and dashed lines to indicate uncertainty and limited evidence.

Development of area and volume with time

The peak in total ice-sheet area (5.5 Mkm^2) and volume (~9.7 Mkm^3, ~24 m SLE) occurred 21–20 ka (Fig. 7; Table S5); this largely reflects the evolution of the SIS, particularly the relatively late timing of ice reaching the eastern terrestrial limit. Both BIIS and SBKIS reach their maximum volumes earlier; before 25 and 24–20 ka respectively, and appear to maintain a size close to their peak for several thousand years. Minor fluctuations in the size of the BIIS that occur throughout the glacial are related to expansion and retreat of posited ice lobes onto the surrounding continental shelf, the dimensions of which are poorly defined. For the SBKIS and BIIS, the continental-shelf edge is a major limit on growth. Any increase in extent requires ice expansion south in the case of the BIIS and to the east and southeast for the SBKIS. The western margin of the SIS was also limited by the shelf edge and most of the ice-sheet expansion after 25 ka was along the eastern and southern terrestrial margins. At our 1000-year resolution, the rate of ice-sheet build-up (40–21 ka) was almost as fast as the rate of retreat (21–10 ka) (Fig. 7). Initial retreat soon after 19 ka was dominated by the loss of ice over Novaya Zemlya and the adjacent sea floor. After 19 ka ice loss was relatively constant but slowed down for both the SIS and SBKIS between 14 and 12 ka. Note that the BIIS and SBKIS were contributing <1 m SLE after 17 and 15 ka, respectively, with only the SIS remaining as a significant ice sheet until ~11 ka. The former SBKIS was reduced to ice caps centred over the island archipelagos of Svalbard and Franz Josef Land by 14 ka. There does not appear to have been a net total ice-sheet growth from 13 to 11 ka, i.e. during the Younger Dryas (12.7–11.5 ka); despite local and regional evidence for a significant advance of many of the SIS margins during this time (Andersen *et al.* 1995a). Large uncertainty in defining the position of the ice-sheet margin during

Fig. 6. DATED-1 time-slice reconstruction of the evolution of the extent of the Eurasian ice sheets 25–10 ka (A–P). The ice-sheet area is represented every 1000 years. Three lines are shown: maximum (black dashed), minimum (black dotted) and most-credible (solid white line and shaded white area) to represent uncertainty in the data. Note that for some time periods and sectors of the ice-sheet margin the distances between maximum and minimum (i.e. total uncertainty) are over 500 km. Small ice caps and glaciers (<500 km^2) are not shown. Ice-sheet outlines shown in this figure are available to download as Supporting Information (Data S1). As in Fig. 5 maps are projected as North Pole Lambert Azimuthal Equal Area, enabling accurate comparison and measurement of ice-sheet areas.

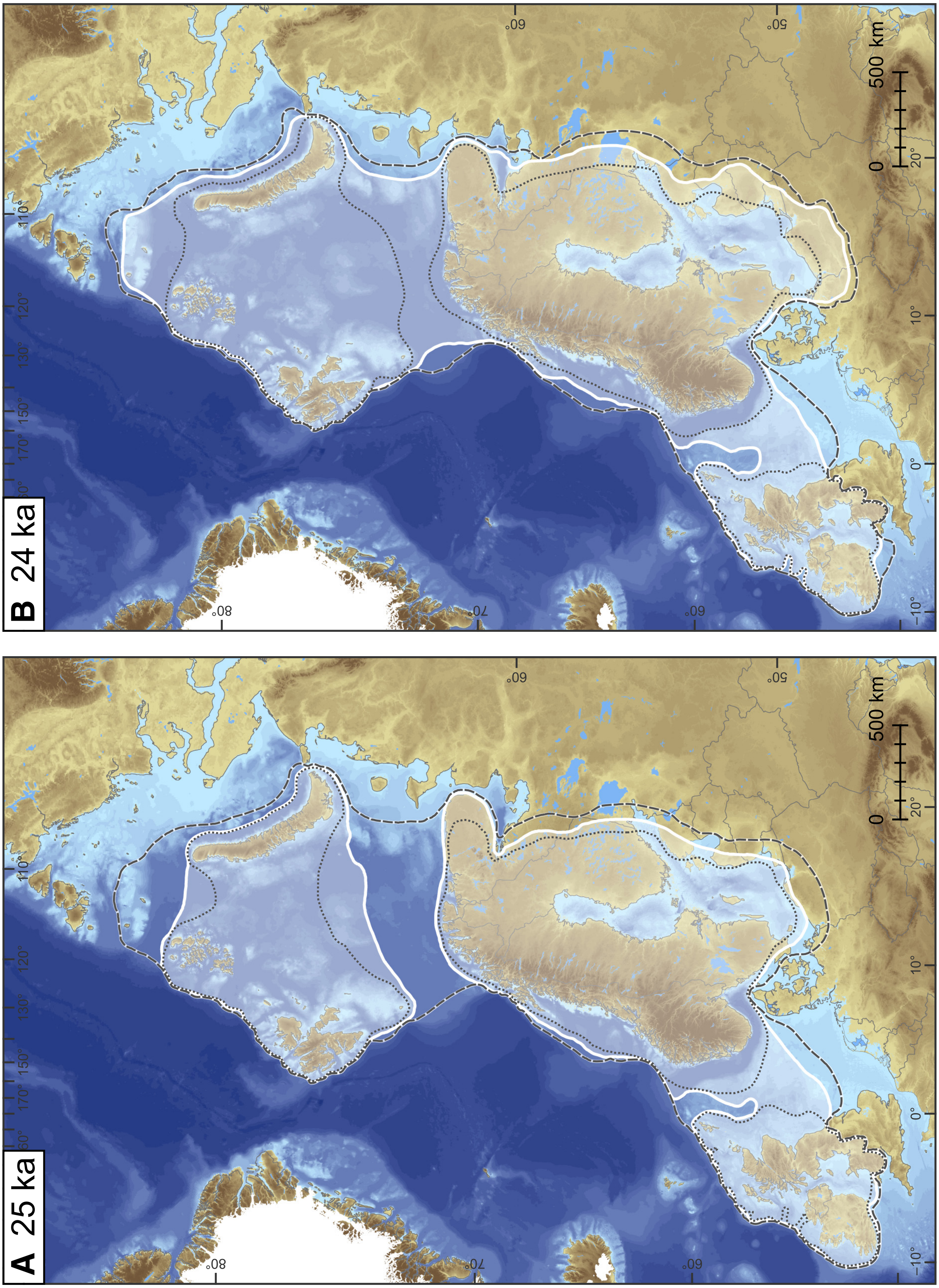

B 24 ka
A 25 ka
500 km
0

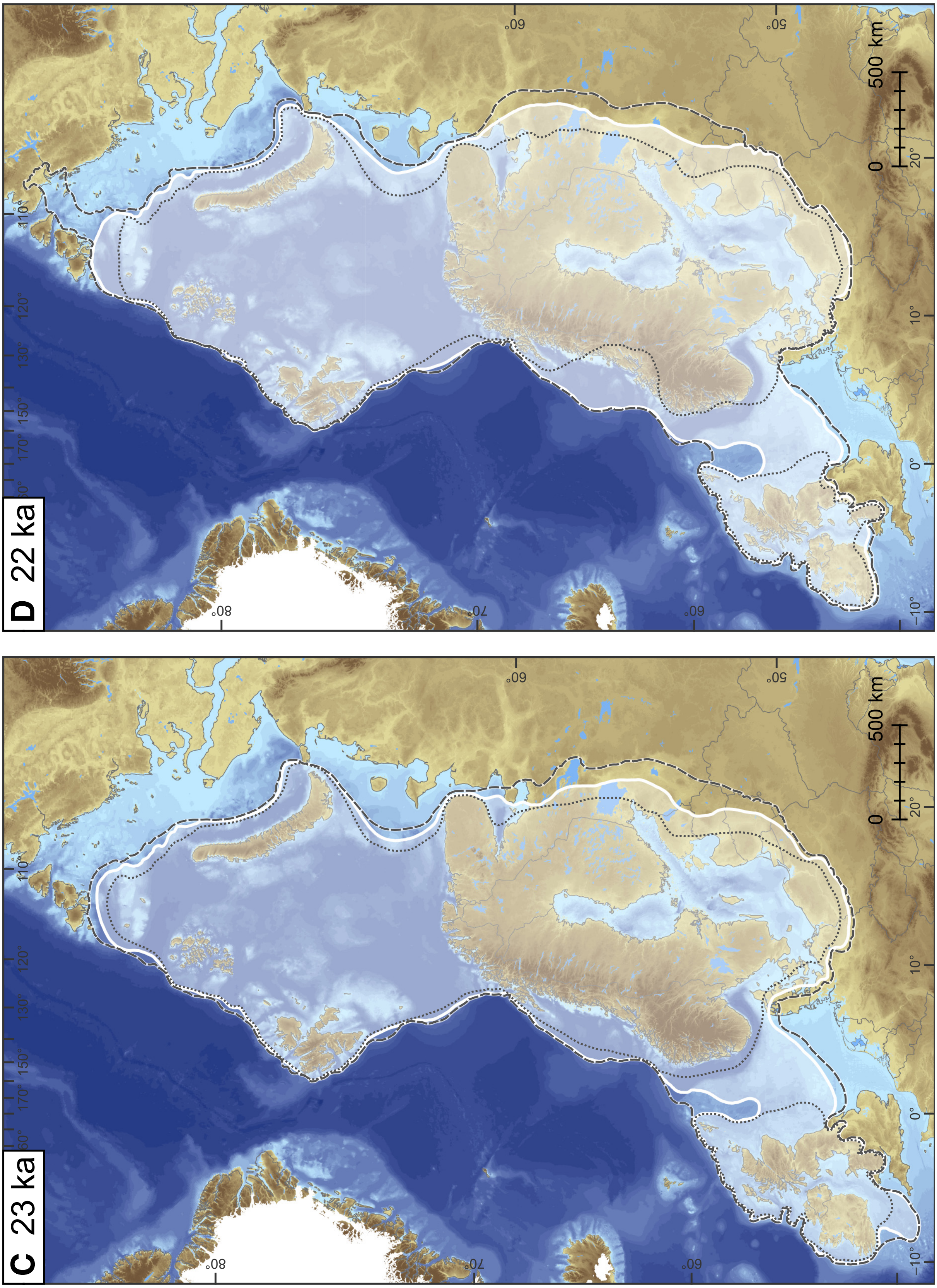

Fig. 6. (continued).

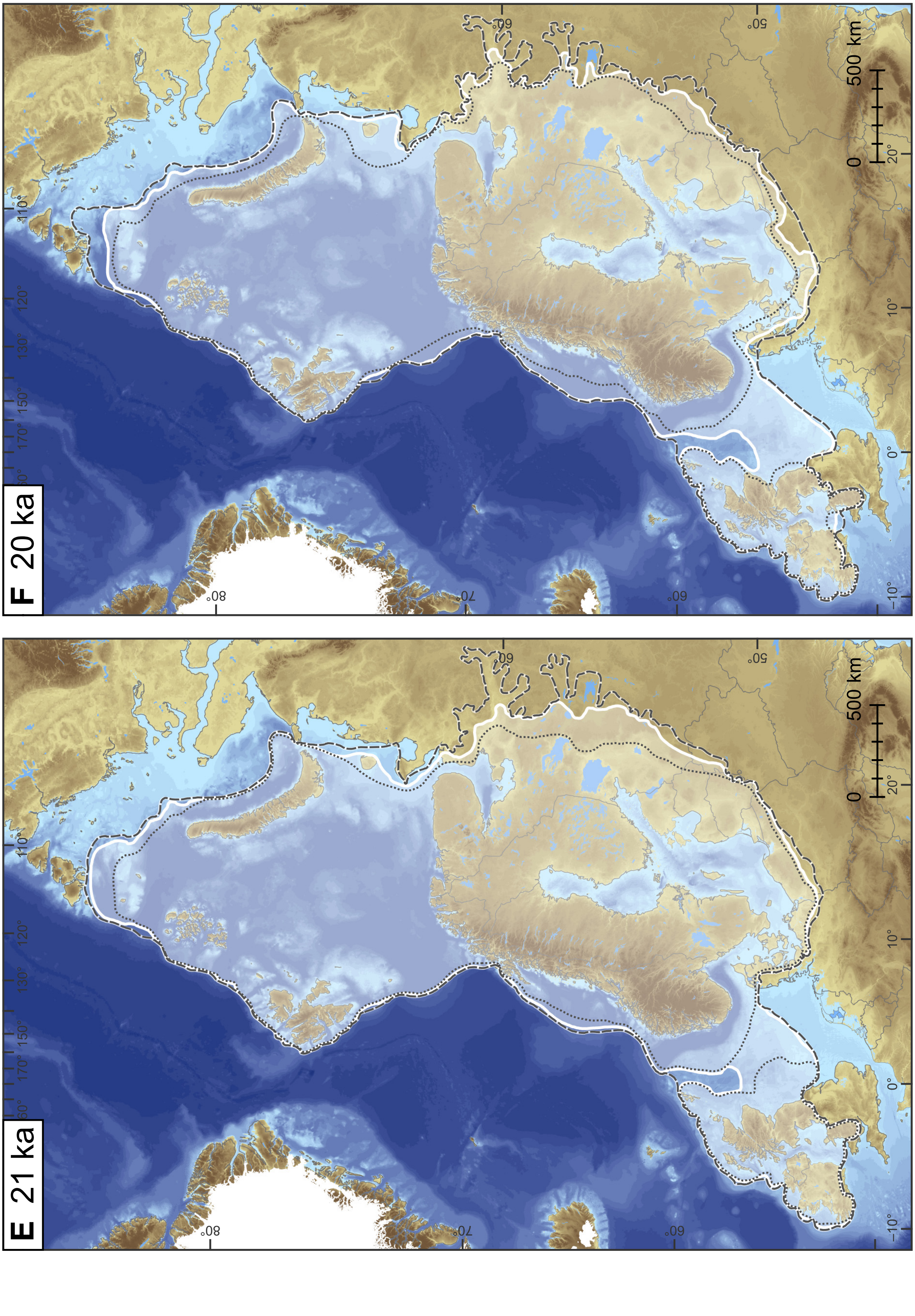

Fig. 6. (continued).

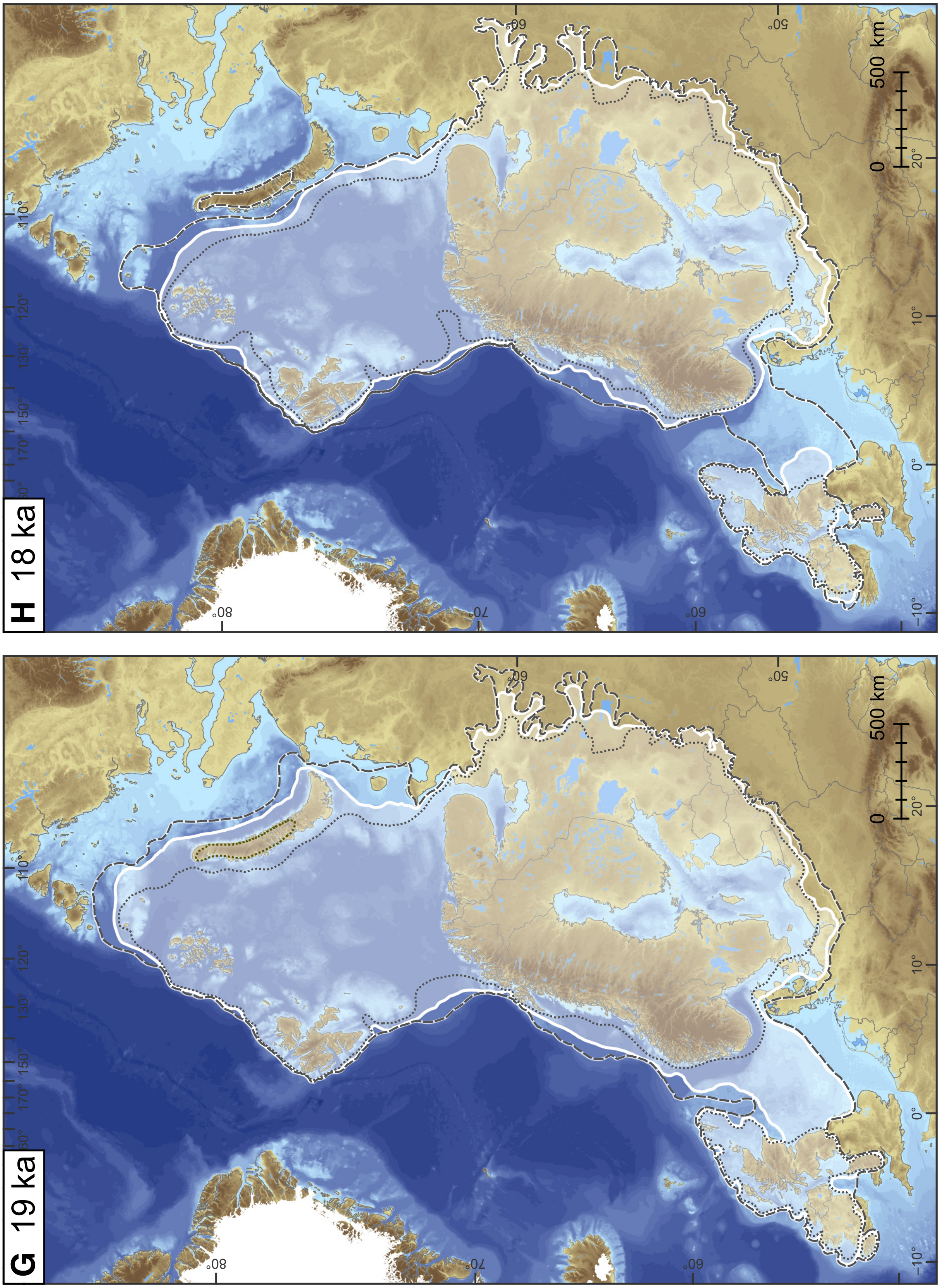

Fig. 6. (continued).

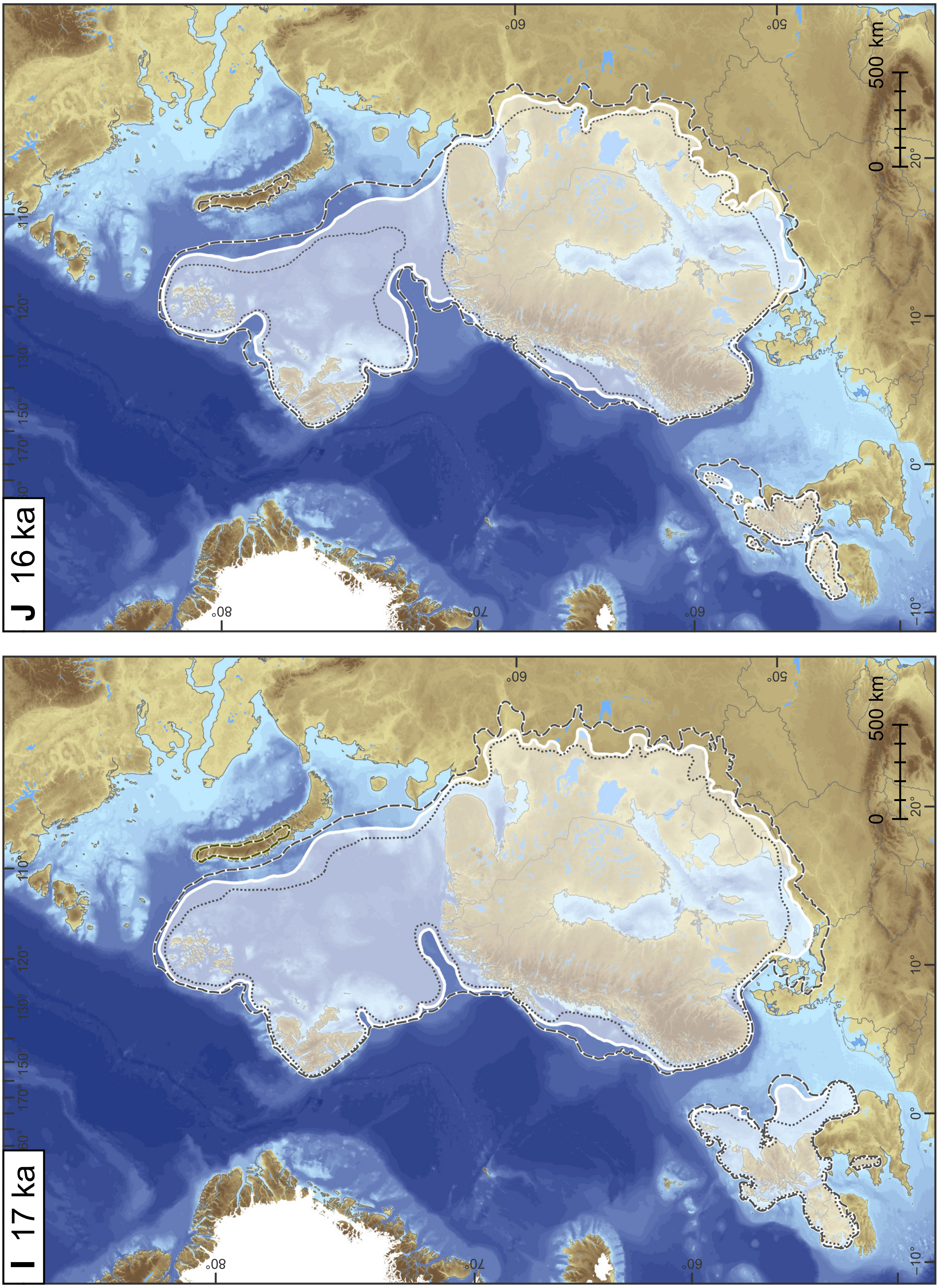

Fig. 6. (continued).

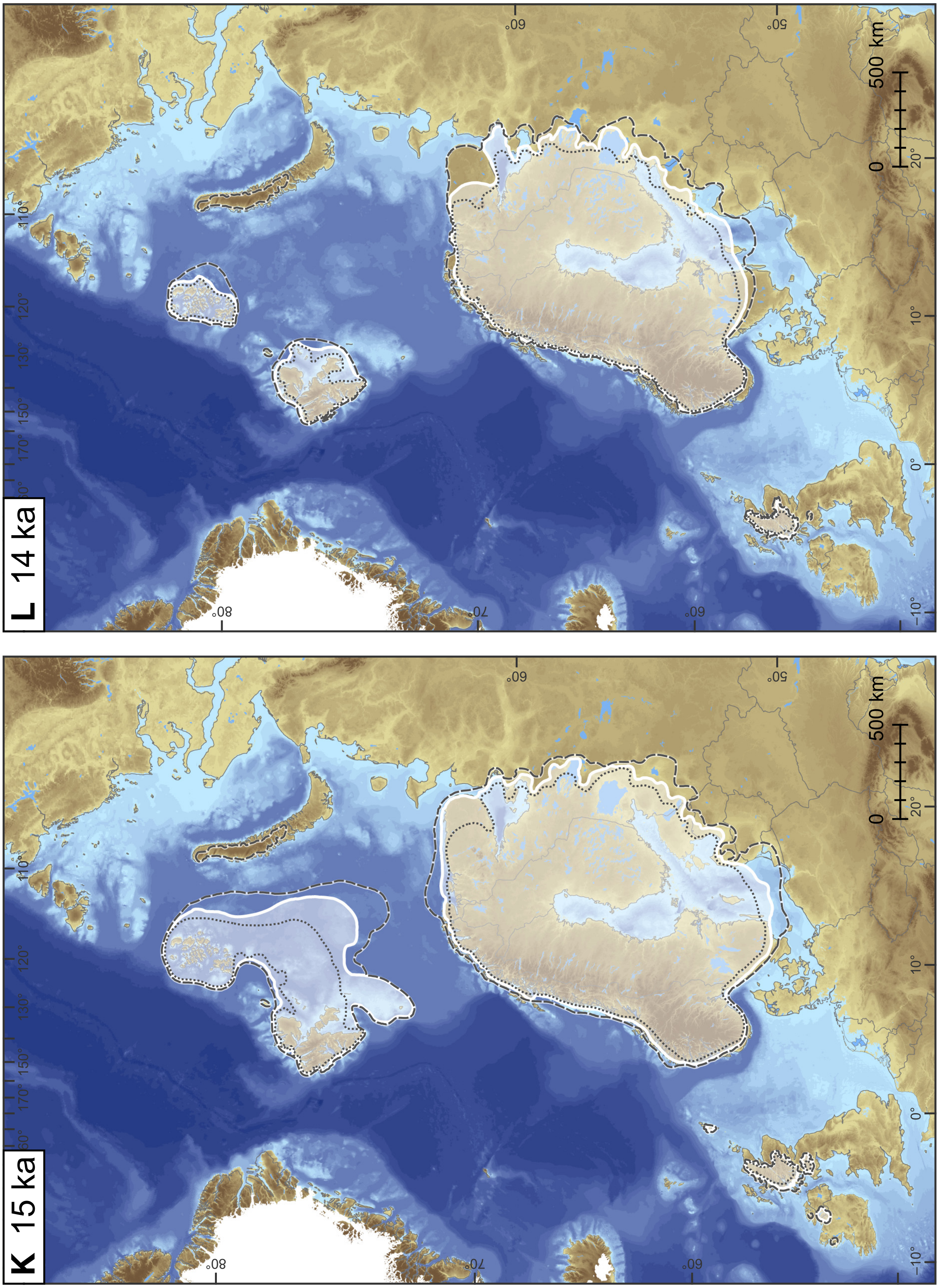

Fig. 6. (continued).

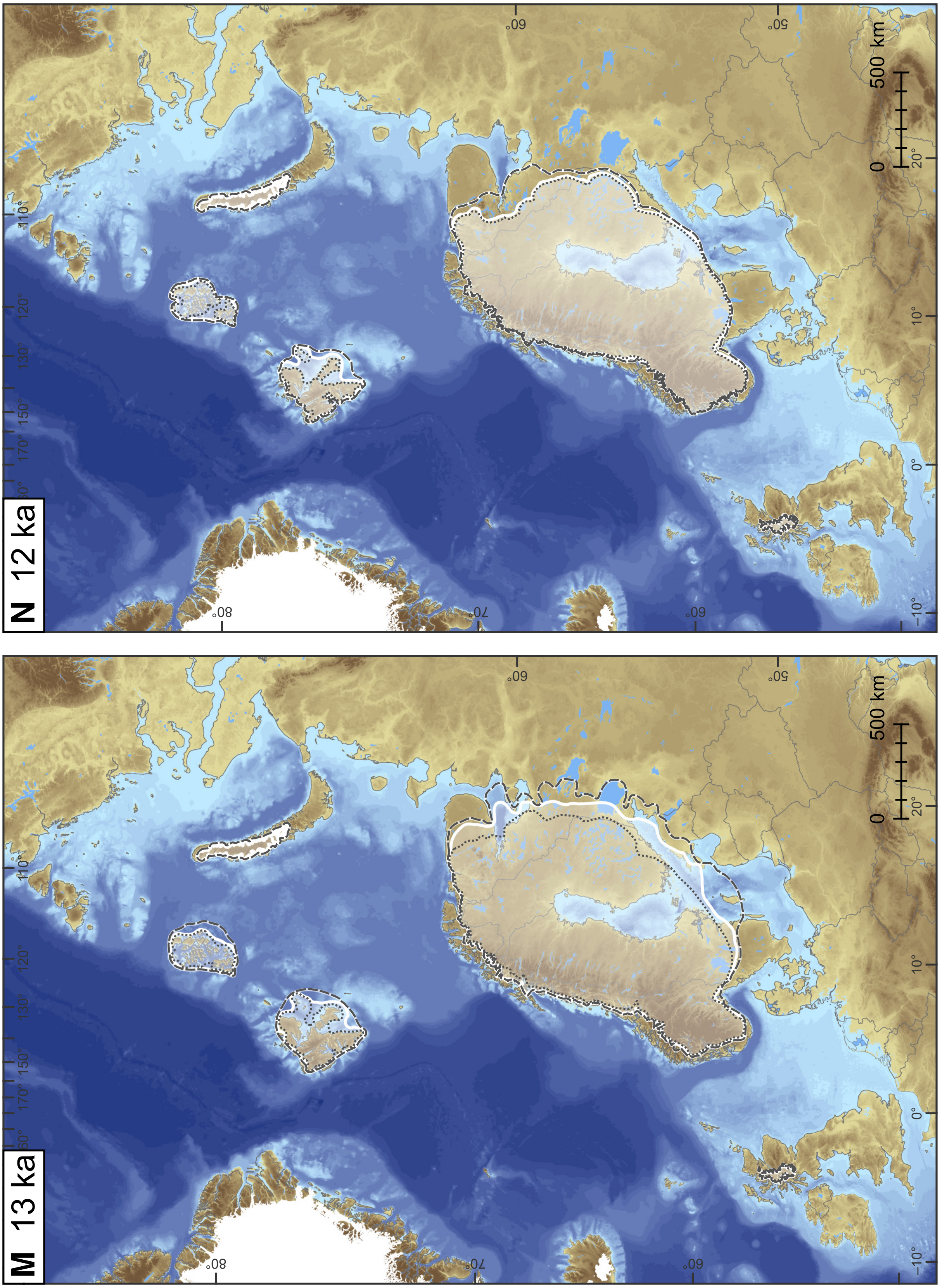

Fig. 6. (continued).

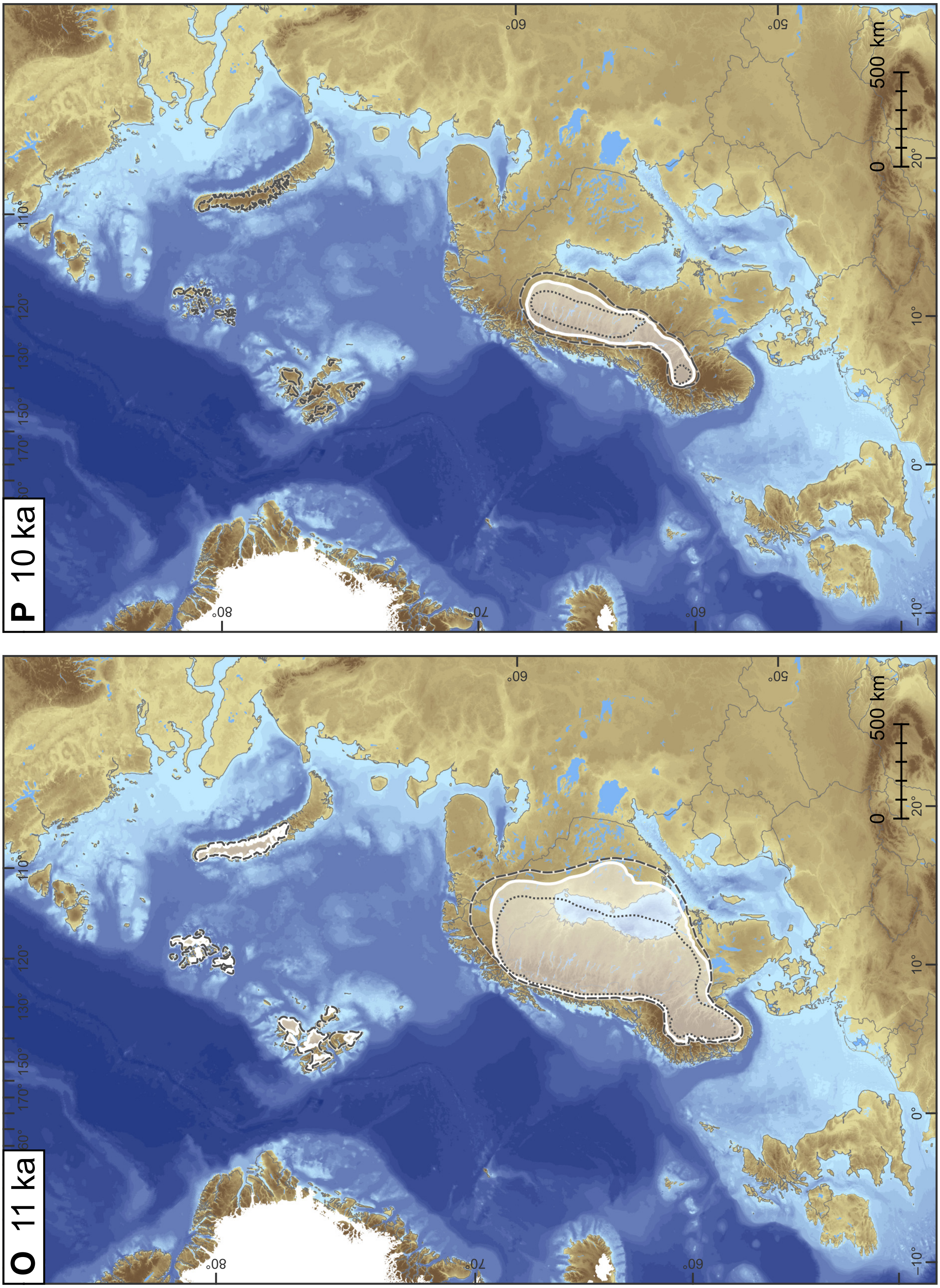

Fig. 6. (continued).

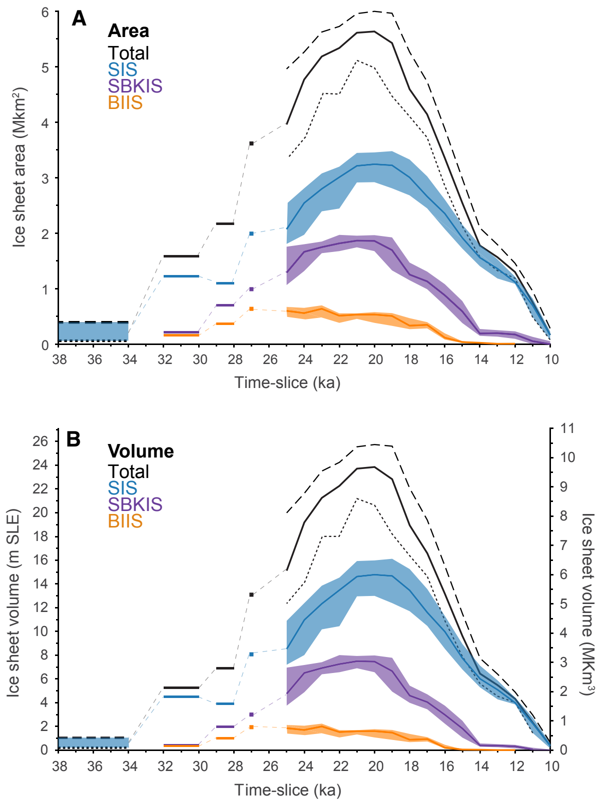

Fig. 7. Area (A) and volume (B) evolution of the Eurasian ice sheets *c.* 38 to 10 ka. From 25 to 10 ka we have drawn three continuous curves for the most-credible, maximum and minimum lines, respectively. For the more uncertain pre-25 ka period only one best estimate is shown derived from the areas depicted in Fig. 5. Individual ice-sheet volume was estimated in km^3 based on the ice-sheet area as shown in Figs 5 and 6 and converted to m SLE (see Table S5 and Methods for details). Contiguous ice-sheet complexes were split into individual ice sheets along the boundaries shown in Fig. 1. Note that values for the SBKIS between 25 and 15 ka likely overestimate the contribution of this ice sheet to global sea level by a maximum of ~1 m, as most of the ice sheet was grounded (~210 m) below present-day sea level during this time period.

the older part of the record is translated into differences of up to 2 m SLE between maximum and minimum lines for time-slices older than 19 ka (Fig. 7).

Discussion

First we discuss the major characteristics of each time-slice map, with a focus on locations where there are large uncertainties and the timing of key events. Note that we do not cite here all of the supporting data behind each line placement. All references are cited in the accompanying DATED-1 database (Table S1) and listed in the Supporting Information (Data S1). Second we describe in detail two of the most uncertain locations.

Pre-25 ka time-slice reconstructions

The SIS that existed during MIS 4 had probably almost entirely melted by the early part of MIS 3 (60–45 ka BP) (Wohlfarth 2010). Subsequently the SIS re-grew, passing the coast of western Norway at the time of the Laschamp palaeomagnetic excursion (*c.* 41 ka BP) (Valen *et al.* 1995; Mangerud *et al.* 2010). This glacial advance was followed by ice retreat during the milder Ålesund Interstadial (38–34 ka). Less is known about the spatial extent of the BIIS and SBKIS during this time. In this first version (DATED-1), we present only four time-slice maps for the period before 25 ka based on ~1800 dates, of which ~1500 are >30 ka and predominantly derived using luminescence and radiocarbon methods. Considering that samples older than 25 ka have often provided erroneous radiocarbon ages, that the typical error bounds of luminescence dating are large (±1000s of years) and that the potential for short-lived oscillations of the ice margin during build-up is high (Houmark-Nielsen 2010), all pre-25 ka lines should be regarded with some caution.

38–34 ka. – We present two suggestions for the SIS ice extent during the Ålesund Interstadial, dated to 38–34 cal. ka BP. There are over 40 (mainly AMS) radiocarbon dates from bones and molluscs from the type-site at Skjonghelleren in western Norway (DATED-1, Site 1240), and ages are confirmed by bracketing palaeomagnetic (Laschamp and Mono Lake) excursions (Mangerud *et al.* 2003, 2010). Finds of reindeer antlers indicate that at least a wide coastal area was ice-free during this period (Sites 1236, 1244; Valen *et al.* 1996). The Sandnes Interstadial identified from exposed shallow marine sediments on the southwest coast of Norway is correlated with the Ålesund Interstadial (Raunholm *et al.* 2004). Several bulk-sample radiocarbon ages from inland Norway have given Ålesund Interstadial ages (Sites 1124, 1135-6, 1205, 1269, 1278, 1302, 1304, 1307, 1314, 1316, 1318, 1335, 1359-63, 1370-1, 1374, 1382, 1384, 1394, 1418, 1437; Thoresen & Bergersen 1983; Olsen *et al.* 2001; Wohlfarth 2010), but for most samples the organic content is well below 1% (Olsen *et al.* 2001) and the samples are therefore vulnerable to contamination and reworking of older organic matter. Although some of these ages may be correct, most are too uncertain to prove ice-free conditions throughout Scandinavia during this interstadial. Furthermore, several of these samples yielded conflicting ages. The most reliable basis for asserting ice-free conditions extending inland during the Ålesund Interstadial is from an AMS date from terrestrial plant macrofossils (34.7 ka BP; Site 1205, DATED-ID 2380) at Djupdalsbekken in central Norway (Paus *et al.* 2011). If correct, these data imply that the SIS was small and restricted to the high mountain areas (e.g. Arnold *et al.* 2002; Olsen *et al.* 2002; Vorren & Mangerud 2008; Lambeck *et al.* 2010; Wohlfarth 2010; Mangerud *et al.* 2011). However, we do not consider such a major reduction of the ice sheet to be well supported by the existing observations, and we therefore present two alternative scenarios; a ‘minimum’ version where ice is restricted to the highest Scandinavian mountains and a ‘maximum’ reconstruction depicting a more extensive ice sheet. In both versions the west coast of Norway and most lowland areas of Sweden and Finland were ice free. The proto-BIIS and SBKIS are not depicted in our reconstruction. Ice-rafted debris flux to the west of Scotland indicates that the BIIS was large enough to produce icebergs at times during MIS 3 (Hibbert *et al.* 2010), but the precise limits of the early BIIS are poorly constrained for this time period. After initiation around 35–32 ka, the BIIS was likely small until *c.* 30 ka based on the available terrestrial radiocarbon chronology (Hall *et al.* 2003; Brown *et al.* 2007). On Svalbard, it has been calculated from amino acid racemization that the ice-covered area was not larger than present-day conditions during MIS 3 (~50–30 ka) and relative sea levels were lower than present (Mangerud *et al.* 1992, 1998), a view that seems generally accepted (e.g. Ingólfsson & Landvik 2013).

32–30 ka. – We correlate evidence for ice advance across the Norwegian coastline at Ålesund after 34 ka (Mangerud *et al.* 2010) with a documented short-lived advance of ice over eastern Denmark dated to between 34 and 30 ka, the Klintholm Ice Stream (Houmark-Nielsen & Kjær 2003; Houmark-Nielsen 2010). The northern and eastern margins of the SIS are highly uncertain. The few available constraining dates suggest ice advance across northern Sweden and Finland after *c.* 34 ka (Sites 1052, 1696, 1703, 1708, 2171, 2176, 2180; Korpela 1969; Kujansuu 1975; Donner *et al.* 1979; Hirvas & Kujansuu 1979; Lagerbäck & Robertsson 1988) but in Finnmark sand and silt below till has been OSL dated to 26±3 ka (Site 1493), suggesting that the northernmost tip of Norway may have been ice free at this time (Olsen *et al.* 1996). Dates from central and southern Finland indicate ice-free conditions until after *c.* 33–27 ka (Sites 2133, 2154, 2158-9; Ukkonen *et al.* 1999). An ice-margin position west of the Gulf of Bothnia is incompatible with ice advance into eastern Denmark (Klintholm) and evidence for ice incursion into northern Poland between 30 and 29 ka (Sites 1801, 1807-8, 1814, 1816; Wysota *et al.* 2002, 2009). Therefore, we draw a dashed line running south of the Baltic Sea, and although we think it likely that this southern expansion was matched by ice growth to the east we keep the eastern SIS margin along the Finnish coastline. Marine cores record ice-rafted debris delivery to the continental shelf between Franz Josef Land and Svalbard 34–16 ka (Site 225; Knies *et al.* 2001), and so we draw tentative margins centred over Svalbard and Franz Josef Land extending beyond the present-day coastline. In support of this, a shell contained within till has been dated to 32.5 ka on Danskøya, NW Spitsbergen (Site 2443; Salvigsen 1977; Landvik *et al.* 1998). A small ice cap is depicted centred on Novaya Zemlya slightly larger than the present-day ice cover, but not extending beyond sites with shells radiocarbon dated to 34–30 ka along the coastline (Sites 2345-2366; Forman *et al.* 1999; Mangerud *et al.* 2008a). A small ice cap over Scotland is tentatively depicted after Hughes *et al.* (2014).

29–28 ka. – We assume continued growth of the BIIS following evidence for increased ice-rafted debris delivery to the Rosemary Bank and Barra-Donegal Fan at 29 ka (Scourse *et al.* 2009) and ice at the western continental-shelf edge 28–27 ka (Sites 748–754; Everest *et al.* 2013). We use flow-pattern configurations from Hughes *et al.* (2014) and Greenwood & Clark (2009b) to assist in defining the ice-margin position in this region. The southern SIS margin is shown retreated from the previous time-slice in southern Denmark (Krohn *et al.* 2009; Larsen *et al.* 2009b), southern Sweden (Houmark-Nielsen 2003; Houmark-Nielsen & Kjær 2003) and northern Poland (Wysota *et al.* 2009) largely based on the Danish stratigraphic record (Houmark-Nielsen 2010). Early ice advance into northern Poland followed by retreat is supported by exposure ages of 27–28 ka from erratics located in the Suwałki Lakeland, which suggest that nunataks may have existed during later ice advances in this region (Dzierżek & Zreda 2007). Close to Ålesund the western SIS margin is drawn inside of the Norwegian coastline (Mangerud *et al.* 2010) but elsewhere the western SIS margin is tentatively depicted close to the present-day coastline, and we keep the eastern SIS margin along the Finnish coastline. Although it is possible that ice had retreated west of the Gulf of Bothnia into Sweden, thus satisfying mammoth bone finds dated to 28.5 ka along the Finnish coastline (Site 2134) and molars found in glacifluvial sediments in central Sweden dated to 30 and 29 ka (Sites 1682, 1678; Ukkonen *et al.* 2007, 2011).

27 ka. – The BIIS was at its maximum shelf-edge position in the west and north and we depict confluent ice cover in the North Sea between the BIIS and SIS (Wilson *et al.* 2002; Bradwell *et al.* 2008b; Sejrup *et al.* 2009; Clark *et al.* 2012). We extend the western margin of the SIS to a shelf-edge position, although north of the Norwegian Channel this is tentative due to a lack of dates from the Norwegian shelf (Dahlgren & Vorren 2003; Johnsen *et al.* 2012) but is supported by marine core evidence for ice-proximal conditions close to the shelf edge *c.* 27.6 ka (Site 50; Rørvik *et al.* 2010) and a date for ice advance after 27.8 ka south of Lofoten (Site 44; Knies *et al.* 2001). The southern limit in the North Sea is tentatively assigned to the Dogger Bank following the southernmost extent of tunnel valleys attributed to be of Weichselian age (after Graham *et al.* 2011). This is ~40 km further north than the limit shown in Clark *et al.* (2012) and Sejrup *et al.* (2009). Across Denmark the defined extent of the Kattegatt Fm is used, although 27 ka is the youngest possible age assigned to this, probably short-lived, advance (Houmark-Nielsen 2003; Larsen *et al.* 2009a). Radiocarbon dates (from a compiled database supplied by Knut Kaiser; Sites 1871, 1875–6, 1880) imply that the Polish coast was ice free until after *c.* 26 ka, supporting full retreat if we accept ice advance into northern Poland 32–30 ka (Wysota *et al.* 2009). The youngest advance dates preceding the LGM from Estonia, Latvia and Lithuania are varied but collectively indicate ice advance to this region after *c.* 26 ka (Saks *et al.* 2012; Lasberg & Kalm 2013). We therefore place the southeastern margin of the SIS north of the Baltic coast. Dates considered reliable from mammoth bones located beneath till imply ice advance across Finland after *c.* 27–26 ka (Sites 2154, 2133; Ukkonen *et al.* 1999). Although, we treat ages derived from bones with caution as many lack stratigraphical information and may be anomalously young due to contamination or otherwise erroneous (Wohlfarth 2010). In some cases it is now recognized that insufficient pretreatment may explain anomalous bone ages (Ukkonen *et al.* 2011), as has been demonstrated in Britain where bone samples re-dated using ultrafiltration techniques resulted in older ages (Jacobi *et al.* 2009). The southwestern part of the Barents Sea remained ice free based on the youngest age for shell fragments incorporated within till and glacially reworked sediments from cores within Bjørnøyrenna dated to 26±1 ka (Elverhøi *et al.* 1993) and 25.9±0.6 ka (Hald *et al.* 1990) (Sites 193, 183, 187).

25–14 ka time-slice reconstructions

For many sectors of the EurIS the detailed local geographic pattern of retreat, i.e. the configuration and orientation of the ice margin during deglaciation, is well known from end moraines and/or the direction of glacial striae and lineations (e.g. Sollid *et al.* 1973; Rainio *et al.* 1995). In addition, the geometry of ice divides during ice-sheet evolution and the general pattern of ice-sheet advance is known in outline in areas where generations of flow-patterns have been mapped and their relative age has been determined (e.g. Kleman *et al.* 1997; Greenwood & Clark 2009b; Hughes *et al.* 2014). In some terrestrial areas the main geomorphic features and patterns have been known for a century (Flint 1971; Andersen 1981; Boulton *et al.* 1985, 2001) and in recent years similar well-preserved and highly detailed sea-floor observations have been added (Ottesen *et al.* 2002; Dowdeswell *et al.* 2007). However, the lateral correlation of synchronous ice-margin positions is in most cases far from unambiguous and the degree of uncertainty when attempting to correlate between regions is high. Even morphologically distinct moraines are now recognized as laterally time-transgressive (e.g. Böse *et al.* 2012). We do not attempt to show all documented re-advance positions during retreat as many are likely to occur below our 1000-year resolution and instead use the known geographic pattern of moraines to construct the ice-sheet outlines.

For example, multiple moraines mark the ultimate limit and indicate the pattern of retreat of the southern and southeastern margin of the SIS across the European and Russian plains (e.g. Kalm 2012) and, supported by glacial lineations, indicate a lobate ice margin influenced by competing ice streams (Punkari 1997). Both the arrangement of moraines and existing dates suggest that retreat was episodic and/or that oscillations of the ice front may have occurred. In recent years a large number of TCN exposure ages has been added to the existing radiocarbon and OSL chronology of the southeastern SIS margin (Fig. 3; e.g. Rinterknecht *et al.* 2006). Yet, the timing of ice advance and retreat, and correlation of moraines, remains unstraightforward with many conflicting dates (Lasberg & Kalm 2013). The thick and unstable deposits along this margin combined with permafrost conditions persisting until the Holocene (Bitinas 2012) mean that the likelihood of post-exposure rotation and upfreezing of boulders along this southeastern margin of the SIS is high, both effects resulting in too-young ages (Heyman *et al.* 2011; Houmark-Nielsen *et al.* 2012; Lüthgens & Böse 2012), in addition to too-old ages arising from isotopic inheritance. Available luminescence ages from this region exhibit considerable scatter and large errors, with many samples giving older ages than their stratigraphic position would suggest, and many are considered unreliable owing to incomplete bleaching (Raukas 2004; Raukas & Stankowski 2005; Raukas *et al.* 2010). Further, some radiocarbon ages from Estonia are older than regional correlations suggest (Lasberg & Kalm 2013). The result is that several conflicting morphological correlations of the moraine systems that have been proposed (e.g. Kalm 2006, 2012; Marks 2011, 2012; Zelčs *et al.* 2011; Bitinas 2012) are difficult to resolve.

25 ka. – Our maximum line shows the SBKIS, SIS and BIIS connected as an integrated ice sheet, but the minimum and most-credible lines keep the SBKIS and SIS separated until 23 and 24 ka, respectively, reflecting the scarcity of dates within the area of coalescence of these two ice sheets (note ~500 km discrepancy between maximum and minimum lines in this time-slice for this sector). In contrast, a radiocarbon date within glacimarine sediments resting above till from the central part of the northern North Sea (Sejrup *et al.* 1994) suggests an opening between the BIIS and SIS already by 25 ka (Site 126, DATED-ID 1193). Our minimum line follows a scenario of complete break-up of ice cover over the North Sea and our most-credible line restricts break-up to the opening of an embayment in the northern North Sea (after Bradwell *et al.* 2008b; Clark *et al.* 2012). However, we consider that the persistence of a narrow embayment in the northern North Sea for over 5000 years is glaciologically implausible and therefore maintain full ice cover over the North Sea in our maximum lines until 23 ka. Ice is shown close to the shelf edge along the western SIS margin but rapid fluctuations of up to 30–40 km may have occurred on the Norwegian shelf (Dahlgren & Vorren 2003; Brendryen *et al.* 2015) and the BIIS may have started to retreat from the shelf edge (Clark *et al.* 2012; Everest *et al.* 2013). Bulk basal glacilacustrine sediments from Æråsvatn (Site 1465) on the northern tip of Andøya, only ~20 km from the Norwegian shelf edge, have returned radiocarbon ages as old as 26.5 ka (Alm 1993). However, in line with more recent results from this area we restrict deglaciation of northern Andøya to our minimum line only at 25 ka (after Vorren *et al.* 2013). Moraines and marine core data indicate that the ice-sheet margin was located near the shelf edge (Egga I) before 24 ka (Vorren *et al.* 2015). The highest mountain summits (300–400 m a.s.l.) on northern Andøya may either have remained as nunataks or were covered by non-erosive cold-based ice during the peak of the last glaciation (Sites 1456, 1458–9, 1462, 1466–7; Nesje *et al.* 2007).

Ice had retreated to the north of Denmark following the Kattegatt advance (Houmark-Nielsen 2003; Kjær *et al.* 2006b) and ice likely re-advanced across southern Sweden and the southwestern Baltic Sea after *c.* 25 ka (Kramarska 1998; Kjær *et al.* 2006b). This is supported by dates indicating advance across Poland after 25–29 ka (Pazdur *et al.* 1983), western Latvia after *c.* 26 ka (Saks *et al.* 2012; Lasberg & Kalm 2013) and central and southern Lithuania after *c.* 25 ka (Lasberg & Kalm 2013). The most-credible line sits north of the Estonian coastline to accommodate the youngest obtained OSL ages from kame and delta sediments dated to 21±2.5 and 23±6 ka (Sites 2077, 2085; Raukas 2004), although these dates are described as not being in stratigraphical order and the large error bounds on these dates renders them almost useless for constraining our reconstruction at a 1000-year resolution. The timing of ice advance into Russia is imprecisely dated and we maintain a large distance between minimum and maximum lines in this region.

Ice masses over Svalbard, Novaya Zemlya and Franz Josef Land are shown as an integrated SBKIS, although the precise eastern and southern boundaries of this ice mass are highly uncertain due to the low density of chronological control, especially over the central Barents Sea. The shelf edge remains as a limiting boundary for ice-sheet growth to the west and so all lines are placed within ~30 km of the shelf break.

24 ka. – We draw the maximum line of the BIIS depicting expansion of ice into the Irish Sea as a precursor to the advance of the Irish Sea Ice Stream to the Scilly Isles occurring *c.* 23 ka (Ó Cofaigh & Evans 2007). There is some evidence for retreat followed by a re-advance of ice over northern Andøya 24–23 ka (Vorren *et al.* 1988, 2013; Vorren & Plassen 2002), possibly reflecting fluctuations of the western SIS margin as it sits close to the shelf edge (Rørvik *et al.* 2010; Brendryen *et al.* 2015). Lines for the eastern SIS are expanded out towards the maximum limit from the previous time-slice but remain far apart (up to 450 km), reflecting poor dating control on the timing of ice advance across the European and Russian plains (Fig. 3). We follow the interpretation of Lasberg & Kalm (2013) for an earlier ice maximum (*c.* 24.4–19.6 ka) in the southwestern compared with the northeastern European Plain (*c.* 19.4–17.8 ka; see later time-slices). As at 25 ka the minimum line is drawn to accommodate a small number of 'ice-free' dates from the Polish (Kaiser database) and Estonian (Raukas 2004) coastlines although many OSL dates from the southeastern Baltic are regarded as possibly erroneous and have large error bounds (Raukas & Stankowski 2005; Raukas *et al.* 2010), and we question the reliability of these ages in the context of surrounding data. The maximum line for the southern SIS is placed close to the Brandenburg and Leszno moraine positions in Germany and western Poland, respectively (Pazdur *et al.* 1983; Lüthgens & Böse 2011; Böse *et al.* 2012; Marks 2012), but evidence suggests that the ice front did not advance into Denmark until the following stage (Houmark-Nielsen & Kjær 2003; Houmark-Nielsen 2010).

23 ka. – A short-lived advance of the Irish Sea Ice Stream of the BIIS to the maximum position over the Scilly Isles is placed in this stage (after Clark *et al.* 2012; Ó Cofaigh *et al.* 2012). Dates from trough-mouth fans west of Svalbard and the timing of offshore ice-rafted debris pulses indicate an ice margin close to the shelf edge for the northern and western SBKIS (Andersen *et al.* 1996; Landvik *et al.* 1998; Kleiber *et al.* 2000) and SIS west of the Lofoten Islands (Rørvik *et al.* 2010). After 23.5–22.4 ka lake sedimentation is continuous in Øvre Æråsvatn (Site 1463, 43 m a.s.l.) and Endlevatn (Site 1464, 36 m a.s.l.) on Andøya, indicating that the northern tip of the island was finally deglaciated at the latest by 22 ka (Vorren *et al.* 1988, 2013, 2015; Alm 1993). Ice started to advance again into northern Denmark, the maximum position is placed along the Main Stationary Line, and the minimum encroaching over the northern tip based on the timing for the Mid-Danish till *c.* 23–21 ka (Larsen *et al.* 2009b). Maximum and most-credible lines are placed at, or close to, the maximum limit in Germany and Poland and uncertainty in the precise timing of ice expansion increases from west to east, as in the previous time-slice. We no longer keep the minimum line north of the Estonian coastline, thus using the oldest error bound for the constraining OSL ages dated to 21±2.5 ka (Raukas 2004). There exist no dates on the timing of ice advance into the Kara Sea towards Taimyr; however, we tentatively place the ice margin in this time-slice at the maximum ice-extent position (Polyak *et al.* 2008).

22 ka. – In the Irish Sea the ice front is stepped back reflecting rapid retreat of the Irish Sea Ice Stream (e.g. Chiverrell *et al.* 2013). We maintain a connection between the SIS and BIIS in the southern North Sea, although the persistence and existence of the postulated ice dome that this requires remains unconfirmed. In the northern North Sea the postulated embayment is widened to represent the uncertain distance of retreat eastward before the documented Tampen re-advance (22–19 ka) (Sejrup *et al.* 1994, 2005). Minimum and most-credible lines are placed at the Main Stationary Line in Denmark (Houmark-Nielsen 2004, 2008; Larsen *et al.* 2009b). The maximum and most-credible lines are close to the maximum position in northeast Poland, Lithuania and northwest Belarus (Lasberg & Kalm 2013) with only the minimum line kept west of central Latvia (Raukas *et al.* 2010) and southeastern Estonia (Kalm 2005). Separation between the lines increases towards the east, reflecting a low density of dates and large errors on available OSL dates (e.g. Raukas 2004; Kalm 2005). The margins of the SBKIS remain similar to the previous stage with the exception of the maximum line where a lobe of ice extends out to the northeast impinging onto the Taimyr Peninsula. This is based on two shell dates from melt-out till indicating ice advance onto the Peninsula from the west after 23 ka (Site 2342; Alexanderson *et al.* 2001); see later discussion. We follow Polyak *et al.* (2008) for the shape of this lobe, which is reduced from that shown in Svendsen *et al.* (2004).

The western minimum margin of the SIS is shown inland of the present-day coastline. In central Norway the line is ~350 km east of the maximum and most-credible lines, which remain close to the Norwegian shelf edge. This minimum line is to accommodate evidence mainly from bulk radiocarbon dates but also OSL ages for a substantial retreat of the SIS during MIS 2 (Olsen & Hammer 2005; Johnsen *et al.* 2012; Kolstrup & Olsen 2012). This evidence clearly is in conflict and difficult to resolve with some marine evidence that places the western SIS margin advanced on the shelf (Elliot *et al.* 2001; Dahlgren & Vorren 2003; Rørvik *et al.* 2010) and the southern and eastern SIS margins close to their maximum extent at this time (Larsen *et al.* 2006; Lasberg & Kalm 2013). Radiocarbon dates in support of this retreat are predominantly from bulk samples (the majority of which we rate as QC = 3 and therefore ignore) and the available OSL ages differ by as much as 4000 years depending upon the water saturation history of the samples. The available dating is imprecise (mean 22.3±1.7 ka) and the event, if it existed, is regarded as short-lived (Johnsen *et al.* 2012). On the balance of evidence we consider such a dramatic retreat of the western SIS margin, up to 150 km inland of the Norwegian coastline, at a time when the eastern SIS margin was close to the ultimate limit unlikely, but not impossible. Therefore, we accommodate it in the minimum reconstruction for this single time-slice only; the line is drawn within the limit of dates supporting the retreat that we give a QC rating of 2 or 1 (Sites 983, 1269, 1271-3, 1276–8, 1285, 1305, 1311–3).

21 ka. – In the absence of evidence to the contrary we make small changes for most of the ice-sheet sectors between 22 and 21 ka. We do not, in this first version of DATED, reconstruct surface elevation of the ice sheets but, based on exposure dating of mountain summits, by 21 ka the BIIS had started to thin (Ballantyne & Stone 2015). Lowering of the SBKIS surface in northern and western Svalbard may have commenced even earlier (~26±4 ka, Hormes *et al.* 2013). The SIS margin is shown expanded in the maximum and most-credible lines into the northern North Sea from the previous stage (Tampen Re-advance 22–19 ka; Rokoengen *et al.* 1982; Rise & Rokoengen 1984; Sejrup *et al.* 2015). Across Germany there is uncertainty in the timing of retreat from the maximum limit, with a wide range of ages presented for mapped and correlated moraines (Lüthgens *et al.* 2010; Lüthgens & Böse 2011); we place all lines between the Frankfurt and Pomeranian limits in Germany and western Poland. All lines are close to the ultimate limit across northeastern Poland, Lithuania and northwest Belarus (Lasberg & Kalm 2013). The ultimate MIS 2 ice-sheet limit in mainland Russia was reached after 22 ka based primarily on OSL dates (Kjær *et al.* 2006a) and we place the maximum line at (and step the minimum and most-credible towards) the ultimate limit in the Russian Plain based on ice-dammed lake sedimentation dated to 21–20.9 ka (Site 2225; Lyså *et al.* 2001, 2011). We use the ultimate limit for this sector as mapped by Larsen *et al.* (2014), which is slightly more extensive than shown in Svendsen *et al.* (2004).

20 ka. – Available data show that the BIIS was retreating at almost all margins at this time (Clark *et al.* 2012 and references therein). In addition, high-altitude TCN ages and flow-pattern evidence indicate that retreat was preceded by lowering of the ice-sheet surface (Ballantyne *et al.* 2006; Glasser *et al.* 2012;

Hughes *et al.* 2014). Glacigenic debris flow sediments from the North Sea Fan (Sites 145–7) indicate that the calving front of the Norwegian Channel Ice Stream was close to the channel mouth until *c.* 19 ka (King *et al.* 1998) and had retreated south of the Troll core (Site 132) at 60.6° N by 18.5 ka (Sejrup *et al.* 1994). However, recently published TCN dates for final deglaciation of the islands of Karmøy and Utsira, located ~300 km up-flow at ~59.3° N, suggest that the ice stream had retreated all the way back to these islands by *c.* 20 ka (Svendsen *et al.* 2015) but these new dates are not included in the DATED-1 database because of our 1 January 2013 census date. The timing of retreat from the Norwegian shelf is poorly constrained; we therefore depict the minimum line along the mid-shelf but keep the maximum and most-credible lines close to the shelf edge in this time-slice. Retreat from the Main Stationary Line (Denmark) commenced, indicated by proglacial sediments dated to 20–19 ka (Larsen *et al.* 2009b). Dates constraining the timing of the Pomeranian limit across Germany and Poland return a large spread of ages (Lüthgens & Böse 2011); sandur deposition at this margin in northeast Germany is dated to 21.7–18.1 ka using OSL (Site 1759), suggesting an older age than implied by some TCN (*c.* 13–21 ka) and radiocarbon (*c.* 16–19 ka) ages for this margin (Rinterknecht *et al.* 2005, 2012; Houmark-Nielsen *et al.* 2006; Heine *et al.* 2009; Marks 2012). There is no equivocal evidence for significant retreat followed by a re-advance to the Pomeranian position and we keep a separation between the lines to reflect this uncertainty. The range of returned ages strongly supports the interpretation of the 'Pomeranian moraine' as a suite of time-transgressive features. All lines remain close to the ultimate limit on the Russian Plain, but separation is maintained between the lines owing to the large error bounds on the available OSL chronology (Demidov *et al.* 2006). It is probable that the lobes of ice that extended this far east had a very low surface profile (Larsen *et al.* 2014).

19 ka. – By 19 ka the Irish Sea was deglaciated (Telfer *et al.* 2009). The Norwegian Channel Ice Stream probably started to retreat from the shelf break west of Norway *c.* 19 ka (King *et al.* 1998) or a little earlier (see later discussion) and we step the margin in the channel back from the shelf edge. Sectors of the southern SIS margin appear to have experienced minor (10s km) oscillations of the ice front as the margin retreated back from the ultimate terrestrial limit; ice re-advanced over southern Denmark (e.g. Young Baltic advance; Kjær *et al.* 2003; Larsen *et al.* 2009b). We follow Lasberg & Kalm (2013) and place the most-credible and maximum ice margins at the ultimate limit in the southeastern European Plain. We disregard two radiocarbon dates from mammoth bones found in southern Sweden that give ages of *c.* 19 ka (Site 2134; Ukkonen *et al.* 1999), as the balance of evidence indicates they are likely to be erroneous (Ukkonen *et al.* 2011) although not rejected following our quality control assessment. Using the 'Arctic' production rate some 'deglacial' ^{10}Be exposure ages from boulders and streamlined bedrock from the island of Bornholm, south of Sweden (Sites 789-90, 794-5, 799-800, 805-6; Houmark-Nielsen *et al.* 2012) give ages of 19.8–17.1 ka (two ages using ^{36}Cl of 21–23 ka are assumed to overestimate the true age). Similarly some boulders (Sites 1622, 1612, 1610, 1593, 1578–9) from the Halland Coastal Moraines, southwestern Sweden, return seemingly anomalously old ages (15–19 ka; Larsen *et al.* 2012). The older range of these dates appears to conflict with evidence for ice re-advance over southern Denmark and is older than both dates that imply deglaciation of the southwestern Baltic Sea *c.* 17 ka (Kramarska 1998) and the youngest age estimates for the Pomeranian ice margin over Germany (Lüthgens *et al.* 2011). Intriguingly, the apparently overestimated TCN ages from the Halland Coastal Moraines correspond to a handful of shells radiocarbon dated to *c.* 19 ka previously considered to be contaminated with old carbon (Sites 1592, 1595; Påsse 1992). We draw the minimum line only north of Bornholm in the following time-slice and step the margin back towards the island here. Exposure ages indicate deglaciation of northern Germany and Poland between 17.2–13.6 and 20.7–12.4 ka, respectively (Rinterknecht *et al.* 2006, 2012). This large spread of ages probably reflects inheritance issues and postdepositional rotation of boulders in an unstable postglacial landscape incorporating dead-ice and mobile sediments (Lüthgens & Böse 2012). The SBKIS started to retreat from the western shelf edge (Elverhøi *et al.* 1995; Cadman 1996; Landvik *et al.* 1998; Rasmussen *et al.* 2007), and we depict deglaciation of Novaya Zemlya in our minimum reconstruction as a precursor to the following time-slice.

18 ka. – The SIS and BIIS are shown as fully separated in all but the maximum reconstruction. Based on the balance of available OSL dates constraining the Bobrovo till, the eastern margin of the SIS is at the maximum limit in our most-credible line, comprising a thin, highly lobate margin terminating into ice-dammed lakes (Demidov *et al.* 2006; Larsen *et al.* 2006, 2014; Lyså *et al.* 2011, 2014; Fredin *et al.* 2012). The timing of deglaciation on Novaya Zemlya is not well dated (see discussion below), but two radiocarbon dates (Sites 2356, 2346) from the southwestern coast suggest deglaciation occurring before *c.* 18 ka (Serebryanny *et al.* 1998). We show the SBKIS as retreated from Novaya Zemlya in all reconstructions, leaving a remnant ice cap in the maximum reconstruction only. The pattern of retreat is poorly constrained in the eastern Barents Sea and we maintain a separation between the lines here. We consider that the large but poorly dated 'Admirality Bank Moraines' are partly bedrock features (Gataullin & Polyak 1997) and are too big to have been formed during the most recent deglaciation, and so we ignored them (also omitted in a recent review by Jakobsson *et al.* 2014). Exposure ages from western Svalbard indicate lowering of the ice surface due to thinning after *c.* 18.5 ka (Site 2437; Landvik *et al.* 2013).

17 ka. – By 17 ka the BIIS was restricted to Ireland and Scotland, although the North Sea Lobe is depicted running down the eastern coastline of England (Eyles *et al.* 1994). In the northern North Sea we follow the Fladen 1 re-advance moraine dated to 17.5 ka by Sejrup *et al.* (2015) in our maximum line. The Skagerrak is deglaciated and all lines are close to the Halland Coastal Moraines along the southwest Swedish coast (Larsen *et al.* 2012). Over Denmark the maximum line follows the limit of the Bælthav Ice Stream incursion and it is known that the ice margin here terminated into proglacial lakes (Houmark-Nielsen & Kjær 2003). The SIS is depicted starting to retreat from the maximum limits across the Russian (Lunkka *et al.* 2001; Demidov *et al.* 2006) and Eastern European plains (Lasberg & Kalm 2013). Shells within till (Rokoengen & Frengstad 1999) and shelf moraines (Nygård *et al.* 2004) indicate fluctuations of the western SIS margin on the Norwegian shelf during retreat. The connection between the SIS and SBKIS is maintained, based on mapped ice-flow directions from the western Barents Sea (Bjarnadóttir *et al.* 2014). Several ice streams were in operation in the southern Barents Sea and around Svalbard. It is probable that the ice-sheet margin re-advanced multiple times during retreat and separation of the SBKIS and SIS (e.g. Winsborrow *et al.* 2010; Rüther *et al.* 2012; Bjarnadóttir *et al.* 2014). The timing of separation of these two ice sheets is poorly dated and we depict separation occurring across three time-slices 17–15 ka. The margin positions in the eastern Barents Sea remain speculative.

16 ka. – Moraines on the Norwegian shelf indicate that the western margin of the SIS oscillated during retreat from the Norwegian shelf, e.g. the Bremanger advance (<18–16 ka; Nygård *et al.* 2004; Sejrup *et al.* 2009), which has been correlated with a second ice advance into the northern North Sea by the BIIS (Fladen 2 dated to 16.2 ka; Sejrup *et al.* 2015). Here we follow Clark *et al.* (2012) and show the BIIS as discrete ice masses on Ireland, Highland Scotland and Shetland in the most-credible and minimum lines, and close to the Fladen 2 position in the maximum line only. In contrast, the southwestern SIS margin had retreated onshore at Jæren, southwestern Norway by 17–16 ka (Sites 903–4906; Knudsen 2006). All lines are placed close to the western Swedish coast based on dates constraining the Halland Coastal Moraines to between 17 and 16 ka (Lundqvist & Wohlfarth 2001; Larsen *et al.* 2012). This is supported by recent (post-DATED-1 census) ages for the Göteborg moraine <16 ka (Anjar *et al.* 2014). We use mapped margin positions (Saarnisto *et al.* 1995; Uścinowicz 1999; Saarnisto & Saarinen 2001; Demidov *et al.* 2004; Kalm 2012) to guide placement of the lines in the Baltic Sea and east of Poland. In northernmost Norway deglaciation of the coastal plateau above ~300 m is indicated by exposure dating (Sites 1501, 1504; Fjellanger *et al.* 2006). Although, marine evidence supports extensive ice remaining offshore north of Norway (Rüther *et al.* 2011) at this time, and basal lake radiocarbon dates support later deglaciation of northernmost Norway *c.* 14 ka (Sites 1507-9; Romundset *et al.* 2011). Only in our minimum reconstruction is the SBKIS separated from the SIS as the timing of separation is imprecisely defined from the current data. Seabed geomorphology demonstrates that separation of the SIS and SBKIS progressed as ice retreated along Bjørnøyrenna (Bjarnadóttir *et al.* 2014) and was accompanied by ice streaming along the northern Norwegian coast (Winsborrow *et al.* 2010). The pattern of retreat from the eastern Barents Sea is as yet undefined, although there is some indication of late-stage ice flow from an ice centre located close to the central bank of the Barents Sea (Bjarnadóttir *et al.* 2014).

15 ka. – A number of radiocarbon dates demonstrate that the SIS had largely retreated within the Norwegian coastline, and some of the highest peaks (over 900–1000 m) may have existed as nunataks after 16–15 ka (Goehring *et al.* 2008). The maximum extent of the eastern SIS follows the Haanja and Luga moraines in Russia (Demidov *et al.* 2004; Kalm 2012) and the North Lithuanian moraine (Kalm 2006, 2012). The minimum line follows the Sakla and Otepää moraine positions (Kalm 2012). The SIS and SBKIS are shown as separated in all three reconstructions. In the north the SBKIS retreated back towards the central Barents Sea, Svalbard and Franz Josef Land. Lines around Svalbard follow Klitgaard Kristensen *et al.* (2013) and Hogan *et al.* (2010) and the minimum line is drawn so that Bjørnøya is additionally deglaciated. Ice is depicted close to the western coastlines of Svalbard (Forman *et al.* 1987; Svendsen *et al.* 1992; Landvik *et al.* 1998) and Franz Josef Land (Forman *et al.* 1996; Lubinski *et al.* 1996, 2001; Landvik *et al.* 1998). Marine sedimentation commenced *c.* 15 ka (Polyak *et al.* 1995; Landvik *et al.* 1998; Sites 173, 175, 182) and after 14.4 ka (Rüther *et al.* 2012; Sites 189–192) in the eastern and western Barents Sea, respectively.

14 ka. – For the BIIS we use the limits of the Wester Ross re-advance moraines in western Scotland (Everest *et al.* 2006; Bradwell *et al.* 2008a; Ballantyne *et al.* 2009). The SIS is shown retreated from the entire western coast, from the northern tip of Norway (Romundset *et al.* 2011) to the southern tip of Sweden (Johnsen *et al.* 2009). We depict continued retreat of the eastern margin of the SIS, but note that the rate of retreat here is poorly constrained, and may have been more rapid, with local and regional re-advances of the ice margin (Kalm 2006). Lake Onega was deglaciated *c.* 14 ka based on varve counts (Saarnisto & Saarinen 2001). The SBKIS had separated into two over Svalbard and Franz Josef Land, and the Barents Sea is shown as deglaciated, although note that there are very few constraining dates (Landvik *et al.* 1998, 2005; Klitgaard Kristensen *et al.* 2013).

Younger Dryas time-slices 13–12 ka

The SIS at the end of the Younger Dryas (~1.6 Mkm^3 or 4 m SLE) was comparable in volume to present-day estimates for the Greenland Ice Sheet (~2.85 Mkm^3 or 7 m SLE). Moraines attributed to the Younger Dryas cold period (12.7–11.5 ka; Lohne *et al.* 2013) have been mapped almost continuously around Scandinavia and provide the means to reconstruct precisely the marginal extent of the SIS during this time period (Fig. 8; Andersen *et al.* 1995b). Across Norway moraines have been established as documenting a re-advance of the SIS although in some areas the moraines were formed at the start of the Younger Dryas and in other areas towards the end of the stadial; i.e. up to 1200 years apart (Andersen *et al.* 1995a,b). Additionally, lateral moraines are found along many fjords and valleys in western Norway, providing opportunities to reconstruct the ice thickness for this time period. Across Scotland numerous moraines have been mapped, correlated and attributed to a re-advance (or re-growth) of ice during this period, locally termed the Loch Lomond Stadial (Sissons 1979; Lowe *et al.* 1999; Bradwell *et al.* 2008a). Over Britain we use the Loch Lomond Stadial ice limits from Clark *et al.* (2004) and Golledge (2010) and depict similar ice-sheet limits in Scotland in both our 13 and 12 ka time-slices. In order to maintain a consistent 1000-year resolution in DATED-1 we do not specifically make a Younger Dryas time-slice; instead, our time-slices at 13 and 12 ka loosely follow the known ice boundaries. Small (<500 Mkm^2) ice caps and glaciers outside the limits of the main ice sheets are not shown.

13 ka. – There has been a long discussion on whether Scotland was fully deglaciated before the start of the Younger Dryas/Loch Lomond Stadial (e.g. Bradwell *et al.* 2008a). Over Scotland our lines show ice cover restricted to the western Highlands, although it is likely that there were also several small ice caps and glaciers in the Southern Uplands and Scottish Islands (see Golledge 2010 for a review) and in Ireland, Wales and northern England. In western Norway we draw all lines inland of the mapped Younger Dryas re-advance moraines (Mangerud 2000, 2004; Mangerud *et al.* 2011) but place the maximum and most-credible lines close to the Tautra Moraine in Trøndelag (Reite 1994) and Tromsø-Lyngen moraines in northern Norway (Andersen 1975). Numerous local glaciers beyond the SIS limit in western (Sollid & Reite 1983; Larsen *et al.* 1984) and northern (Andersen 1968, 1975) Norway are not shown. Around Oslofjorden we use the Onsøy Moraine located shortly distal of the Ra Moraine (Sørensen 1992). We follow the accepted Younger Dryas extent across Sweden (Lundqvist & Wohlfarth 2001). There is uncertainty in the position of the ice front over the Baltic Sea, although all Baltic States were likely ice free before 13.3 ka (Lasberg & Kalm 2013) and the freshwater Baltic Ice Lake had developed before *c.* 13 ka (Björck *et al.* 2002; Donner 2010; Grigoriev *et al.* 2011; Saarse *et al.* 2012). In the east the SIS is depicted close to the Finnish-Russian border and we use the Salpaussellkä I and Rugozera moraine positions as the minimum and the Pandivere and Neva margins as the maximum lines at 13 ka (Donner 2010; Saarse *et al.* 2012). The most-credible line follows the Palivere line across Estonia (Fig. 8). By 13 ka ice was close to the coast in southern Svalbard (Salvigsen & Elgersma 1993; Mangerud & Landvik 2007).

12 ka. – In our 12 ka time-slice we show the ice margin as it was at the end of the Younger Dryas. In western Norway all lines follow the mapped Herdla-Halsnøy moraines (Lohne *et al.* 2012). In Trøndelag the most-credible line follows the Hoklingen Moraine position and around Oslofjorden the Ås Moraine (Andersen *et al.* 1995b). Elsewhere along the Norwegian coast the maximum line follows the mapped moraines and the most-credible line is drawn slightly inland of this position. Across Finland we follow the Salpaussellkä I and II for the maximum and most-credible lines, respectively (Donner 2010). Both the minimum and most-credible lines sit close to the Kalevala Moraine in westernmost Russia. Much of the low-lying southern islands of Franz Josef Land and outer fjords of Svalbard were ice free by 12 ka (Forman *et al.* 1996; Landvik *et al.* 2013).

Post-Younger Dryas time-slices 11–10 ka

After 12 ka the SIS ice sheet margin was likely very crenulated and split into lobes and valley/fjord glaciers; we do not depict the detail of this ice margin. Meltwater channels are found almost at the summits of the highest peaks in the inland mountains of Norway and Sweden (1500–2000 m a.s.l.). Such channels are only formed below the equilibrium line altitude (ELA) and thus demonstrate that during deglaciation the ELA

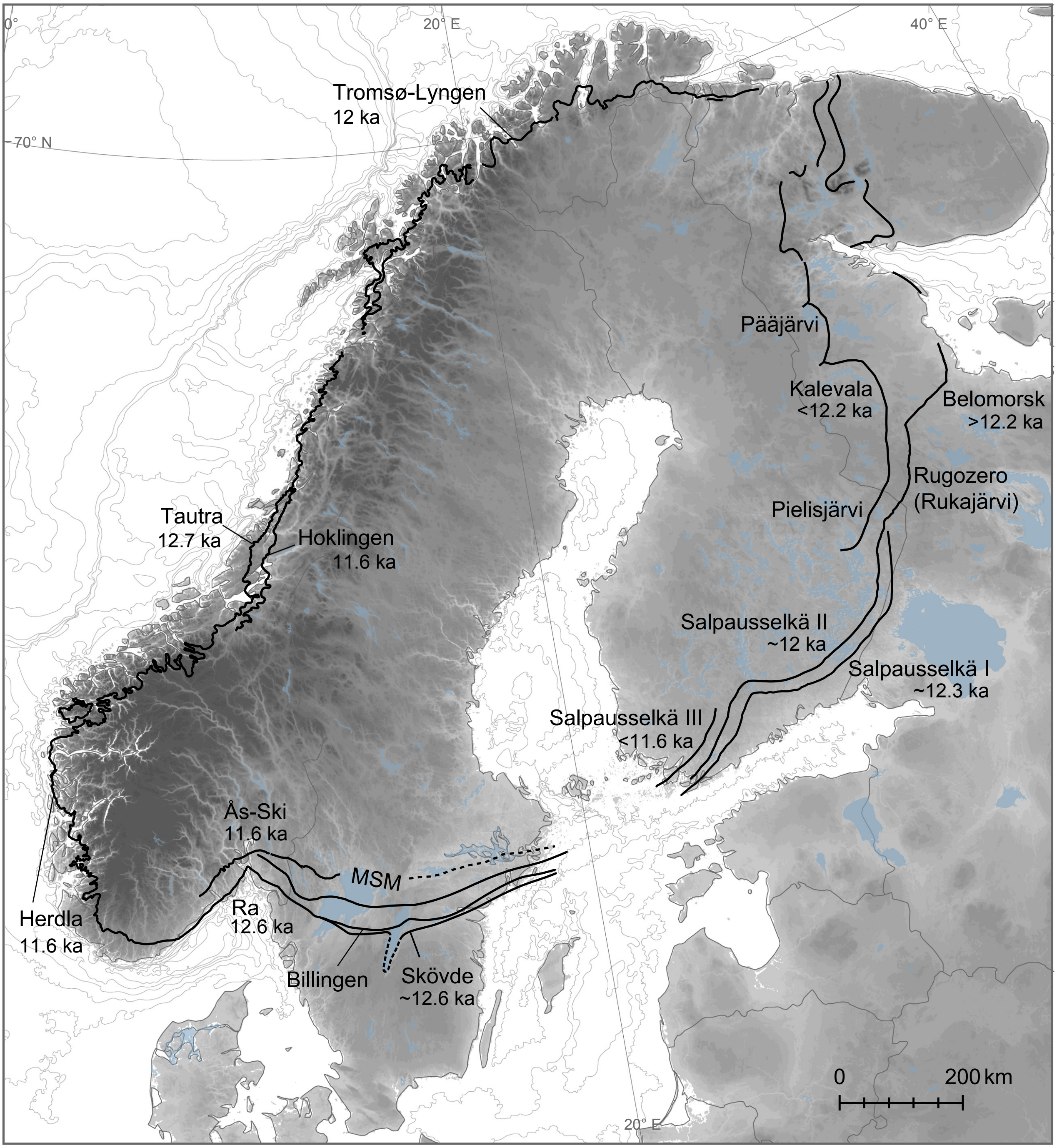

Fig. 8. Moraine positions attributed to the Younger Dryas (12.5–11.7 ka) extent of the Scandinavian Ice Sheet (after Andersen *et al.* 1995a; Rainio *et al.* 1995; Lundqvist & Wohlfarth 2001; Mangerud 2004; Donner 2010; Pasanen *et al.* 2010; Mangerud *et al.* 2011; Lunkka *et al.* 2012; Olsen *et al.* 2013). Although the ice margin can be traced across Scandinavia, available dates show that the moraines are not synchronous and dating precision for the age of the moraines varies. In some places multiple stages have been mapped. MSM = Middle Swedish Moraines.

was located higher and probably above the summit of the SIS, i.e. the ice sheet had no accumulation area and was climatically dead, with all ice flow occurring due to the existing surface slope (Mannerfelt 1940, 1945; Gjessing 1966). We postulate that the ELA moved above the top of the ice sheet soon after the Younger Dryas/Holocene transition. The implication for our reconstruction is that there was not only a retreating ice margin, but the entire ice sheet also melted down vertically, revealing mountain summits close to the centre of the ice sheet (Linge *et al.* 2006, 2007; Goehring *et al.* 2008) and splitting the ice sheet into numerous individual ice masses, thus creating a more irregular ice margin than shown in our reconstructions at 11 and 10 ka. Above the marine limit the possibility to precisely map the ice-marginal retreat disappears as these higher elevation areas are almost devoid of end moraines or other marginal landforms. In western Norway ice-marginal deltas showing the retreating margin are commonly found below the marine limit, but their location is often determined by topography rather than climate, and continuations of the margin as lateral moraines at higher elevations are very rarely found. Therefore, correlation from fjord to fjord is difficult and to a large extent dependent upon radiocarbon dates of which there are too few for robust correlations. The last remaining glaciers were probably located on the floors of deep valleys near the former ice divide. Thus, final deglaciation did not occur as a retreat of the glaciers towards the highest mountains and present-day glaciers of Norway and Sweden.

11 ka. – Scotland was rapidly deglaciated following the Loch Lomond Stadial (Lowe & Walker 1976; MacLeod *et al.* 2011). Svalbard, Franz Josef Land and Novaya Zemlya were also possibly fully deglaciated at this time (our minimum reconstruction shows no ice on these islands by 11 ka), with any remaining ice restricted within the present-day coastlines (Forwick & Vorren 2009, 2010; Baeten *et al.* 2010). Over Finland we take the Central Finland End Moraine and Salpausselkä III margin positions for the most-credible and maximum lines, respectively, at 11 ka. In western Norway the Eidfjord-Osa and correlated moraines are well dated to 11 ka (Mangerud *et al.* 2013) and around Oslofjorden we use the Aker Moraine position.

10 ka. – After 11 ka ice-margin positions along the Swedish Baltic Sea coast are precisely dated by the varve chronology (Strömberg 1989, 1990, 2005). Together with directions of the youngest glacial striae and in some places (De Geer) moraines a well-defined ice margin can be mapped documenting retreat from the Baltic Sea region (Strömberg 1989, 1990; Donner 1995). It is well established that the last, more-or-less contiguous SIS was located along or close to the earlier ice-divide position, south of the main watershed in southeastern Norway and east of the watershed in Sweden. This is shown by the youngest glacial striae and the many ice-dammed lakes created between the ice divide and the water divide during the down-wasting of the ice surface (Lundqvist 1972; Bertling & Sollid 1999). However, the age relationships between the many lakes – and thus the ice remnants – are unknown; there may be a considerable age difference from south to north. Dates for final deglaciation of the SIS from the Scandinavian Mountains are sparse, the available dates suggesting deglaciation commencing shortly after *c.* 10 ka (Lundqvist & Mejdahl 1995; Rubensdotter & Rosqvist 2009; Bakke *et al.* 2010; Möller *et al.* 2013). The final demise of the SIS progressed rapidly and deglaciation of Scandinavia was likely complete by 9 ka (Lundqvist & Mejdahl 1995; Nesje *et al.* 2004; Harbor *et al.* 2006) or slightly earlier (Fabel *et al.* 2006).

Glaciers on western Svalbard were smaller than present-day glaciers here (Svendsen & Mangerud 1997) and we have depicted all Arctic islands as ice free in the minimum and most-credible reconstructions and use a simplified version of the present-day glacier limits (GLIMS 2005, updated 2012) for the maximum reconstruction.

The most ambiguous sectors

Despite the wealth of geological information that exists there remain problems when attempting to produce maps of former ice-sheet extent at 1000-year resolution across the entire area covered by the EurIS; as apparent from the distances in each time-slice between our most-credible line and bounding maximum and minimum lines, respectively. However, two areas stand out as the most uncertain and will be discussed below, namely the eastern Barents-Kara Sea and the North Sea. In both these regions geomorphological evidence of the ice-margin patterns is sparse or missing and there are few dates.

Eastern SBKIS. – Greatest uncertainty in both the timing and style of glaciation of the EurIS is in the Kara Sea and eastern Barents Sea. The western Barents Sea sea floor (Andreassen *et al.* 2008, 2014; Winsborrow *et al.* 2010; Rüther *et al.* 2011, 2012; Bjarnadóttir *et al.* 2013, 2014) and the area around Svalbard (Landvik *et al.* 2005; Ottesen & Dowdeswell 2006, 2009; Ottesen *et al.* 2007, 2008; Dowdeswell *et al.* 2010; Hogan *et al.* 2010) are now well mapped in terms of glacial ice-flow lineations, end moraines and grounding line wedges, which provide precise information about the pattern of ice flow and ice-margin geometry during ice recession and there exist some radiocarbon dates. In contrast, geomorphological data for the eastern Barents and Kara seas are almost non-existent, and there are extremely few accurate ages for any glacial margin (Fig. 2A). We highlight two main unresolved issues; the maximum extent of the eastern SBKIS and the style and timing of glaciation over Novaya Zemlya.

The maximum achieved extent of the EurIS in the Kara Sea shown in Svendsen *et al.* (2004) has to a large degree been confirmed by more recent investigations (Dittmers *et al.* 2008), but the northeastern extension of the ice sheet onto the Taimyr Peninsula remains problematic. It is clear that the ice front did not reach the islands of Severnaya Zemlya, which hosted only local glaciers not larger than today (Möller *et al.* 2007, 2015). In contrast, it has been proposed that the northwestern part of the Taimyr Peninsula was inundated by a glacier advance from the Kara Sea shelf (Alexanderson *et al.* 2001, 2002; Svendsen *et al.* 2004). This interpretation relies on two AMS radiocarbon dates (Site 2342, DATED-id 5423–4; LuA-4817, 23 642±341 and Lua-4597, 23 500±310 cal. years BP) from mollusc shells (Alexanderson *et al.* 2001) collected from melt-out till draped over remnants of glacier ice correlated to a belt of ice-marginal features, named the North Taimyr ice-marginal zone (Kind & Leonov 1982). These dates implicate an eastward ice advance across the northern Kara Sea reaching the peninsula sometime after 23 ka. Although the near-identical ages for the two molluscs lends credibility to the ages, viewed against the background of other data we find the extension of a ~450 km-long ice lobe from the SBKIS problematic and question this interpretation. First, ice advance reaching the mainland would have blocked northbound fluvial drainage from the continent, creating an ice-dammed lake as in previous glaciations (Mangerud *et al.* 2004; Svendsen *et al.* 2014), but traces of such a lake have not been found (Svendsen *et al.* 2004). Rather, there is evidence that present-day fluvial drainage prevailed throughout MIS 2 with the deposition of aeolian sediments and formation of ice wedges in many areas close to the present-day sea level along the Russian coastline (e.g. Vasil'chuk & Vasil'chuk 1998). Second, and perhaps more significant, based on glaciological considerations we find it remarkable that the postulated advance, which terminated well inland on Taimyr evidently did not encroach into Severnaya Zemlya. Existing radiocarbon dates (Sites 2370, 2373–5, *c.* 30–24 ka) indicate that mammoths were grazing on Severnaya Zemlya at this time and there is nothing to suggest that the ice sheet was located in the near vicinity of these islands (Möller *et al.* 1999, 2007, 2015). Furthermore, two radiocarbon dates on terrestrial peat obtained from the sea floor to the north of the Taimyr River estuary suggest that this area has been ice free since before 19 ka (Site 198; Bolshiyanov *et al.* 1998). In our time-slice reconstructions we depict ice reaching the Taimyr Peninsula for the maximum limit in the 22 ka time-slice reconstruction only; our minimum and most-credible reconstructions leave the Taimyr and adjacent part of the Kara Sea shelf entirely ice free since 40 ka. We suspect that the dates (Site 2342) from Taimyr underestimate the real age of these molluscs, i.e. that the corresponding ice advance is older than 23 ka and relates to the more extensive glaciation established to have occurred during MIS 4 (Svendsen *et al.* 2004; Möller *et al.* 2015).

It is generally assumed that the major glaciations of the Barents-Kara Sea were initiated by expansion of glaciers on the islands surrounding the Barents Sea onto the adjacent sea floor and eventually merging to create a shelf-centred ice sheet, a scenario we also assume in our depiction of ice build-up 40–25 ka. The primary ice divide shifted from the islands towards the central Barents Sea and remained there until the final deglaciation, when the ice sheet split into several domes and retreated back towards the major islands again, mirroring the ice-sheet build-up. For Svalbard and Franz Josef Land this is an accepted interpretation, supported by observations (Ingólfsson & Landvik 2013; Landvik *et al.* 2014). However, the glacial evolution of the eastern SBKIS is still poorly constrained, especially in the vicinity of Novaya Zemlya. It is not clear if Novaya Zemlya was inundated by the shelf-centred Barents Ice Sheet or if a persistent satellite ice dome was located over the islands throughout the last glaciation.

The postglacial marine limit around the entire archipelago of Novaya Zemlya is <15 m a.s.l. and is dated to 6–7.5 ka BP (Zeeberg *et al.* 2001). This contrasts strongly with the situation on Svalbard where the highest relative sea level everywhere was reached several thousand years earlier, and in eastern Svalbard was up to 100 m a.s.l. (Forman *et al.* 1995; Landvik *et al.* 1998). Zeeberg *et al.* (2001) concluded that there was a thin satellite dome over Novaya Zemlya and postulated a late deglaciation in line with marine shells and peat dated to 9.4–12.4 cal. ka BP (Sites 2365, 194, 2357; Serebryanny & Malyasova 1998; Forman *et al.* 1999; Zeeberg *et al.* 2001). We consider these ages as safe minimum ages for deglaciation, but in the time-slice reconstructions presented here we propose that Novaya Zemlya was deglaciated as early as *c.* 18 ka. Two ^{14}C dates (Sites 2346, 2356) from the west coast of Novaya Zemlya have yielded ages of *c.* 18.5 cal. ka BP (Forman *et al.* 1999). According to the descriptions of the investigators both samples were taken from terrestrial peat lenses below silt and clay not covered by till. One sample was found close to present-day sea level suggesting a low relative sea level at the time of the peat formation. We cannot exclude the possibility that the dates are anomalously old due to contamination, and no details of the sample preparation were given. However, if the peat formed as late as 10 000 ^{14}C years BP, then the samples must be contaminated with as much as 65% nonfinite-aged C in order to generate the reported ages (Geyh & Schleicher 1990), which in our opinion is unlikely. Further support for early deglaciation of Novaya Zemlya comes from amino acid analysis of marine molluscs. Palaeo-temperature modelling of shell racemization indicates that during the MIS 2 glaciation the archipelago was covered by warm-based ice that lasted for an integrated time of only 3000 years after 30 ka (Mangerud *et al.* 2008a), although the presence of cold-based ice would permit a longer ice-covered period. The low marine limits around Novaya Zemlya are also consistent with our interpretation, namely that deglaciation took place at an early stage when global sea level was still near the LGM low-stand.

Based on an overall assessment we consider the most probable interpretation to be that an ice cap grew over Novaya Zemlya before the islands were inundated by an eastward expansion of the SBKIS during MIS 2, and that the islands became ice free soon after *c.* 19–20 ka. Early deglaciation of Novaya Zemlya can be explained by precipitation starvation of the eastern lee-side flank of the SBKIS, an idea supported by the fact that glaciers on Severnaya Zemlya (Möller *et al.* 2007) and in the Polar Urals (Mangerud *et al.* 2008b) remained very small during the MIS 2 glaciation.

North Sea ice cover and the Norwegian Channel Ice Stream. – There is now little doubt that the SIS and BIIS were connected and that grounded ice existed in the North Sea during MIS 2 (Graham *et al*. 2007, 2009; Sejrup *et al*. 1994). However the nature and timing of this connection remains in question as there is both limited chronological control and pattern information, especially in the southern part of the North Sea (Hughes *et al.* 2011; Clark *et al.* 2012). The few radiocarbon dates available from below till in the northern North Sea indicate complete ice cover with coalescence of the BIIS and SIS sometime after 33 ka, and dates above till that glacimarine (ice-free) conditions existed in the vicinity of Fladen Ground after 25 ka (Rise & Rokoengen 1984; Sejrup *et al.* 1994). Based on these dates an early separation of the BIIS and SIS has been proposed, either by the opening up of a long and narrow embayment in the northern North Sea (Bradwell *et al.* 2008b) or complete separation of the two ice sheets (Sejrup *et al.* 2005, 2009, 2015). We depict these alternatives for the most-credible and minimum lines, respectively, from 25 to 18 ka. However, glaciologically we find it unlikely that a long narrow embayment into an active ice sheet should have persisted for several thousand years. Partial or full deglaciation of the North Sea as early as 25 ka is also difficult to reconcile with other dates from both the western and eastern side of the North Sea and evidence for former ice-flow geometry (although limited), and we therefore keep full ice cover in the North Sea in our maximum line until *c.* 23 ka.

In the eastern North Sea, the large Norwegian Channel Ice Stream is known to have operated during the last glacial cycle (Sejrup *et al.* 1994). Radiocarbon dates from marine cores constrain the last operation of the ice stream to 20–19 ka (King *et al.* 1998; Nygård *et al.* 2005) and indicate that the ice-stream front had retreated ~220 km (the Troll core) southwards along the channel by 18.5 ka (Sejrup *et al.* 1994). Operation of the ice stream concurrent with ice-free conditions in the northern North Sea to the west of the Norwegian Channel is enigmatic (Clark *et al.* 2012). Although confined to the prominent Norwegian Trough, there is no present-day analogue for an ice stream unbounded by slower-moving ice along one lateral flank. New ^{10}Be exposure ages (published after the census date for DATED-1) from islands (Utsira and southern Karmøy) located ~400 km upstream along the former path of the Norwegian Channel Ice Stream suggest that the islands were deglaciated by *c.* 20 ka (Svendsen *et al.* 2015), i.e. 2000 years earlier than suggested by the marine radiocarbon chronology. This age discrepancy is unresolved, but assuming that the reported exposure ages are accurate Svendsen *et al.* (2015) suggest that an ice-free embayment opened up across almost the entire northern North Sea including the Norwegian Channel as early as 20 ka. In the south-western North Sea, radiocarbon and OSL dates from eastern England implicate ice presence along the coastline after 22 ka (e.g. Bateman *et al.* 2008, 2011) for which Clark *et al.* (2012) proposed two alternative interpretation scenarios. One scenario accepted full deglaciation of the North Sea after 25 ka followed by advancement of the North Sea Lobe eastward out of northern England before turning southeast to follow the coastline to Dimlington (a well-documented feature of the BIIS; Boston *et al.* 2010; Evans & Thomson 2010; Bateman *et al.* 2011; Davies *et al.* 2012; Roberts *et al.* 2013). The alternative scenario restricted break-up of ice to the northern North Sea at 25 ka and proposed a persistent ice dome in the southern North Sea. We note that such an ice dome would require the local equilibrium line to be very low and should give imprints on the relative sea-level evolution of coastlines surrounding the North Sea. Both models rely on the expansion of the North Sea Lobe to explain the presence of ice-dammed Glacial Lake Humber (near Dimlington) at *c.* 17 ka (Bateman *et al*. 2008), although such a large ice lobe is hard to envisage as the majority of evidence indicates that the BIIS was restricted to north and west Ireland and Scotland by this time. In the DATED-1 time-slices we use the two proposed scenarios of Clark *et al.* (2012) to define our minimum and most-credible limits in the North Sea region 25–18 ka.

Recommendations and requests

The collation and archiving of data required by this project leads us to make a number of recommendations and requests for future reporting of chronological data. Dates should always be reported with geographic co-ordinates of the sampling site (not simply a map or location name). Ideally co-ordinates for terrestrial and marine samples should be reported in decimal degrees and the WGS84 projection. For TCN dates all data necessary for recalculating the ages on different production rates must be reported. DATED is an ongoing project and the database will be updated on a rolling basis, with periodic release of updated versions of both the database and time-slice reconstructions. Therefore, we encourage reporting of errors and missing data from DATED-1 to us and we welcome published criticism and alternative interpretations. We anticipate that both the database and maps will become a valuable resource for researchers and welcome suggestions for improvements and developments for future versions.

Conclusions

- To January 2013, over 5000 individual dates have accumulated in the literature that constrain either the build-up, retreat or both of the EurIS during the last glacial cycle.
- Evaluation of the collated dates, considered together with geomorphological evidence for ice-sheet margin positions and flow-pattern configuration, facilitated a series of map reconstructions documenting the build-up and retreat of the EurIS during the last glacial cycle (40–10 ka). The maps demonstrate both what is confidently known and what remains uncertain according to the available geological evidence and provide a new basis on which to compare evidence from disparate regions and against numerical modelling results.
- The combined EurIS reached a maximum areal extent of ~5.5 Mkm^2 between 21 and 20 ka. The SIS was by far the largest ice sheet, comprising over 50% of the total area throughout the last glaciation and reached its maximum size up to ~3000 years later than the smallest component, the BIIS and ~2000 years later than the SBKIS. The BIIS and SBKIS were grounded below present-day sea level across substantial proportions of their former beds at their maximum extents.
- Individual ice sheets of the EurIS reached their maximum limits asynchronously.
- This compilation has revealed many unresolved instances of conflicting evidence leading to some large uncertainties. The largest geographical areas of uncertainty have a low density of dates and pattern information, both in space and time (e.g. the marine sectors and the eastern margins of the SIS and SBKIS). The timing and mode of coalescence and separation of the ice sheets are especially poorly constrained, and in all time-slices before 15 ka there are sectors of the ice margins where uncertainties exceed 500 km.

References for DATED-1 database

The database was compiled using the following sources referenced in the Supporting Information (Data S1):

Aa & Mangerud (1981), Aa & Sønstegaard (1997), Aaris-Sørensen (2006), Aaris-Sørensen & Liljegren (2004), Aaris-Sørensen & Petersen (1984), Aaris-Sørensen *et al.* (1990), Aarseth *et al.* (1997), Aarseth & Mangerud (1974), Aaseth (1990), Āboltiņš *et al.* (1975), Ahlberg *et al.* (1996), Aldhouse-Green (2000), Aldhouse-Green & Pettitt (1998), Alexanderson *et al.* (2001, 2008, 2013), Alexanderson & Murray (2007, 2012), Alm (1993), Andersen (1960, 1968, 1975, 1981), Andersen *et al.* (1979, 1981a,b, 1982, 1983, 1987, 1995, 1996), Andersson *et al.* (1999), Andreassen *et al.* (1985), Andreev *et al.* (2001), Andrén *et al.* (2000), Anundsen (1972, 1977, 1978, 1985), Anundsen *et al.* (1983), Anundsen & Simonsen (1967), Arppe & Karhu (2006, 2010), Arslanov *et al.* (1970, 1975, 1986), Arslanov (1971, 1975, 1987, 1993), Aseyev (1974), Ashworth (1972), Atkinson *et al.* (1986), Austad & Erichsen (1987), Baeten *et al.* (2010), Bakke *et al.* (2005a,b, 2010), Ballantyne & Hall (2008), Ballantyne *et al.* (1998, 2006, 2007a,b, 2008, 2009a,b,c, 2011), Ballantyne & Stone (2009), Banys *et al.* (1991), Barker *et al.* (1969), Bartley & Morgan (1990), Bateman (1995, 2001, 2008, 2011), Baxter *et al.* (1969), Beckett (1981), Bennike *et al.* (1994, 2006), Berger *et al.* (2004), Bergersen *et al.* (1991), Berglund (1979, 1995a,b), Berglund *et al.* (1976, 1994), Bergsten & Nordberg (1992), Bergstrøm (1975, 1984, 1995, 1997, 1999), Bergstrøm *et al.* (1992, 2005), Birkenmajer & Olsson (1998), Birnie *et al.* (1993a,b), Bishop *et al.* (1977), Bishop & Dickson (1970), Bitinas (2007), Bitinas *et al.* (2002), Bjelm (1976), Bjune *et al.* (2004, 2005), Björck *et al.* (1998), Björck & Digerfeldt (1982, 1986), Björck & Håkansson (1982), Björck & Möller (1987), Blackburn (1952), Blake (1975, 1989, 2006), Blaszkiewicz (1998, 2002, 2005), Bluszcz & Pazdur (2003), Blystad (1981), Blystad & Anundsen (1983), Bolshiyanov *et al.* (1998), Bondevik & Mangerud (2002), Bondevik *et al.* (1995, 1999, 2006), Bos *et al.* (2004), Boulton (1979), Bowen (1994), Bowen *et al.* (2002), Braaten & Hermansen (1985), Bradwell *et al.* (2008), Bramer (1972), Brande (2003), Brauer *et al.* (2005), Brown *et al.* (2007), Browne & Graham (1981), Browne *et al.* (1977), Browne *et al.* (1983a,b), Brückner (1996), Brückner & Halfar (1994), Brückner *et al.* (2002), Buckland (1976, 1982), Buckley & Willis (1969, 1970), Bugge (1980), Burleigh *et al.* (1982), Butomo (1965), Bøe *et al.* (2007), Böse (1979), Cadman (1996), Carter (1993), Caseldine & Edwards (1982), Catt (1987), Cepek (1965), Cherdyntsev *et al.* (1969), Cimiotti (1983), Clark *et al.* (2009a,b, 2012), Clark *et al.* (2004), Colhoun *et al.* (1972), Colhoun & Synge (1980), Coope & Brophy (1972), Coope & Joachim (1980), Coope & Lister (1987), Coope & Pennington (1977), Corner & Haugane (1993), Corner *et al.* (1999, 2001), Council for British Archaeology (CBA) (2000 (updated 2008)), Craig (1978), Currant *et al.* (1984), Cwynar & Watts (1989), Dahl & Nesje (1994), Dahl *et al.* (1997, 2002), Dahlgren & Vorren (2003), Danilāns (1973), Dardis *et al.* (1985), Dawson *et al.* (1997), Demidov *et al.*

(2006), Diefendorf *et al.* (2006), Ditlefsen (1991), Dolukhanov & Miklyayev (1975), Donner *et al.* (1979), Donner (1979), Dresser (1980), Duplessy *et al.* (2005), Dzierżek & Zreda (2007), Eilertsen *et al.* (2005), Elverhøi *et al.* (1993, 1995a,b), Elverhøi & Solheim (1987), Engstrand & Östlund (1962), Engstrand (1965, 1967), Evans *et al.* (2005), Everest *et al.* (2006, 2013), Everest & Kubik (2006), Everest & Golledge (2004), Fabel *et al.* (2002, 2006, 2010, 2012), Fareth (1987), Fernlund (1988, 1990, 1993), Feyling-Hansen (1964), Fimreite *et al.* (2001), Fitzpatrick (1965), Fjellanger *et al.* (2006), Flatekval (1991), Follestad (1985, 1986, 1992), Forman (1990), Forman & Ingólfsson (2000), Forman *et al.* (1987, 1995, 1996, 1997, 1999a,b, 2002), Forwick & Vorren (2002, 2007, 2009), Forwick *et al.* (2010), Foster (1968, 1970), Fredén (1975, 1984), Gaigalas (2000), Gaigalas & Fedorowicz (2009), Gaigalas *et al.* (1981, 1986, 1987, 2005, 2007, 2008), García Ambrosiani (1990), Gataullin (1988), Gaunt (1974, 1976), Gaunt *et al.* 1970, 1971), Gemmell *et al.* (2008), Genes (1978), Gheorghiu *et al.* (2012), Gillespie *et al.* (1985), Girling (1974), Gjessing & Spjeldnaes (1979), Glasser *et al.* (2012), Godwin & Willis (1959, 1964), Goehring *et al.* (2008), Golledge *et al.* (2007), Gowlett *et al.* (1986), Graham *et al.* (2010), Gray (1975), Gray & Brooks (1972), Green (1984), Gregory & Currie (1928), Greve (1984), Grigoriev *et al.* (2011), Grøsfjeld *et al.* (1999), Gulliksen *et al.* (1975, 1978, 1998), Guobyte & Satkūnas (2011), Görsdorf & Kaiser (2001), Haflidason *et al.* (1995), Hald *et al.* (1990, 1999, 2003, 2004), Hall (1984), Hall & Jarvis (1989), Hallam *et al.* (1973), Harbor *et al.* (2006), Harkness (1981), Harkness & Wilson (1974, 1979), Harrison *et al.* (2010a,b), Haug (2005), Hedges *et al.* (1987, 1988a,b, 1989, 1990a,b, 1992, 1993, 1994, 1995, 1996, 1997), Heier-Nielsen *et al.* (1995), Heikkinen *et al.* (1974), Heikkinen & Äikää (1977), Heine *et al.* (2009), Heinsalu & Veski (2007), Helle (2008), Helle *et al.* (1997, 2007), Helmens *et al.* (2000, 2007), Henningsen & Hovden (1984), Henningsmoen (1979), Herking (2004), Hibbert *et al.* (2010), Hill & Prior (1968), Hilldén (1979), Hillefors (1974, 1975), Hiller *et al.* (2004), Hirvas (1991), Hirvas & Kujansuu (1979, 1981), Hogan *et al.* (2010), Holloway *et al.* (2002), Holmes (1977), Holtedahl (1960, 1964, 1967), Holtedahl & Bjerkli (1982), Hoppe (1972, 1974), Hormes *et al.* (2011, 2013), Houmark-Nielsen (1994, 2003, 2007, 2008, 2010), Houmark-Nielsen & Kjær (2003), Houmark-Nielsen & Kolstrup (1981), Houmark-Nielsen *et al.* (1996, 2001, 2012), Hughes *et al.* (2011), Hulme & Durno (1980), Hyvärinen (1973, 1975), Häggblom (1982), Håkansson (1969, 1970, 1974, 1976, 1977, 1979, 1980, 1982, 1986, 1988), Idland (1992), Iisalo (1996), Ilves (1980, 1990), Ilves *et al.* (1970, 1974), Ince (1981), Ivanova *et al.* (2002), Jacobi & Higham (2008), Jacobi *et al.* (1986, 2009), Janocko *et al.* (1998), Janowska (1980), Jardine *et al.* (1988), Jensen & Vorren (2008), Jessen *et al.* (2010), John (1965, 1967), John & Ellis-Gruffydd (1970), Johnsen *et al.* (2009, 2012), Jones & Keigwin (1988), Jones (1976, 1977), Jones & Gaunt (1976), Jones & Keen (1993), Jungner (1979), Jungner & Sonninen (1983, 1996), Junttila *et al.* (2010), Kaakinen *et al.* (2009), Kadastik (2004), Kaiser (2004), Kaiser *et al.* (1999, 2007), Kajak *et al.* (1981), Kaland (1988), Kalm (2005, 2006), Karlen (1979), Karlen *et al.* (1987), Karlsen (2008), Kelley *et al.* (2006), Kershaw (1986), Kessel & Punning (1969), Kind (1974), King *et al.* (1998), Kirk & Godwin (1963), Kjemperud (1986), Kjær *et al.* (2006a,b, 2003), Klakegg & NordahI-Olsen (1985), Klakegg & Sørensen (1991), Kleiber *et al.* (2000), Kliewe (1968), Kliewe & Janke (1991), Klingberg (1989), Klitgaard-Kristensen *et al.* (2012), Klovning & Hafsten (1965), Knies *et al.* (2000, 2001, 2007), Knight (2001), Knudsen (1978, 2006), Knutz *et al.* (2002, 2007), Koç *et al.* (2002), Kolstrup (1991, 1992), Kolstrup & Havemann (1984), Kolstrup & Houmark-Nielsen (1991), Kolstrup & Olsen (2012), Kopczynska-Lamparska (1976), Koren *et al.* (2008), Korpela (1969), Kortekaas & Murray (2007), Kortekaas *et al.* (2007), Kozarski & Nowaczyk (1995), Kramarska (1998), Kramarska & Jurowska (1991), Kremenetski *et al.* (2004), Kristensen *et al.* (1998), Kristiansen *et al.* (1988), Krog & Tauber (1974), Krohn *et al.* (2009), Kronborg (1983), Krzymińska *et al.* (2005), Krzywinski & Stabell (1984), Kubischta *et al.* (2011), Kujansuu (1975), Kvamme (1984), Laberg *et al.* (2007), Laberg & Vorren (1995, 2004), Laberg *et al.* (2002), Lagerbäck & Robertsson (1988), Lagerlund & Houmark-Nielsen (1993), Lampe (2005), Landvik *et al.* (1987, 1992, 1995, 1998, 2003, 2005, 2013), Landvik & Hamborg (1987), Landvik & Mangerud (1985), Larsen *et al.* (1984, 1987, 1988, 1998, 1999, 2000, 2006, 2009a,b, 2012), Larsson *et al.* (2007), Lasberg (2014), Lasberg & Kalm (2013), Lawson (1984), Lehman & Forman (1992), Lehman *et al.* (1991), Levitan *et al.* (2003), Lie *et al.* (1983), Lien (1985), Liiva *et al.* (1966, 1968, 1979), Lindén *et al.* (2006), Linge *et al.* (2006a,b, 2007), Lister (2009), Lohne (2006), Lohne *et al.* (2004, 2007a,b, 2012), Lokrantz *et al.* (2003), Longva (1994), Longva & Thoresen (1989, 1991), Lõugas *et al.* (2002), Lowe (1978), Lowe & Walker (1976), Lowe *et al.* (2004), Lubinski *et al.* (2001), Lukas & Bradwell (2010), Lundqvist (1955, 1964, 1978), Lundqvist & Mejdahl (1995), Lundqvist & Miller (1992), Lundqvist & Mook (1981), Lundqvist & Wohlfarth (2001), Lunkka *et al.* (2001, 2008, 2012), Lykke-Andersen (1981, 1982, 1987), Lyså *et al.* (2001, 2004, 2011), Lüthgens & Böse (2011), Lüthgens *et al.* (2010a,b, 2011), Lønne *et al.* (2001), Lønne & Mangerud (1991), MacLeod *et al.* (2011), Malakhovsky & Markov (1969), Mangerud (1970, 1977, 2000, 2004), Mangerud & Landvik (2007), Mangerud & Svendsen (1990), Mangerud *et al.* (1979, 1981, 1992, 1999, 2008, 2010), Manikowska (1995), Manley *et al.* (2001), Mardal (2007), Markots *et al.* (2007), Markov (1939), Matthews (1970), Matthews *et al.* (2000, 2005, 2011), Mausbacher *et al.* (2002), McCabe & Clark (1998, 2003), McCabe & Haynes (1996), McCabe *et al.* (1978, 1986, 2005, 2007a,b,c), McCarroll *et al.* (2010), McCormack *et al.* (2011), Meirons (1986, 1992), Meirons & Juskevics (1984), Meirons *et al.* (1981), Mellars (1990), Micas (1963), Midtun (2009), Milecka (2005), Miller (1977), Milling (1975), Mitchell (1976), Mol (1997), Molleson & Burleigh (1978), Molodkov (2007), Molodkov *et al.* (1998), Moora (1998), Moora *et al.* (2002), Morgan (1973a,b), Murton *et al.* (2009), Myklebust (1992), Mykura & Phemister (1976), Mäkinen (1985, 2005), Møller *et al.* (1992), Möller *et al.* (1999, 2007, 2007a,b), Mörner (1969), Nenonen (1995), Nenonen *et al.* (1986), Nese & Lauritzen (1996), Nesje *et al.* (2004, 2007), Neustadt (1971), Niemelä & Tynni (1979), Niewiarowski (2003), Nikiforova *et al.* (1985), Nitz *et al.* (1995), Noe-Nygaard & Heiberg (2001), Nordahl Olsen (1987), Nowaczyk (1994), Nowaczyk & Knies (2000), Nydal (1960, 1962), Nydal *et al.* (1964, 1970, 1972, 1985), Nygård *et al.* (2004), Ó Cofaigh & Evans (2007), Ó Cofaigh *et al.* (2012), Oakley (1968), Odgaard (1982), Olsen & Hammar (2005), Olsen & Løwe (1984), Olsen (1988, 2002, 2010), Olsen & Bergstrøm (2007), Olsen *et al.* (1996, 2001, 2013), Olsson *et al.* (1969), Otlet & Walker (1979), Page (1972), Pasda (2002), Paus (1988, 1989a,b, 1990, 2010), Paus *et al.* (2011), Pazdur *et al.* (1979, 1982, 1983, 1985, 1994), Peacock (1971, 1995, 1999, 2002, 2008), Peacock & Browne (1998), Peacock *et al.* (1977, 1978, 1992), Peacock & Long (1994), Pearson (1979), Pedersen (2005), Pennington (1975, 1977), Penny *et al.* (1969), Perkins & Rhodes (1994), Phillips *et al.* (1994, 2006, 2008), Plassen & Vorren (2003), Polyak *et al.* (1995, 1997, 2000a,b), Polyak & Solheim (1994), Prentice (1981, 1982), Przegiętka *et al.* (2008), Prøsch-Danielsen (1993), Punning *et al.* (1967, 1968a,b, 1971, 1973, 1974, 1980, 1981, 1982, 1983), Punning & Raukas (1985), Putikinen & Lunkka (2008), Putkinen *et al.* (2011), Påsse (1986, 1987, 1990, 1992), Raab (2003), Rae (1976), Rainio & Lahermo (1976), Rajamäe (1981, 1982), Ralska-Jasiewiczowa & Rzetkowska (1987), Rasmussen (1981, 1984), Rasmussen *et al.* (2007), Rattas *et al.* (2001, 2010), Raukas (2004), Raukas & Stankowski (2005), Raukas *et al.* (2010), Raunholm *et al.* (2002, 2004), Reite (1968, 1982), Reite *et al.* (1992), Repo & Tynni (1967), Richardt (1996, 1998), Ringen (1964), Rinterknecht *et al.* (2004, 2005, 2006, 2007, 2008, 2012), Rise *et al.* (2006, 2008), Rise & Rokoengen (1984), Risebrobakken *et al.* (2010), Roberts *et al.* (2006, 2011), Robertsson (1988), Robertsson & Ambrosiani (1988), Rokoengen (1979), Rokoengen & Frengstad (1999), Rokoengen *et al.* (1977, 1979, 1982), Rolfe *et al.* (2012), Rolfe (1966), Romundset *et al.* (2010, 2011), Ronnert (1988), Rose & Jardine (1980), Ross (1996), Rotnicki & Borowka (1990, 1995), Rowinsky (1995), Rowlands (1971), Rowlands & Shotton (1971), Rubensdotter & Rosqvist (2009), Rye (1970), Rye *et al.* 1987, Rüther *et al.* (2012, 2011), Rørvik *et al.* (2010), Saarse & Liiva (1995), Saarse *et al.* (2009, 2012a,b), Saks *et al.* (2012), Salvigsen (1977, 1978, 1981, 1984), Salvigsen & Elgersma (1993), Salvigsen *et al.* (1990, 1991), Salvigsen & Høgvard (2005), Salvigsen & Mangerud (1991), Salvigsen & Nydal (1981), Salvigsen & Osterholm (1982), Sandgren *et al.* (1999), Sanko & Gaigalas (2008), Sarala (2005), Sarv & Ilves (1975), Satkūnas (1993), Satkūnas *et al.* (2007), Schlaak & Schoknecht (2002), Schulz & Strahl (2001), Scourse (1991, 2006), Scourse & Austin (1994), Scourse *et al.* (2004), Scourse & Rhodes (2006a,b), Seglinš (1988, 1991), Seglinš *et al.* (1988), Seidenkrantz & Knudsen (1993), Seiriene *et al.* (2006), Sejrup *et al.* (1994, 2009), Serebryanny *et al.* (1998), Serebryanny (1978), Serebryanny & Malyasova (1998), Shotton (1977), Shotton *et al.* (1969, 1970, 1974), Shotton & Williams (1971, 1973), Simm (1986), Simms & Coxon (2005), Simpson (1933), Sindre (1980), Šinkūnas *et al.* (2001), Sissons (1967), Sissons & Walker (1974), Skirbekk *et al.* (2010), Ślubowska-Woldengen *et al.* (2007), Small *et al.* (2012), Smith & Goddard (1991), Smith *et al.* (1971, 1990), Snyder *et al.* (2000), Sohar & Kalm (2008), Sokołowski (2007), Solem (2011), Sollid & Reite (1983), Sommer & Benecke (2009), Spjeldnæs (1978), Stančikaitė *et al.* (1998, 2008, 2009), Stankowska & Stankowski (1988), Stein *et al.* (2001, 2002), Stelle *et al.* (1975a,b), Stelle & Veksler (1975), Stoker *et al.* (2009), Stone & Ballantyne (2006), Strahl (2005), Strickertsson & Murray (1999), Stuart (1982), Suggate & West (1959), Sutherland (1981, 1984, 1986), Sutherland *et al.* (1984), Sutherland & Walker (1984), Svendsen & Mangerud (1990), Svendsen *et al.* (1992, 1996), Svendsen & Warren (2001), Switsur & West (1972), Sønstegaard *et al.* (1999), Sørensen (1979a,b, 1982, 1992, 1999), Sørensen *et al.* (2012), Tauber (1964, 1966), Telfer *et al.* (2009), Thomas (1977), Thomas *et al.* (2004, 2006), Thomsen (1982, 1989), Thoresen & Bergersen (1983), Thrasher *et al.* (2009), Tomczak *et al.* (1999), Tooley (1977), Tooley *et al.* (1977), Tornivaara (2007), Tschudi *et al.* (2000), Turkowska (1995), Tveranger *et al.* (1995), Ukkonen *et al.* (1999, 2006, 2007, 2011), Undås (1963), Uścinowicz (1999), Valchik *et al.* (1990), Valen *et al.* (1996, 1997), van Asch *et al.* (2012), Vasari *et al.* (1977), Vasil'chuk & Vasil'chuk (1998), Veksler (1989), Veksler & Stelle (1986), Ventris (1985), Vigdorchik *et al.* (1970, 1974), Vincent *et al.* (2010), Vinogradov *et al.* (1966, 1968), von Weymarn & Edwards (1973), Vorren (1973, 1978), Vorren & Alm (1999), Vorren & Kristoffersen (1986), Vorren & Laberg (1996), Vorren & Plassen (2002), Vorren *et al.* (1988), Vozniachuk *et al.* (1981), Walker *et al.* (2012), Walker (1980, 1982), Walker & Lowe (1979), Watson *et al.* (2010), Wedel (1969), Whittington *et al.* (1998), Whittington & Hall (2002), Winsborrow *et al.* (2010), Wintle (1981), Wintle & Catt (1985), Wisniewski *et al.* (2009), Wohlfarth (2009), Wohlfarth *et al.* (1995a,b, 1999), Wojciechowski (2000), Woodman *et al.* (1997), Worsley (1967), Wysota *et al.* (2002, 2009), Yakushko *et al.* (1975), Yamasaki *et al.* (1969), Yelovicheva & Sanko (1999), Zachowicz (1995), Zeeberg *et al.* (2001), Zelčs & Markots (2004), Zernitskaya *et al.* (2007), Zimenkov (1985, 1989), Zimenkov & Kuznetsov (1985), Zimenkov *et al.* (1985), Zobens *et al.* (1969), Zubakov (1974), Zurek *et al.* (2002), Östlund & Engstrand (1960), Øvstedahl & Aarseth 1975.

Acknowledgements. – All authors contributed to the compilation of the database and producing the time-slice reconstructions, and are listed alphabetically after A. L. C. Hughes and R. Gyllencreutz. The idea for DATED was originally conceived by J. Mangerud and developed into a project proposal together with J. I. Svendsen, who has been project leader since the start in 2005. The database was initially compiled by R. Gyllencreutz, 2005–2011. Responsibility for maintenance and updates was handed from R. Gyllencreutz to A. L. C. Hughes in 2012. We thank Mikael Berglund, Chris Clark, Sarah Greenwood, Anne Hormes, Volli Kalm, Knut Kaiser, Veli-Pekka Salonen and Barbara Wolfarth for providing their carefully compiled regional datasets. We thank Colin Ballantyne, Jorie Clark, Jeremy Everest, Derek Fabel and Henriette Linge for supplying additional data for recalculation of some TCN dates published before full data reporting became standard. We additionally thank Thomas Andrén, Chris Clark, Michael Houmark-Nielsen (for our discussion at the Nordic Geological Winter Meeting in 2013), Johan Kleman, Lev Tarasov, David Small and Barbara Wohlfarth (amongst a host of colleagues at various conferences and meetings) for fruitful discussions. This work has received funding from the Norwegian Research Council through several projects: Impact of changing freshwater flows and thermohaline circulation and European Climate (under the RAPID programme), The Ice Age development and human settlement in northern Eurasia (ICEHUS, project no. 176048), Eurasian Ice Sheet and Climate Interaction (EISCLIM project no. 229788/E10). DATED is a contribution to the activities of the Bjerknes Centre for Climate Research (BCCR), and we are grateful for their long-standing and continued support of the project. Michael Houmark-Nielsen and Jürgen Ehlers are thanked for their constructive reviews. We thank the University of Bergen for supporting Open Access publication of this paper. We thank J. A. Piotrowski as Editor In Chief for excellent editorial support and the invitation to submit this paper in Boreas.

References

Note that this list only includes those cited in the main text – references for the database are listed separately in the Supporting Information (Data S1).

Alexanderson, H. & Murray, A. S. 2012: Problems and potential of OSL dating Weichselian and Holocene sediments in Sweden. *Quaternary Science Reviews 44*, 37–50.

Alexanderson, H., Adrielsson, L., Hjort, C., Möller, P., Antonov, O., Eriksson, S. & Pavlov, M. 2002: Depositional history of the North Taymyr ice-marginal zone, Siberia-a landsystem approach. *Journal of Quaternary Science 17*, 361–382.

Alexanderson, H., Hjort, C., Möller, P., Antonov, O. & Pavlov, M. 2001: The North Taymyr ice-marginal zone, Arctic Siberia-a preliminary overview and dating. *Global and Planetary Change 31*, 427–445.

Alm, T. 1993: Øvre Æråsvatn - palynostratigraphy of a 22,000 to 10,000 BP lacustrine record on Andøya, northern Norway. *Boreas 22*, 171–188.

Andersen, B. G. 1968: Glacial geology of Western Troms, North Norway. *Norges Geologiske Undersøkelse 256*, 160.

Andersen, B. G. 1975: Glacial geology of northern Nordland, North Norway. *Norges Geologiske Undersøkelse 320*, 1–74.

Andersen, B. G. 1981: Late Weichselian ice sheets in Eurasia and Greenland. *In* Denton, D. H. & Hughes, P. D. (eds.): *The Last Great Ice Sheets*, 1–65. John Wiley, New York.

Andersen, B. G., Lundqvist, J. & Saarnisto, M. 1995a: The Younger-Dryas margin of the Scandinavian Ice-Sheet - an introduction. *Quaternary International 28*, 145–146.

Andersen, B. G., Mangerud, J., Sørensen, R., Reite, A., Sveian, H., Thoresen, M. & Bergström, B. 1995b: Younger Dryas ice-marginal deposits in Norway. *Quaternary International 28*, 147–169.

Andersen, E. S., Dokken, T. M., Elverhøi, A., Solheim, A. & Fossen, I. 1996: Late Quaternary sedimentation and glacial history of the western Svalbard continental margin. *Marine Geology 133*, 123–156.

André, M.-F. 2002: Rates of postglacial rock weathering on glacially scoured outcrops (Abisko-Riksgränsen area, 68°N). *Geografiska Annaler, Series A 84*, 139–150.

Andreassen, K., Laberg, J. S. & Vorren, T. O. 2008: Seafloor geomorphology of the SW Barents Sea and its glaci-dynamic implications. *Geomorphology 97*, 157–177.

Andreassen, K., Winsborrow, M. C. M., Bjarnadóttir, L. R. & Rüther, D. C. 2014: Ice stream retreat dynamics inferred from an assemblage of landforms in the northern Barents Sea. *Quaternary Science Reviews 92*, 246–257.

Andrén, T., Björck, J. & Johnsen, S. 1999: Correlation of Swedish glacial varves with the Greenland (GRIP) oxygen isotope record. *Journal of Quaternary Science 14*, 361–371.

Anjar, J., Larsen, N. K., Håkansson, L., Möller, P., Linge, H., Fabel, D. & Xu, S. 2014: A ^{10}Be-based reconstruction of the last deglaciation in southern Sweden. *Boreas 43*, 132–148.

Arnold, N. S., van Andel, T. H. & Valen, V. 2002: Extent and dynamics of the Scandinavian Ice Sheet during Oxygen Isotope Stage 3 (65,000–25,000 yr B.P.). *Quaternary Research 57*, 38–48.

Baeten, N. J., Forwick, M., Vogt, C. & Vorren, T. O. 2010: Late Weichselian and Holocene sedimentary environments and glacial activity in Billefjorden, Svalbard. *Geological Society, London, Special Publications 344*, 207–223.

Bakke, J., Dahl, S. O., Paasche, Ø., Simonsen, J. R., Kvisvik, B., Bakke, K. & Nesje, A. 2010: A complete record of Holocene glacier variability at Austre Okstindbreen, northern Norway: an integrated approach. *Quaternary Science Reviews 29*, 1246–1262.

Balco, G., Briner, J., Finkel, R. C., Rayburn, J. A., Ridge, J. C. & Schaefer, J. M. 2009: Regional beryllium-10 production rate calibration for late-glacial northeastern North America. *Quaternary Geochronology 4*, 93–107.

Balco, G., Stone, J. O., Lifton, N. A. & Dunai, T. J. 2008: A complete and easily accessible means of calculating surface exposure ages or erosion rates from ^{10}Be and ^{26}Al measurements. *Quaternary Geochronology 3*, 174–195.

Ballantyne, C. K. & Stone, J. O. 2015: Trimlines, blockfields and the vertical extent of the last ice sheet in southern Ireland. *Boreas 44*, 277–287.

Ballantyne, C. K., McCarroll, D. & Stone, J. O. 2006: Vertical dimensions and age of the Wicklow Mountains ice dome, Eastern Ireland, and implications for the extent of the last Irish ice sheet. *Quaternary Science Reviews 25*, 2048–2058.

Ballantyne, C. K., Schnabel, C. & Xu, S. 2009: Readvance of the last British-Irish Ice Sheet during Greenland Interstade 1 (GI-1): the Wester Ross Readvance, NW Scotland. *Quaternary Science Reviews 28*, 783–789.

Bateman, M. D., Buckland, P. C., Chase, B., Frederick, C. D. & Gaunt, G. D. 2008: The Late Devensian proglacial Lake Humber:

new evidence from littoral deposits at Ferrybridge, Yorkshire, England. *Boreas 37*, 195–210.

Bateman, M. D., Buckland, P. C., Whyte, M. A., Ashurst, R. A., Boulter, C. & Panagiotakopulu, E. 2011: Re-evaluation of the Last Glacial Maximum typesite at Dimlington, UK. *Boreas 40*, 573–584.

van den Berg, J., van de Wal, R. & Oerlemans, H. 2008: A mass balance model for the Eurasian Ice Sheet for the last 120,000 years. *Global and Planetary Change 61*, 194–208.

Berglund, M. 2004: Holocene shore displacement and chronology in Ångermanland, eastern Sweden, the Scandinavian glacio-isostatic uplift centre. *Boreas 33*, 48–60.

Bertling, I. & Sollid, J. L. 1999: The drainage history of glacial lake Nedre Glåmsjø, southern Central Norway. *Norsk Geografisk Tidsskrift 53*, 190–201.

Bitinas, A. 2012: New insights into the last deglaciation of the south-eastern flank of the Scandinavian Ice Sheet. *Quaternary Science Reviews 44*, 69–80.

Bjarnadóttir, L. R., Rüther, D. C., Winsborrow, M. C. M. & Andreassen, K. 2013: Grounding-line dynamics during the last deglaciation of Kveithola, W Barents Sea, as revealed by seabed geomorphology and shallow seismic stratigraphy. *Boreas 42*, 84–107.

Bjarnadóttir, L. R., Winsborrow, M. C. M. & Andreassen, K. 2014: Deglaciation of the central Barents Sea. *Quaternary Science Reviews 92*, 208–226.

Björck, J., Andrén, T., Wastegård, S. & Possnert, G. 2002: An event stratigraphy for the Last Glacial-Holocene transition in eastern middle Sweden: results from investigations of varved clay and terrestrial sequences. *Quaternary Science Reviews 21*, 1489–1501.

Bolshiyanov, D. Y., Savatyugin, L., Shneider, G. & Molodkov, A. 1998: New data about modern and ancient glaciations of the Taimyr-Severnaya Zemlya Region. *Materialy Glaciologocheskikh Issledovanii 85*, 219–222.

Bondevik, S., Mangerud, J., Birks, H. H., Gulliksen, S. & Reimer, P. 2006: Changes in North Atlantic radiocarbon reservoir ages during the Allerod and Younger Dryas. *Science 312*, 1514–1517.

Böse, M., Lüthgens, C., Lee, J. R. & Rose, J. 2012: Quaternary glaciations of northern Europe. *Quaternary Science Reviews 44*, 1–25.

Boston, C. M., Evans, D. J. A. & Ó Cofaigh, C. 2010: Styles of till deposition at the margin of the Last Glacial Maximum North Sea lobe of the British-Irish Ice Sheet an assessment based on geochemical properties of glacigenic deposits in eastern England. *Quaternary Science Reviews 29*, 3184–3211.

Boulton, G. S., Dongelmans, P., Punkari, M. & Broadgate, M. 2001: Palaeoglaciology of an ice sheet through a glacial cycle: the European ice sheet through the Weichselian. *Quaternary Science Reviews 20*, 591–625.

Boulton, G. S., Hulton, N. & Vautravers, M. 1995: Ice-sheet models as tools for palaeoclimatic analysis: the example of the European ice sheet through the last glacial cycle. *Annals of Glaciology 21*, 103–110.

Boulton, G. S., Smith, G. D., Jones, A. S. & Newsome, J. 1985: Glacial geology and glaciology of the last mid-latitude ice sheets. *Journal of the Geological Society of London 142*, 447–474.

Bradwell, T., Fabel, D., Stoker, M., Mathers, H., McHargue, L. & Howe, J. 2008a: Ice caps existed throughout the Lateglacial interstadial in northern Scotland. *Journal of Quaternary Science 23*, 401–407.

Bradwell, T., Stoker, M. S., Golledge, N. R., Wilson, C. K., Merritt, J. W., Long, D., Everest, J. D., Hestvik, O. B., Stevenson, A. G., Hubbard, A. L., Finlayson, A. G. & Mathers, H. E. 2008b: The northern sector of the last British Ice Sheet: maximum extent and demise. *Earth-Science Reviews 88*, 207–226.

Brendryen, J., Haflidason, H., Rise, L., Chand, S., Vanneste, M., Longva, O., L'Heureux, J. S. & Forsberg, C. F. 2015: Ice sheet dynamics on the Lofoten-Vesterålen shelf, north Norway, from Late MIS-3 to Heinrich Stadial 1. *Quaternary Science Reviews 119*, 136–156.

Briner, J. P., Miller, G. H., Davis, P. T. & Finkel, R. C. 2006: Cosmogenic radionuclides from fiord landscapes support differential erosion by overriding ice sheets. *Geological Society of America Bulletin 118*, 406–420.

Briner, J. P., Young, N. E., Goehring, B. M. & Schaefer, J. M. 2012: Constraining Holocene ^{10}Be production rates in Greenland. *Journal of Quaternary Science 27*, 2–6.

Brown, E. J., Rose, J., Coope, R. G. & Lowe, J. J. 2007: An MIS 3 age organic deposit from Balglass Burn, central Scotland: palaeoenvironmental significance and implications for the timing of the onset of the LGM ice sheet in the vicinity of the British Isles. *Journal of Quaternary Science 22*, 295–308.

Cadman, V. 1996: *Glacimarine sedimentation and environments during the Late Weichselian and Holocene in the Bellsund Trough and Van Keulenfjorden, Svalbard*. Ph.D. thesis, University of Cambridge, UK.

Cato, I. 1985: The definitive connection of the Swedish geochronological time scale with the present, and the new date of the zero year in Döviken, northern Sweden. *Boreas 14*, 117–122.

Chiverrell, R. C., Thrasher, I. M., Thomas, G. S. P., Lang, A., Scourse, J. D., van Landeghem, K. J. J., Mccarroll, D., Clark, C. D., Ó Cofaigh, C., Evans, D. J. A. & Ballantyne, C. K. 2013: Bayesian modelling the retreat of the Irish Sea Ice Stream. *Journal of Quaternary Science 28*, 200–209.

Clark, C. D. 1997: Reconstructing the evolutionary dynamics of former ice sheets using multi-temporal evidence, remote sensing and GIS. *Quaternary Science Reviews 16*, 1067–1092.

Clark, C. D., Evans, D. J. A., Khatwa, A., Bradwell, T., Jordan, C. J., Marsh, S. H., Mitchell, W. A. & Bateman, M. D. 2004: Map and GIS database of glacial landforms and features related to the last British Ice Sheet. *Boreas 33*, 359–375.

Clark, C. D., Hughes, A. L. C., Greenwood, S. L., Jordan, C. & Sejrup, H. P. 2012: Pattern and timing of retreat of the last British-Irish Ice Sheet. *Quaternary Science Reviews 44*, 112–146.

Clark, P. U., Dyke, A. S., Shakun, J. D., Carlson, A. E., Clark, J., Wohlfarth, B., Mitrovica, J. X., Hostetler, S. W. & McCabe, A. M. 2009: The last glacial maximum. *Science 325*, 710–714.

Clason, C. C., Applegate, P. J. & Holmlund, P. 2014: Modelling Late Weichselian evolution of the Eurasian ice sheets forced by surface meltwater-enhanced basal sliding. *Journal of Glaciology 60*, 29–40.

Dahlgren, K. I. T. & Vorren, T. O. 2003: Sedimentary environment and glacial history during the last 40 ka of the Voring continental margin, mid-Norway. *Marine Geology 193*, 93–127.

Davies, B. J., Roberts, D. H., Bridgland, D. R. & Ó Cofaigh, C. 2012: Dynamic Devensian ice flow in NE England: a sedimentological reconstruction. *Boreas 41*, 337–366.

De Geer, G. 1935: The transbaltic extension of the Swedish Timescale. *Geografiska Annaler 17*, 533–549.

Demidov, I. N., Houmark-Nielsen, M., Kjær, K. H. & Larsen, E. 2006: The last Scandinavian Ice Sheet in northwestern Russia: ice flow patterns and decay dynamics. *Boreas 35*, 425–443.

Demidov, I. N., Houmark-Nielsen, M., Kjær, K. H., Larsen, E., Lyså, A., Funder, S., Lunkka, J.-P. & Saarnisto, M. 2004: Valdaian glacial maxima in the Arkhangelsk district of northwestern Russia. *In* Ehlers, J. & Gibbard, P. L. (eds.): *Quaternary Glaciations Extent and Chronology Part I: Europe*, 321–336. Elsevier, Amsterdam.

Dittmers, K., Niessen, F. & Stein, R. 2008: Acoustic facies on the inner Kara Sea Shelf: implications for Late Weichselian to Holocene sediment dynamics. *Marine Geology 254*, 197–215.

Donner, J. J. 1995: *The Quaternary History of Scandinavia*. 200 pp. Cambridge University Press, Cambridge.

Donner, J. J. 2010: The Younger Dryas age of the Salpausselkä moraines in Finland. *Bulletin of the Geological Society of Finland 82*, 69–80.

Donner, J., Jungner, H. & Kurtén, B. 1979: Radiocarbon dates of mammoth finds in Finland compared with radiocarbon dates of Weichselian and Eemian deposits. *Bulletin of the Geological Society of Finland 51*, 45–54.

Dowdeswell, J. A., Hogan, K. A., Evans, J., Noormets, R., Ó Cofaigh, C. & Ottesen, D. 2010: Past ice-sheet flow east of Svalbard inferred from streamlined subglacial landforms. *Geology 38*, 163–166.

Dowdeswell, J. A., Ottesen, D., Rise, L. & Craig, J. 2007: Identification and preservation of landforms diagnostic of past ice-sheet

activity on continental shelves from three-dimensional seismic evidence. *Geology 35*, 359–362.
Duller, G. A. T. 2006: Single grain optical dating of glacigenic deposits. *Quaternary Geochronology 1*, 296–304.
Duller, G. A. T. 2008: Single-grain optical dating of Quaternary sediments: why aliquot size matters in luminescence dating. *Boreas 37*, 589–612.
Dyke, A. S., Andrews, J. T., Clark, P. U., England, J. H., Miller, G. H., Shaw, J. & Veillette, J. J. 2002: The Laurentide and Innuitian ice sheets during the Last Glacial Maximum. *Quaternary Science Reviews 21*, 9–31.
Dzierżek, J. & Zreda, M. 2007: Timing and style of deglaciation of north eastern Poland from cosmogenic ^{36}Cl dating of glacial and glaciofluvial deposits. *Geological Quarterly 51*, 203–216.
Ehlers, J. & Gibbard, P. L. (eds.) 2004: *Quaternary Glaciations - Extent and Chronology, Part 1: Europe*. 475 pp. Elsevier, Amsterdam.
Ehlers, J., Gibbard, P. L. & Hughes, P. D. (eds.) 2011: *Quaternary Glaciations - Extent and Chronology: A Closer Look*. 1108 pp. Elsevier, Amsterdam.
Elliot, M., Labeyrie, L., Dokken, T. & Manthe, S. 2001: Coherent patterns of ice-rafted debris deposits in the Nordic regions during the last glacial (10-60 ka). *Earth and Planetary Science Letters 194*, 151–163.
Elverhøi, A., Andersen, E. S., Dokken, T., Hebbeln, D., Spielhagen, R., Svendsen, J. I., Sørflaten, M., Rørnes, A., Hald, M. & Forsberg, C. F. 1995: The growth and decay of the Late Weichselian ice sheet in western Svalbard and adjacent areas based on provenance studies of marine sediments. *Quaternary Research 44*, 303–316.
Elverhøi, A., Fjeldskaar, W., Solheim, A., Nylandberg, M. & Russwurm, L. 1993: The Barents Sea-Ice Sheet - a model of its growth and decay during the last ice maximum. *Quaternary Science Reviews 12*, 863–873.
England, J., Dyke, A. S., Coulthard, R. D., McNeely, R. & Aitken, A. 2013: The exaggerated radiocarbon age of deposit-feeding molluscs in calcareous environments. *Boreas 42*, 362–373.
Evans, D. J. A. & Thomson, S. A. 2010: Glacial sediments and landforms of Holderness, eastern England: a glacial depositional model for the North Sea Lobe of the British-Irish Ice Sheet. *Earth-Science Reviews 101*, 147–189.
Everest, J., Bradwell, T., Fogwill, C. J. & Kubik, P. W. 2006: Cosmogenic ^{10}Be age constraints for the Wester Ross readvance moraine: insights into British Ice-Sheet behaviour. *Geografiska Annaler, Series A 88*, 9–17.
Everest, J. D., Bradwell, T., Stoker, M. & Dewey, S. 2013: New age constraints for the maximum extent of the last British-Irish Ice Sheet (NW sector). *Journal of Quaternary Science 28*, 2–7.
Eyles, N., McCabe, A. M. & Bowen, D. Q. 1994: The stratigraphic and sedimentological significance of Late Devensian ice-sheet surging in Holderness, Yorkshire, UK. *Quaternary Science Reviews 13*, 727–759.
Fabel, D., Fink, D., Fredin, O., Harbor, J., Land, M. & Stroeven, A. P. 2006: Exposure ages from relict lateral moraines overridden by the Fennoscandian ice sheet. *Quaternary Research 65*, 136–146.
Fabel, D., Stroeven, A. P., Harbor, J., Kleman, J., Elmore, D. & Fink, D. 2002: Landscape preservation under Fennoscandian ice sheets determined from in situ produced ^{10}Be and ^{26}Al. *Earth and Planetary Science Letters 201*, 397–406.
Fenton, C. R., Hermanns, R. L., Blikra, L. H., Kubik, P. W., Bryant, C., Niedermann, S., Meixner, A. & Goethals, M. M. 2011: Regional ^{10}Be production rate calibration for the past 12 ka deduced from the radiocarbon-dated Grøtlandsura and Russenes rock avalanches at 69° N, Norway. *Quaternary Geochronology 6*, 437–452.
Fjellanger, J., Sørbel, L., Linge, H., Brook, E. J., Raisbeck, G. M. & Yiou, F. 2006: Glacial survival of blockfields on the Varanger Peninsula, northern Norway. *Geomorphology 82*, 255–272.
Flint, R. 1971: *Glacial and Quaternary Geology*. 906 pp. John Wiley and Sons, New York.
Forman, S. L., Lubinski, D., Miller, G. H., Matishov, G. G., Korsun, S., Snyder, J., Herlihy, F., Weihe, R. & Myslivets, V. 1996: Postglacial emergence of western Franz Josef Land, Russia, and retreat of the Barents Sea ice sheet. *Quaternary Science Reviews 15*, 77–90.
Forman, S. L., Lubinski, D., Miller, G. H., Snyder, J., Matishov, G., Korsun, S. & Myslivets, V. 1995: Postglacial emergence and distribution of late Weichselian ice-sheet loads in the northern Barents and Kara seas, Russia. *Geology 23*, 113–116.
Forman, S. L., Lubinski, D. J., Zeeberg, J. J., Polyak, L., Miller, G. H., Matishov, G. & Tarasov, G. 1999: Postglacial emergence and Late Quaternary glaciation on northern Novaya Zemlya, Arctic Russia. *Boreas 28*, 133–145.
Forman, S. L., Mann, D. H. & Miller, G. H. 1987: Late Weichselian and Holocene relative sea-level history of Broggerhalvoya, Spitsbergen. *Quaternary Research 27*, 41–50.
Forsström, P.-L., Sallasmaa, O., Greve, R. & Zwinger, T. 2003: Simulation of fast-flow features of the Fennoscandian ice sheet during the Last Glacial Maximum. *Annals of Glaciology 37*, 383–389.
Forwick, M. & Vorren, T. O. 2009: Late Weichselian and Holocene sedimentary environments and ice rafting in Isfjorden, Spitsbergen. *Palaeogeography, Palaeoclimatology, Palaeoecology 280*, 258–274.
Forwick, M. & Vorren, T. O. 2010: Stratigraphy and deglaciation of the Isfjorden area, Spitsbergen. *Norwegian Journal of Geology 90*, 163–179.
Fredén, C. 2009: *National Atlas of Sweden - Geology*. 208 pp. Norstedts, Stockholm.
Fredin, O., Rubensdotter, L., van Welden, A., Larsen, E. & Lyså, A. 2012: Distribution of ice marginal moraines in NW Russia. *Journal of Maps 8*, 236–241.
Funder, S., Kjeldsen, K. K., Kjær, K. & Ó Cofaigh, C. 2011: The Greenland Ice Sheet during the past 30,000 years: a review. *In* Ehlers, J., Gibbard, P. & Hughes, P. D. (eds.): *Quaternary Glaciations - Extent and Chronology: A Closer Look*, 699–714. Elsevier, Amsterdam.
Gataullin, V. & Polyak, L. 1997: Morainic Ridge Complex, Eastern Barents Sea. *In* Davies, T. A., Bell, T., Cooper, A. K., Josenhans, H., Polyak, L., Solheim, A., Stoker, M. S. & Stravers, J. A. (eds.): *Glaciated Continental Margins: An Atlas of Acoustic Images*, 82–83. Chapman and Hall, London.
Geirsdóttir, Á. 2011: Pliocene and Pleistocene glaciations of Iceland: a brief overview of the glacial history. *In* Ehlers, J., Gibbard, P. & Hughes, P. D. (eds.): *Quaternary Glaciations - Extent and Chronology: A Closer Look*, 199–210. Elsevier, Amsterdam.
Geyh, M. A. & Schleicher, H. 1990: *Absolute age Determination: Physical and Chemical Dating Methods and Their Application*. 503 pp. Springer-Verlag, Berlin.
Gjessing, J. 1966: Deglaciation of southeast and east-central Norway. *Norsk Geografisk Tidsskrift 20*, 133–149.
Glasser, N. F., Hughes, P. D., Fenton, C., Schnabel, C. & Rother, H. 2012: ^{10}Be and ^{26}Al exposure-age dating of bedrock surfaces on the Aran ridge, Wales: evidence for a thick Welsh Ice Cap at the Last Glacial Maximum. *Journal of Quaternary Science 27*, 97–104.
GLIMS 2005: Updated 2012. *GLIMS Glacier Database*. Boulder, Colorado. Available at: http://dx.doi.org/10.7265/N5V98602.
Goehring, B. M., Brook, E. J., Linge, H., Raisbeck, G. M. & Yiou, F. 2008: Beryllium-10 exposure ages of erratic boulders in southern Norway and implications for the history of the Fennoscandian Ice Sheet. *Quaternary Science Reviews 27*, 320–336.
Goehring, B. M., Lohne, Ø. S., Mangerud, J., Svendsen, J. I., Gyllencreutz, R., Schaefer, J. & Finkel, R. 2012: Late glacial and Holocene ^{10}Be production rates for western Norway. *Journal of Quaternary Science 27*, 89–96.
Golledge, N. R. 2010: Glaciation of Scotland during the Younger Dryas stadial: a review. *Journal of Quaternary Science 25*, 550–566.
Görsdorf, J. & Kaiser, K. 2001: Radiokohlenstoffdaten aus dem Spätpleistozän und Frühholozän von Mecklenburg-Vorpommern. *Meyniana 53*, 91–118.
Graham, A. G. C., Lonergan, L. & Stoker, M. S. 2007: Evidence for Late Pleistocene ice stream activity in the Witch Ground Basin, central North Sea, from 3D seismic reflection data. *Quaternary Science Reviews 26*, 627–643.
Graham, A. G. C., Lonergan, L. & Stoker, M. S. 2009: Seafloor glacial features reveal the extent and decay of the last British Ice Sheet, east of Scotland. *Journal Of Quaternary Science 24*, 117–138.

Graham, A. G. C., Stoker, M. S., Lonergan, L., Bradwell, T. & Stewart, M. A. 2011: The Pleistocene glaciations of the North Sea basin. *In* Ehlers, J., Gibbard, P. & Hughes, P. D. (eds.): *Quaternary Glaciations - Extent and Chronology: A Closer Look*, 261–278. Elsevier, Amsterdam.

Greenwood, S. L. & Clark, C. D. 2008: Subglacial bedforms of the Irish Ice Sheet. *Journal of Maps 2008*, 332–357.

Greenwood, S. L. & Clark, C. D. 2009a: Reconstructing the last Irish Ice Sheet 1: changing flow geometries and ice flow dynamics deciphered from the glacial landform record. *Quaternary Science Reviews 28*, 3085–3100.

Greenwood, S. L. & Clark, C. D. 2009b: Reconstructing the last Irish Ice Sheet 2: a geomorphologically-driven model of ice sheet growth, retreat and dynamics. *Quaternary Science Reviews 28*, 3101–3123.

Grigoriev, A., Zhamoida, V., Spiridonov, M., Sharapova, A., Sivkov, V. & Ryabchuk, D. 2011: Late-glacial and Holocene palaeoenvironments in the Baltic Sea based on a sedimentary record from the Gdansk Basin. *Climate Research 48*, 13–21.

Gyllencreutz, R., Mangerud, J., Svendsen, J.-I. & Lohne, Ø. S. 2007: DATED – A GIS-based reconstruction and dating database of the Eurasian deglaciation. *Geological Survey of Finland, Special Paper 46*, 113–120.

Hald, M., Saettem, J. & Nesse, E. 1990: Middle and Late Weichselian stratigraphy in shallow drillings from the southwestern Barents Sea - foraminiferal, amino-acid and radiocarbon evidence. *Norsk Geologisk Tidsskrift 70*, 241–257.

Hall, A. M., Peacock, J. D. & Connell, E. R. 2003: New data for the Last Glacial Maximum in Great Britain and Ireland: a Scottish perspective on the paper by Bowen et al. (2002). *Quaternary Science Reviews 22*, 1551–1554.

Harbor, J., Stroeven, A. P., Fabel, D., Clarhäll, A., Kleman, J., Li, Y., Elmore, D. & Fink, D. 2006: Cosmogenic nuclide evidence for minimal erosion across two subglacial sliding boundaries of the late glacial Fennoscandian ice sheet. *Geomorphology 75*, 90–99.

Heine, K., Reuther, A. U., Thieke, H. U., Schulz, R., Schlaak, N. & Kubik, P. W. 2009: Timing of Weichselian ice marginal positions in Brandenburg (northeastern Germany) using cosmogenic in situ ^{10}Be. *Zeitschrift für Geomorphologie 53*, 433–454.

Heyman, J. 2014: Paleoglaciation of the Tibetan Plateau and surrounding mountains based on exposure ages and ELA depression estimates. *Quaternary Science Reviews 91*, 30–41.

Heyman, J., Stroeven, A. P., Harbor, J. M. & Caffee, M. W. 2011: Too young or too old: evaluating cosmogenic exposure dating based on an analysis of compiled boulder exposure ages. *Earth and Planetary Science Letters 302*, 71–80.

Hibbert, F. D., Austin, W. E. N., Leng, M. J. & Gatliff, R. W. 2010: British Ice Sheet dynamics inferred from North Atlantic ice-rafted debris records spanning the last 175 000 years. *Journal of Quaternary Science 25*, 461–482.

Hirvas, H. & Kujansuu, R. 1979: On glacial, interstadial and interglacial deposits in Northern Finland. *IGCP Project 73/I/24 Quaternary Glaciations in the Northern Hemisphere: Report No. 5*, 146–164 pp. Prague.

Hogan, K. A., Dowdeswell, J. A., Noormets, R., Evans, J. & Ó Cofaigh, C. 2010: Evidence for full-glacial flow and retreat of the Late Weichselian Ice Sheet from the waters around Kong Karls Land, eastern Svalbard. *Quaternary Science Reviews 29*, 3563–3582.

Holmlund, P. & Fastook, J. 1995: A time-dependent glaciological model of the Weichselian ice-sheet. *Quaternary International 27*, 53–58.

Hormes, A., Gjermundsen, E. F. & Rasmussen, T. L. 2013: From mountain top to the deep sea – deglaciation in 4D of the northwestern Barents Sea ice sheet. *Quaternary Science Reviews 75*, 78–99.

Houmark-Nielsen, M. 2003: Signature and timing of the Kattegat Ice Stream: onset of the Last Glacial Maximum sequence at the southwestern margin of the Scandinavian Ice Sheet. *Boreas 32*, 227–241.

Houmark-Nielsen, M. 2004: The Pleistocene of Denmark: a review of stratigraphy and glaciation history. *In* Ehlers, J. & Gibbard, P. L. (eds.): *Quaternary Glaciations Extent and Chronology Part I: Europe*, 35–46. Elsevier, Amsterdam.

Houmark-Nielsen, M. 2008: Testing OSL failures against a regional Weichselian glaciation chronology from southern Scandinavia. *Boreas 37*, 660–677.

Houmark-Nielsen, M. 2010: Extent, age and dynamics of Marine Isotope Stage 3 glaciations in the southwestern Baltic Basin. *Boreas 39*, 343–359.

Houmark-Nielsen, M. & Kjær, K. H. 2003: Southwest Scandinavia, 40–15 kyr BP: palaeogeography and environmental change. *Journal of Quaternary Science 18*, 769–786.

Houmark-Nielsen, M., Björck, S. & Wohlfarth, B. 2006: 'Cosmogenic 10 Be ages on the Pomeranian Moraine, Poland': comments. *Boreas 35*, 600–604.

Houmark-Nielsen, M., Linge, H., Fabel, D., Schnabel, C., Xu, S., Wilcken, K. M. & Binnie, S. 2012: Cosmogenic surface exposure dating the last deglaciation in Denmark: discrepancies with independent age constraints suggest delayed periglacial landform stabilisation. *Quaternary Geochronology 13*, 1–17.

Hubbard, A., Bradwell, T., Golledge, N., Hall, A., Patton, H., Sugden, D., Cooper, R. & Stoker, M. 2009: Dynamic cycles, ice streams and their impact on the extent, chronology and deglaciation of the British-Irish ice sheet. *Quaternary Science Reviews 28*, 758–776.

Hughes, A. L. C., Clark, C. D. & Jordan, C. J. 2010: Subglacial bedforms of the last British Ice Sheet. *Journal of Maps 6*, 543–563.

Hughes, A. L. C., Clark, C. D. & Jordan, C. J. 2014: Flow-pattern evolution of the last British Ice Sheet. *Quaternary Science Reviews 89*, 148–168.

Hughes, A. L. C., Greenwood, S. L. & Clark, C. D. 2011: Dating constraints on the last British-Irish Ice Sheet: a map and database. *Journal of Maps 7*, 156–184.

Ingólfsson, Ó. & Landvik, J. Y. 2013: The Svalbard-Barents Sea icesheet – historical, current and future perspectives. *Quaternary Science Reviews 64*, 33–60.

Jacobi, R. M., Rose, J., MacLeod, A. & Higham, T. F. G. 2009: Revised radiocarbon ages on woolly rhinoceros (*Coelodonta antiquitatis*) from western central Scotland: significance for timing the extinction of woolly rhinoceros in Britain and the onset of the LGM in central Scotland. *Quaternary Science Reviews 28*, 2551–2556.

Jakobsson, M. 2002: Hypsometry and volume of the Arctic Ocean and its constituent seas. *Geochemistry Geophysics Geosystems 3*, 1–18.

Jakobsson, M., Andreassen, K., Bjarnadóttir, L. R., Dove, D., Dowdeswell, J. A., England, J. H., Funder, S., Hogan, K., Ingólfsson, Ó., Jennings, A., Larsen, N. K., Kirchner, N., Landvik, J. Y., Mayer, L., Mikkelsen, N., Möller, P., Niessen, F., Nilsson, J., O'Regan, M., Polyak, L., Nørgaard-Pedersen, N. & Stein, R. 2014: Arctic Ocean glacial history. *Quaternary Science Reviews 92*, 40–67.

Jakobsson, M., Björck, S., Alm, G., Andrén, T., Lindeberg, G. & Svensson, N.-O. 2007: Reconstructing the Younger Dryas ice dammed lake in the Baltic Basin: bathymetry, area and volume. *Global and Planetary Change 57*, 355–370.

Johnsen, T. F., Alexanderson, H., Fabel, D. & Freeman, S. P. H. T. 2009: New ^{10}Be cosmogenic ages from the Vimmerby moraine confirm the timing of Scandinavian ice sheet deglaciation in southern Sweden. *Geografiska Annaler, Series A, Physical Geography 91*, 113–120.

Johnsen, T. F., Olsen, L. & Murray, A. 2012: OSL ages in central Norway support a MIS 2 interstadial (25–20 ka) and a dynamic Scandinavian ice sheet. *Quaternary Science Reviews 44*, 96–111.

Kalm, V. 2005: Chronological data from Estonian Pleistocene. *Proceedings of the Estonian Academy of Sciences, Geology 54*, 5–25.

Kalm, V. 2006: Pleistocene chronostratigraphy in Estonia, southeastern sector of the Scandinavian glaciation. *Quaternary Science Reviews 25*, 960–975.

Kalm, V. 2012: Ice-flow pattern and extent of the last Scandinavian Ice Sheet southeast of the Baltic Sea. *Quaternary Science Reviews 44*, 51–59.

Kind, N. V. & Leonov, B. N. 1982: *The Antropogen of the Taimyr Peninsula*. 184 pp. Nauka, Moscow. (in Russian).

King, E. L., Haflidason, H., Sejrup, H. P. & Løvlie, R. 1998: Glacigenic debris flows on the North Sea Trough Mouth Fan during ice stream maxima. *Marine Geology 152*, 217–246.

Kjær, K., Larsen, E., Funder, S., Demidov, I., Jensen, M., Håkansson, L. & Murray, A. 2006a: Eurasian ice-sheet interaction in northwestern Russia throughout the late Quaternary. *Boreas 35*, 444–475.

Kjær, K. H., Houmark-Nielsen, M. & Richardt, N. 2003: Ice-flow patterns and dispersal of erratics at the southwestern margin of the last Scandinavian Ice Sheet: signature of palaeo-ice streams. *Boreas 32*, 130–148.

Kjær, K. H., Lagerlund, E., Adrielsson, L., Thomas, P., Murray, A. & Sandgren, P. 2006b: The first independent chronology for Middle and Late Weichselian sediments from southern Sweden and the Island of Bornholm. *GFF 128*, 209–220.

Kleiber, H. P., Knies, J. & Niessen, F. 2000: The Late Weichselian glaciation of the Franz Victoria Trough, northern Barents Sea: ice sheet extent and timing. *Marine Geology 168*, 25–44.

Kleman, J., Hättestrand, C., Borgström, I. & Stroeven, A. 1997: Fennoscandian palaeoglaciology reconstructed using a glacial geological inversion model. *Journal of Glaciology 43*, 283–299.

Klitgaard Kristensen, D., Rasmussen, T. L. & Koç, N. 2013: Palaeoceanographic changes in the northern Barents Sea during the last 16 000 years - new constraints on the last deglaciation of the Svalbard-Barents Sea Ice Sheet. *Boreas 42*, 798–813.

Knies, J., Kleiber, H. P., Matthiessen, J., Muller, C. & Nowaczyk, N. 2001: Marine ice-rafted debris records constrain maximum extent of Saalian and Weichselian ice-sheets along the northern Eurasian margin. *Global and Planetary Change 31*, 45–64.

Knudsen, C. G. 2006: *Glacier dynamics and Lateglacial environmental changes – evidences from SW Norway and Iceland*. Ph.D. thesis, University of Bergen.

Kolstrup, E. & Olsen, L. 2012: Palaeoenvironmental developments in the central Scandinavian mountains during deglaciation – a discussion. *Norsk Geografisk Tidsskrift - Norwegian Journal of Geography 66*, 30–51.

Korpela, K. 1969: Die Weichsel-Eiszeit und ihr Interstadial in Peräpohjola (nördliches Nordfinnland) im Licht von submoränen Sedimenten. *Annales Academiæ Scientiarum Fennicae, Series A III 99*, 1–108.

Kramarska, R. 1998: Origin and development of the Odra Bank in the light of the geologic structure and radiocarbon dating. *Geological Quarterly 42*, 277.

Krohn, C. F., Larsen, N. K., Kronborg, C., Nielsen, O. B. & Knudsen, K. L. 2009: Litho- and chronostratigraphy of the Late Weichselian in Vendsyssel, northern Denmark with special emphasis on tunnel-valley infill in relation to a receding ice margin. *Boreas 38*, 811–833.

Kujansuu, R. 1975: Interstadial esker at Marrasjärvi, Finnish Lapland. *Geologi 27*, 45–50 (in Finnish).

Lagerbäck, R. & Robertsson, A.-M. 1988: Kettle holes - stratigraphical archives for Weichselian geology and palaeoenvironment in northernmost Sweden. *Boreas 17*, 439–468.

Lal, D. 1991: Cosmic ray labeling of erosion surfaces: in situ nuclide production rates and erosion models. *Earth and Planetary Science Letters 104*, 424–439.

Lambeck, K., Purcell, A., Zhao, J. & Svensson, N. O. 2010: The Scandinavian Ice Sheet: from MIS 4 to the end of the Last Glacial Maximum. *Boreas 39*, 410–435.

Landvik, J. Y., Alexanderson, H., Henriksen, M. & Ingólfsson, Ó. 2014: Landscape imprints of changing glacial regimes during ice-sheet build-up and decay: a conceptual model from Svalbard. *Quaternary Science Reviews 92*, 258–268.

Landvik, J. Y., Bondevik, S., Elverhøi, A., Fjeldskaar, W., Mangerud, J., Salvigsen, O., Siegert, M. J., Svendsen, J. I. & Vorren, T. O. 1998: The Last Glacial Maximum of Svalbard and the Barents Sea area: ice sheet extent and configuration. *Quaternary Science Reviews 17*, 43–75.

Landvik, J. Y., Brook, E. J., Gualtieri, L., Linge, H., Raisbeck, G., Salvigsen, O. & Yiou, F. 2013: ^{10}Be exposure age constraints on the Late Weichselian ice-sheet geometry and dynamics in inter-ice-stream areas, western Svalbard. *Boreas 42*, 43–56.

Landvik, J. Y., Ingólfsson, Ó., Mienert, J., Lehman, S. J., Solheim, A., Elverhøi, A. & Ottesen, D. 2005: Rethinking Late Weichselian ice-sheet dynamics in coastal NW Svalbard. *Boreas 34*, 7–24.

Larsen, E., Eide, F., Longva, O. & Mangerud, J. 1984: Allerod-Younger Dryas climatic inferences from cirque glaciers and vegetational development in the Nordfjord area, Western Norway. *Arctic and Alpine Research 16*, 137–160.

Larsen, E., Fredin, O., Jensen, M., Kuznetsov, D., Lyså, A. & Subetto, D. 2014: Subglacial sediment, proglacial lake-level and topographic controls on ice extent and lobe geometries during the Last Glacial Maximum in NW Russia. *Quaternary Science Reviews 92*, 369–387.

Larsen, E., Kjær, K., Demidov, I., Funder, S., Grøsfjeld, K., Houmark-Nielsen, M., Jensen, M., Linge, H. & Lyså, A. 2006: Late Pleistocene glacial and lake history of northwestern Russia. *Boreas 35*, 394–424.

Larsen, N. K., Knudsen, K. L., Krohn, C. F., Ronborg, C., Murray, A. S. & Nielsen, O. B. 2009b: Late Quaternary ice sheet, lake and sea history of southwest Scandinavia - a synthesis. *Boreas 38*, 732–761.

Larsen, N. K., Krohn, C. F., Kronborg, C., Nielsen, O. B. & Knudsen, K. L. 2009a: Lithostratigraphy of the Late Saalian to Middle Weichselian Skærumhede Group in Vendsyssel, northern Denmark. *Boreas 38*, 762–786.

Larsen, N. K., Linge, H., Håkansson, L. & Fabel, D. 2012: Investigating the last deglaciation of the Scandinavian Ice Sheet in southwest Sweden with ^{10}Be exposure dating. *Journal of Quaternary Science 27*, 211–220.

Lasberg, K. & Kalm, V. 2013: Chronology of Late Weichselian glaciation in the western part of the East European Plain. *Boreas 42*, 995–1007.

Linge, H., Brook, E. J., Nesje, A., Raisbeck, G. M., Yiou, F. & Clark, H. 2006: In situ ^{10}Be exposure ages from southeastern Norway: implications for the geometry of the Weichselian Scandinavian ice sheet. *Quaternary Science Reviews 25*, 1097–1109.

Linge, H., Olsen, L., Brook, E. J., Darter, J. R., Mickelson, D. M., Raisbeck, G. M. & Yiou, F. 2007: Cosmogenic nuclide surface exposure ages from Nordland, northern Norway: implications for deglaciation in a coast to inland transect. *Norwegian Journal of Geology 87*, 269–280.

Lohne, Ø. S., Mangerud, J. A. N. & Birks, H. H. 2013: Precise ^{14}C ages of the Vedde and Saksunarvatn ashes and the Younger Dryas boundaries from western Norway and their comparison with the Greenland Ice Core (GICC05) chronology. *Journal of Quaternary Science 28*, 490–500.

Lohne, Ø. S., Mangerud, J. & Svendsen, J. I. 2012: Timing of the Younger Dryas glacial maximum in western Norway. *Journal of Quaternary Science 27*, 81–88.

Lowe, J. J. & Walker, M. J. C. 1976: Radiocarbon-dates and deglaciation of Rannoch Moor, Scotland. *Nature 264*, 632–633.

Lowe, J. J., Birks, H. H., Brooks, S. J., Coope, G. R., Harkness, D. D., Mayle, F. E., Sheldrick, C., Turney, C. S. M. & Walker, M. J. C. 1999: The chronology of palaeoenvironmental changes during the Last Glacial-Holocene transition: towards an event stratigraphy for the British Isles. *Journal of the Geological Society, London 156*, 397–410.

Lubinski, D., Polyak, L. & Forman, S. 2001: Freshwater and Atlantic water inflows to the deep northern Barents and Kara seas since ca 13 ^{14}C ka: foraminifera and stable isotopes. *Quaternary Science Reviews 20*, 1851–1879.

Lubinski, D. J., Korsun, S., Polyak, L., Forman, S. L., Lehman, S. J., Herlihy, F. A. & Miller, G. F. 1996: The last deglaciation of the Franz Victoria Trough, northern Barents Sea. *Boreas 25*, 89–100.

Lundqvist, J. 1972: Ice-lake types and deglaciation pattern along the Scandinavian mountain range. *Boreas 1*, 27–54.

Lundqvist, J. & Mejdahl, V. 1995: Luminescence dating of the deglaciation in northern Sweden. *Quaternary International 28*, 193–197.

Lundqvist, J. & Wohlfarth, B. 2001: Timing and east-west correlation of south Swedish ice marginal lines during the Late Weichselian. *Quaternary Science Reviews 20*, 1127–1148.

Lunkka, J.-P., Putkinen, N. & Miettinen, A. 2012: Shoreline displacement in the Belomorsk area, NW Russia during the Younger Dryas Stadial. *Quaternary Science Reviews 37*, 26–37.

Lunkka, J. P., Saarnisto, M., Gey, V., Demidov, I. & Kiselova, V. 2001: Extent and age of the Last Glacial Maximum in the southeastern sector of the Scandinavian Ice Sheet. *Global and Planetary Change 31*, 407–425.

Lüthgens, C. & Böse, M. 2011: Chronology of Weichselian main ice marginal positions in north-eastern Germany. *Eiszeitalter und Gegenwart 60*, 236–247.

Lüthgens, C. & Böse, M. 2012: From morphostratigraphy to geochronology – on the dating of ice marginal positions. *Quaternary Science Reviews 44*, 26–36.

Lüthgens, C., Böse, M. & Krbetschek, M. 2010: On the age of the young morainic morphology in the area ascribed to the maximum extent of the Weichselian glaciation in north-eastern Germany. *Quaternary International 222*, 72–79.

Lüthgens, C., Böse, M. & Preusser, F. 2011: Age of the Pomeranian ice-marginal position in northeastern Germany determined by Optically Stimulated Luminescence (OSL) dating of glaciofluvial sediments. *Boreas 40*, 598–615.

Lyså, A., Demidov, I., Houmark-Nielsen, M. & Larsen, E. 2001: Late Pleistocene stratigraphy and sedimentary environment of the Arkhangelsk area, northwest Russia. *Global and Planetary Change 31*, 179–199.

Lyså, A., Jensen, M. A., Larsen, E., Fredin, O. & Demidov, I. N. 2011: Ice-distal landscape and sediment signatures evidencing damming and drainage of large pro-glacial lakes, northwest Russia. *Boreas 40*, 481–497.

Lyså, A., Larsen, E., Buylaert, J.-P., Fredin, O., Jensen, M. A., Kuznetsov, D., Murray, A. S., Subetto, D. A. & van Welden, A. 2014: Late Pleistocene stratigraphy and sedimentary environments of the Severnaya Dvina-Vychegda region in northwestern Russia. *Boreas 43*, 759–779.

MacLeod, A., Palmer, A., Lowe, J., Rose, J., Bryant, C. & Merritt, J. 2011: Timing of glacier response to Younger Dryas climatic cooling in Scotland. *Global and Planetary Change 79*, 264–274.

Mangerud, J. 1972: Radiocarbon dating of marine shells, including a discussion of apparent age of Recent shells from Norway. *Boreas 1*, 143–172.

Mangerud, J. 2000: Was Hardangerfjorden, western Norway, glaciated during the Younger Dryas? *Norsk Geologisk Tidsskrift 80*, 229–234.

Mangerud, J. 2004: Ice sheet limits on Norway and the Norwegian continental shelf. *In* Ehlers, J. & Gibbard, P. (eds.): *Quaternary Glaciations - Extent and Chronology. Vol. 1 Europe*, 271–294. Elsevier, Amsterdam.

Mangerud, J. 2008: Scandinavian Ice Sheet. *In* Gornitz, V. (ed.): *Encylopedia of Paleoclimatology and Ancient Environments*, 877–879. Springer, Dordrecht.

Mangerud, J. & Gulliksen, S. 1975: Apparent radiocarbon ages of recent marine shells from Norway, Spitsbergen, and Arctic Canada. *Quaternary Research 5*, 263–273.

Mangerud, J. & Landvik, J. Y. 2007: Younger Dryas cirque glaciers in western Spitsbergen: smaller than during the Little Ice Age. *Boreas 36*, 278–285.

Mangerud, J., Bolstad, M., Elgersma, A., Helliksen, D., Landvik, J. Y., Lonne, I., Lycke, A. K., Salvigsen, O., Sandahl, T. & Svendsen, J. I. 1992: The Last Glacial Maximum on Spitsbergen, Svalbard. *Quaternary Research 38*, 1–31.

Mangerud, J., Bondevik, S., Gulliksen, S., Karin Hufthammer, A. & Høisæter, T. 2006: Marine ^{14}C reservoir ages for 19th century whales and molluscs from the North Atlantic. *Quaternary Science Reviews 25*, 3228–3245.

Mangerud, J., Dokken, T., Hebbeln, D., Heggen, B., Ingólfsson, Ó., Landvik, J. Y., Mejdahl, V., Svendsen, J. I. & Vorren, T. O. 1998: Fluctuations of the Svalbard-Barents Sea ice sheet during the last 150,000 years. *Quaternary Science Reviews 17*, 11–42.

Mangerud, J., Goehring, B. M., Lohne, Ø. S., Svendsen, J. I. & Gyllencreutz, R. 2013: Collapse of marine-based outlet glaciers from the Scandinavian Ice Sheet. *Quaternary Science Reviews 67*, 8–16.

Mangerud, J., Gosse, J., Matiouchkovc, A. & Dolvik, T. 2008b: Glaciers in the Polar Urals, Russia, were not much larger during the Last Global Glacial Maximum than today. *Quaternary Science Reviews 27*, 1047–1057.

Mangerud, J., Gulliksen, S. & Larsen, E. 2010: ^{14}C-dated fluctuations of the western flank of the Scandinavian Ice Sheet 45-25 kyr BP compared with Bølling-Younger Dryas fluctuations and Dansgaard-Oeschger events in Greenland. *Boreas 39*, 328–342.

Mangerud, J., Gyllencreutz, R., Lohne, Ø. & Svendsen, J. I. 2011: Glacial history of Norway. *In* Ehlers, J., Gibbard, P. & Hughes, P. D. (eds.): *Quaternary Glaciations - Extent and Chronology: A Closer Look*, 279–298. Elsevier, Amsterdam.

Mangerud, J., Jakobsson, M., Alexanderson, H., Astakhov, V., Clarke, G. K. C., Henriksen, M., Hjort, C., Krinner, G., Lunkka, J. P., Moller, P., Murray, A., Nikolskaya, O., Saarnisto, M. & Svendsen, J. I. 2004: Ice-dammed lakes and rerouting of the drainage of northern Eurasia during the Last Glaciation. *Quaternary Science Reviews 23*, 1313–1332.

Mangerud, J., Kaufman, D., Hansen, J. & Svendsen, J. I. 2008a: Ice-free conditions in Novaya Zemlya 35,000 to 30,000 cal years BP, as indicated by radiocarbon ages and amino acid racemization evidence from marine molluscs. *Polar Research 27*, 187–208.

Mangerud, J., Løvlie, R., Gulliksen, S., Hufthammer, A.-K., Larsen, E. & Valen, V. 2003: Paleomagnetic correlations between Scandinavian ice-sheet fluctuations and Greenland Dansgaard–Oeschger events, 45000–25000 yr B.P. *Quaternary Research 59*, 213–222.

Mannerfelt, C. M. S. 1940: Glacialmorfologiska studier i norska högfjäll. *Norsk Geografisk Tidsskrift 8*, 9–47.

Mannerfelt, C. M. S. 1945: Några glacialmorfologiska formelement. *Geografiska Annaler, SeriesA 27*, 1–239.

Marks, L. 2011: Quaternary glaciations in Poland. *In* Ehlers, J., Gibbard, P. & Hughes, P. D. (eds.): *Quaternary Glaciations - Extent and Chronology: A Closer Look*, 299–304. Elsevier, Amsterdam.

Marks, L. 2012: Timing of the Late Vistulian (Weichselian) glacial phases in Poland. *Quaternary Science Reviews 44*, 81–88.

Möller, P., Alexanderson, H., Funder, S. & Hjort, C. 2015: The Taimyr Peninsula and the Severnaya Zemlya archipelago, Arctic Russia: a synthesis of glacial history and palaeo-environmental change during the Last Glacial cycle (MIS 5e-2). *Quaternary Science Reviews 107*, 149–181.

Möller, P., Bolshiyanov, D. Y. & Bergsten, H. 1999: Weichselian geology and palaeoenvironmental history of the central Taymyr Peninsula, Siberia, indicating no glaciation during the last global glacial maximum. *Boreas 28*, 92–114.

Möller, P., Lubinski, D. J., Ingólfsson, Ó., Forman, S. L., Seidenkrantz, M.-S., Bolshiyanov, D. Y., Lokrantz, H., Antonov, O., Pavlov, M., Ljung, K., Zeeberg, J. J. & Andreev, A. 2007: Erratum to: Severnaya Zemlya, Arctic Russia: a nucleation area for Kara Sea ice sheets during the Middle to Late Quaternary: [Quaternary Science Reviews 25 (21–22) (2006) 2894–2936]. *Quaternary Science Reviews 26*, 1149–1191.

Möller, P., Östlund, O., Barnekow, L., Sandgren, P., Palmbo, F. & Willerslev, E. 2013: Living at the margin of the retreating Fennoscandian Ice Sheet: the early Mesolithic sites at Aareavaara, northernmost Sweden. *The Holocene 23*, 104–116.

Nesje, A., Dahl, S. O. & Bakke, J. 2004: Were abrupt Lateglacial and early-Holocene climatic changes in northwest Europe linked to freshwater outbursts to the North Atlantic and Arctic Oceans? *The Holocene 14*, 299–310.

Nesje, A., Dahl, S. O., Linge, H., Ballantyne, C. K., McCarroll, D., Brook, E. J., Raisbeck, G. M. & Yiou, F. 2007: The surface geometry of the Last Glacial Maximum ice sheet in the Andøya-Skånland region, northern Norway, constrained by surface exposure dating and clay mineralogy. *Boreas 36*, 227–239.

Nygård, A., Sejrup, H. P., Haflidason, H. & Bryn, P. 2005: The glacial North Sea Fan, southern Norwegian Margin: architecture and evolution from the upper continental slope to the deep-sea basin. *Marine and Petroleum Geology 22*, 71–84.

Nygård, A., Sejrup, H. P., Haflidason, H., Cecchi, M. & Ottesen, D. 2004: Deglaciation history of the southwestern Fennoscandian Ice Sheet between 15 and 13 ^{14}C ka BP. *Boreas 33*, 1–17.

Ó Cofaigh, C. & Evans, D. J. A. 2007: Radiocarbon constraints on the age of the maximum advance of the British-Irish Ice Sheet in the Celtic Sea. *Quaternary Science Reviews 26*, 1197–1203.

Ó Cofaigh, C., Telfer, M. W., Bailey, R. M. & Evans, D. J. A. 2012: Late Pleistocene chronostratigraphy and ice sheet limits, southern Ireland. *Quaternary Science Reviews 44*, 160–179.

Olsen, L. & Hammer, Ø. 2005: A 6-ka climatic cycle during at least the last 50,000 years. *Norges Geologiske Undersøkelse, Bulletin 445*, 89–100.

Olsen, L., Mejdahl, V. & Selvik, S. F. 1996: Middle and late Pleistocene stratigraphy, chronology and glacial history in Finnmark, north Norway. *Norges Geologiske Undersøkelse, Bulletin 429*, 1–111.

Olsen, L., Sveian, H., van der Borg, K., Bergstrøm, B. & Broekmans, M. 2002: Rapid and rhythmic ice sheet fluctuations in western Scandinavia 15-40 kyr - a review. *Polar Research 21*, 235–242.

Olsen, L. O., Van der Borg, K., Bergström, B., Sveian, H., Lauritzen, S. E. & Hansen, G. 2001: AMS radiocarbon dating of glacigenic sediments with low organic carbon content - an important tool for reconstructing the history of glacial variations in Norway. *Norwegian Journal of Geology 81*, 59–92.

Olsen, L. R., Fredin, O. & Olesen, O. (eds.) 2013: *Quaternary geology of Norway.* 173 pp. Geological Survey of Norway.

Ottesen, D. & Dowdeswell, J. A. 2006: Assemblages of submarine landforms produced by tidewater glaciers in Svalbard. *Journal of Geophysical Research 111*, F01016, doi: 10.1029/2005JF000330.

Ottesen, D. & Dowdeswell, J. A. 2009: An inter-ice-stream glaciated margin: submarine landforms and a geomorphic model based on marine-geophysical data from Svalbard. *Geological Society of America Bulletin 121*, 1647–1665.

Ottesen, D., Dowdeswell, J. A., Benn, D. I., Kristensen, L., Christiansen, H. H., Christensen, O., Hansen, L., Lebesbye, E., Forwick, M. & Vorren, T. O. 2008: Submarine landforms characteristic of glacier surges in two Spitsbergen fjords. *Quaternary Science Reviews 27*, 1583–1599.

Ottesen, D., Dowdeswell, J. A., Landvik, J. Y. & Mienert, J. 2007: Dynamics of the Late Weichselian ice sheet on Svalbard inferred from high-resolution sea-floor morphology. *Boreas 36*, 286–306.

Ottesen, D., Dowdeswell, J. A., Rise, L., Rokoengen, K. & Henriksen, S. 2002: Large-scale morphological evidence for past ice-stream flow on the mid-Norwegian continental margin. *Geological Society, London, Special Publications 203*, 245–258.

Pasanen, A., Lunkka, J. P. & Putkinen, N. 2010: Reconstruction of the White Sea Basin during the late Younger Dryas. *Boreas 39*, 273–285.

Påsse, T. 1992: Erratic flint along the Swedish west coast. *Geologiska Föreningens i Stockholm Förhandlingar 114*, 271–278.

Paterson, W. S. B. 1994: *The Physics of Glaciers.* 480 pp. Elsevier Science Ltd., Oxford.

Paus, A., Velle, G. & Berge, J. 2011: The Lateglacial and early Holocene vegetation and environment in the Dovre mountains, central Norway, as signalled in two Lateglacial nunatak lakes. *Quaternary Science Reviews 30*, 1780–1796.

Payne, A. J. & Baldwin, D. J. 1999: Thermomechanical modelling of the Scandinavian ice sheet: implications for ice-stream formation. *Annals of Glaciology 28*, 83–89.

Pazdur, M. F., Awsiuk, R., Bluszcz, A., Pazdur, A., Walanus, A. & Zastawny, A. 1983: Gliwice radiocarbon dates IX. *Radiocarbon 25*, 843–866.

Polyak, L., Lehman, S. J., Gataullin, V. & Jull, A. J. T. 1995: Two step deglaciation of the southern Barents Sea. *Geology 23*, 567–571.

Polyak, L., Niessen, F., Gataullin, V. & Gainanov, V. 2008: The eastern extent of the Barents-Kara ice sheet during the Last Glacial Maximum based on seismic-reflection data from the eastern Kara Sea. *Polar Research 27*, 162–174.

Punkari, M. 1997: Glacial and glaciofluvial deposits in the interlobate areas of the Scandinavian Ice Sheet. *Quaternary Science Reviews 16*, 741–753.

Rainio, H., Saarnisto, M. & Ekman, I. 1995: Younger-Dryas end moraines in Finland and NW Russia. *Quaternary International 28*, 179–192.

Rasmussen, S. O., Andersen, K. K., Svensson, A. M., Steffensen, J. P., Vinther, B. M., Clausen, H. B., Siggaard-Andersen, M. L., Johnsen, S. J., Larsen, L. B., Dahl-Jensen, D., Bigler, M., Röthlisberger, R., Fischer, H., Goto-Azuma, K., Hansson, M. E. & Ruth, U. 2006: A new Greenland ice core chronology for the last glacial termination. *Journal of Geophysical Research 111*, D06102, doi: 10.1029/2005JD006079.

Rasmussen, T. L., Thomsen, E., Ślubowska, M. A., Jessen, S., Solheim, A. & Koç, N. 2007: Paleoceanographic evolution of the SW Svalbard margin (76°N) since 20,000 ^{14}C yr BP. *Quaternary Research 67*, 100–114.

Raukas, A. 2004: Application of OSL and ^{10}Be techniques to the establishment of deglaciation chronology in Estonia. *Proceedings of the Estonian Academy of Science Geology 53*, 267–287.

Raukas, A. & Stankowski, W. 2005: Influence of sedimentological composition on OSL dating of glaciofluvial deposits: examples from Estonia. *Geological Quarterly 49*, 463–470.

Raukas, A., Stankowski, W., Zelčs, V. & Šinkunas, P. 2010: Chronology of the last deglaciation in the southeastern Baltic region on the basis of recent OSL dates. *Geochronometria 36*, 1–8.

Raunholm, S., Larsen, E. & Sejrup, H. P. 2004: Weichselian interstadial sediments on Jæren (SW Norway) – paleoenvironments and implications for ice sheet configuration. *Norwegian Journal of Geology 84*, 91–106.

Reimer, P. J., Bard, E., Bayliss, A., Beck, J. W., Blackwell, P. G., Bronk Ramsey, C., Buck, C. E., Cheng, H., Edwards, R. L., Friedrich, M., Grootes, P. M., Guilderson, T. P., Haflidason, H., Hajdas, I., Hatté, C., Heaton, T. J., Hoffmann, D. L., Hogg, A. G., Hughen, K. A., Kaiser, K. F., Kromer, B., Manning, S. W., Niu, M., Reimer, R. W., Richards, D. A., Scott, E. M., Southon, J. R., Staff, R. A., Turney, C. S. M. & van der Plicht, J. 2013: IntCal13 and Marine13 radiocarbon age calibration curves 0–50,000 years cal BP. *Radiocarbon 55*, 1869–1887.

Reite, A. J. 1994: Weichselian and Holocene geology of Sør-Trøndelag and adjacent parts of Nord-Trøndelag county, Central Norway. *Norges Geologiske Undersøkelse, Bulletin 426*, 1–30.

Rinterknecht, V., Braucher, R., Böse, M., Bourlès, D. & Mercier, J. L. 2012: Late Quaternary ice sheet extents in northeastern Germany inferred from surface exposure dating. *Quaternary Science Reviews 44*, 89–95.

Rinterknecht, V. R., Clark, P. U., Raisbeck, G. M., Yiou, F., Bitinas, A., Brook, E. J., Marks, L., Zelčs, V., Lunkka, J. P., Pavlovskaya, I. E., Piotrowski, J. A. & Raukas, A. 2006: The last deglaciation of the southeastern sector of the Scandinavian Ice Sheet. *Science 311*, 1449–1452.

Rinterknecht, V., Marks, L., Piotrowski, J., Raisbeck, G., Yiou, F., Brook, E. & Clark, P. 2005: Cosmogenic ^{10}Be ages on the Pomeranian moraine, Poland. *Boreas 34*, 186–191.

Rise, L. & Rokoengen, K. 1984: Surficial sediments in the Norwegian sector of the North Sea between 60°30′ and 62°N. *Marine Geology 58*, 287–317.

Roberts, D. H., Evans, D. J. A., Lodwick, J. & Cox, N. J. 2013: The subglacial and ice-marginal signature of the North Sea Lobe of the British-Irish Ice Sheet during the Last Glacial Maximum at Upgang, North Yorkshire, UK. *Proceedings of the Geologists Association 124*, 503–519.

Rokoengen, K. & Frengstad, B. 1999: Radiocarbon and seismic evidence of ice-sheet extent and the last deglaciation on the mid-Norwegian continental shelf. *Norsk Geografisk Tidsskrift 79*, 129–132.

Rokoengen, K., Løfaldli, M., Rise, L., Løken, T. & Carlsen, R. 1982: Description and dating of a submerged beach in the northern North Sea. *Marine Geology 50*, M21–M28.

Romundset, A., Bondevik, S. & Bennike, O. 2011: Postglacial uplift and relative sea level changes in Finnmark, northern Norway. *Quaternary Science Reviews 30*, 2398–2421.

Rørvik, K. L., Laberg, J. S., Hald, M., Ravna, E. K. & Vorren, T. O. 2010: Behavior of the northwestern part of the Fennoscandian Ice Sheet during the Last Glacial Maximum – a response to external forcing. *Quaternary Science Reviews 29*, 2224–2237.

Rubensdotter, L. & Rosqvist, G. 2009: Influence of geomorphological setting, fluvial-, glaciofluvial- and mass-movement processes on sedimentation in alpine lakes. *The Holocene 19*, 665–678.

Rüther, D. C., Bjarnadóttir, L. R., Junttila, J., Husum, K., Rasmussen, T. L., Lucchi, R. G. & Andreassen, K. 2012: Pattern and timing of the northwestern Barents Sea Ice Sheet deglaciation and indications of episodic Holocene deposition. *Boreas 41*, 494–512.

Rüther, D. C., Mattingsdal, R., Andreassen, K., Forwick, M. & Husum, K. 2011: Seismic architecture and sedimentology of a major grounding zone system deposited by the Bjørnøyrenna Ice Stream during Late Weichselian deglaciation. *Quaternary Science Reviews 30*, 2776–2792.

Saarnisto, M. & Lunkka, J. P. 2004: Climate variability during the last interglacial-glacial cycle in NW Eurasia. *In* Battarbee, R. W. (ed): *Past Climate Variability through Europe and Africa*, 443–464. Springer, Dordrecht.

Saarnisto, M. & Saarinen, T. 2001: Deglaciation chronology of the Scandinavian Ice Sheet from the Lake Onega Basin to the Salpausselka End Moraines. *Global and Planetary Change 31*, 387–405.

Saarnisto, M., Gronlund, T. & Ekman, I. 1995: Lateglacial of Lake Onega - contribution to the history of the Eastern Baltic Basin. *Quaternary International 27*, 111–120.

Saarse, L., Heinsalu, A. & Veski, S. 2012: Deglaciation chronology of the Pandivere and Palivere ice-marginal zones in Estonia. *Geological Quarterly 56*, 353–362.

Saks, T., Kalvans, A. & Zelcs, V. 2012: OSL dating of Middle Weichselian age shallow basin sediments in Western Latvia, Eastern Baltic. *Quaternary Science Reviews 44*, 60–68.

Salvigsen, O. 1977: Radiocarbon datings and the extension of the Weichselian ice-sheet in Svalbard. *Norsk Polarinstitutt Årbok 1976*, 209–224.

Salvigsen, O. & Elgersma, A. 1993: Radiocarbon dating of deglaciation and raised beaches in north-western Sørkapp Land, Spitsbergen, Svalbard. *Prace Geograficzne 94*, 39–47.

Scourse, J. D., Haapaniemi, A. I., Colmenero-Hidalgo, E., Peck, V. L., Hall, I. R., Austin, W. E. N., Knutz, P. C. & Zahn, R. 2009: Growth, dynamics and deglaciation of the last British-Irish ice sheet: the deep-sea ice-rafted detritus record. *Quaternary Science Reviews 28*, 3066–3084.

Sejrup, H. P., Haflidason, H., Aarseth, I., King, E., Forsberg, C. F., Long, D. & Rokoengen, K. 1994: Late Weichselian glaciation history of the northern North Sea. *Boreas 23*, 1–13.

Sejrup, H. P., Hjelstuen, B. O., Nygård, A., Haflidason, H. & Mardal, I. 2015: Late Devensian ice-marginal features in the central North Sea - processes and chronology. *Boreas 44*, 1–13.

Sejrup, H. P., Hjelstuen, B. O., Torbjørn Dahlgren, K. I., Haflidason, H., Kuijpers, A., Nygård, A., Praeg, D., Stoker, M. S. & Vorren, T. O. 2005: Pleistocene glacial history of the NW European continental margin. *Marine and Petroleum Geology 22*, 1111–1129.

Sejrup, H. P., Nygård, A., Hall, A. M. & Haflidason, H. 2009: Middle and Late Weichselian (Devensian) glaciation history of southwestern Norway, North Sea and eastern UK. *Quaternary Science Reviews 28*, 370–380.

Serebryanny, L. R. & Malyasova, E. 1998: The Quaternary vegetation and landscape evolution of Novaya zemlya in the light of palynological records. *Quaternary International 45/46*, 59–70.

Serebryanny, L., Andreev, A., Malyasova, E., Tarasov, P. & Romanenko, F. 1998: Lateglacial and early-Holocene environments of Novaya Zemlya and the Kara Sea Region of the Russian Arctic. *The Holocene 8*, 323–330.

Siegert, M. J., Dowdeswell, J. A., Hald, M. & Svendsen, J. I. 2001: Modelling the Eurasian Ice Sheet through a full (Weichselian) glacial cycle. *Global and Planetary Change 31*, 367–385.

Sissons, J. B. 1979: The Loch Lomond Stadial in the British Isles. *Nature 280*, 198–203.

Sollid, J. L. & Reite, A. J. 1983: The last glaciation and deglaciation of central Norway. *In* Ehlers, J. (ed.): *Glacial Deposits in North-West Europe*, 41–59. A.A. Balkema, Rotterdam.

Sollid, J. L., Andersen, S., Hamre, N., Kjeldsen, O., Salvigsen, O., Sturød, S., Tveitå, T. & Wilhelmsen, A. 1973: Deglaciation of Finnmark, North Norway. *Norsk Geografisk Tidsskrift 27*, 233–325.

Sørensen, R. 1992: The physical environment of Late Weichselian deglaciation of the Oslofjord region, southeastern Norway. *Sveriges Geologiska Undersökning. Series C 81*, 339–346.

Staiger, J., Gosse, J., Toracinta, R., Oglesby, B., Fastook, J. & Johnson, J. V. 2007: Atmospheric scaling of cosmogenic nuclide production: climate effect. *Journal of Geophysical Research 112*, B02205, doi: 10.1029/2005JB003811.

Stone, J. O. 2000: Air pressure and cosmogenic isotope production. *Journal of Geophysical Research: Solid Earth 105*, 23753–23759.

Stroeven, A. P., Heyman, J., Fabel, D., Björck, S., Caffee, M. W., Fredin, O. & Harbor, J. M. 2015: A new Scandinavian reference ^{10}Be production rate. *Quaternary Geochronology 29*, 104–115.

Strömberg, B. 1985: Revision of the Lateglacial Swedish varve chronology. *Boreas 14*, 101–105.

Strömberg, B. 1989: Late Weichselian deglaciation and clay varve chronology in east-central Sweden. *Sveriges Geologiska Undersokning 73*, 1–70.

Strömberg, B. 1990: A connection between the clay varve chronologies in Sweden and Finland. *Annales Academiae Scientiarum Fennicae, Series A. III. Geologica - Geographica 154*, 1–32.

Strömberg, B. 2005: *Clay Varve Chronology and Deglaciation in SW Finland*. 49 pp. Annales Academiae Scientiarum Fennicae, Geologica-Geographica, Vammala.

Stuiver, M. & Polach, H. A. 1977: Reporting of ^{14}C data. *Radiocarbon 19*, 355–363.

Svendsen, J. I. & Mangerud, J. 1997: Holocene glacial and climatic variations on Spitsbergen, Svalbard. *Holocene 7*, 45–57.

Svendsen, J. I., Alexanderson, H., Astakhov, V. I., Demidov, I., Dowdeswell, J. A., Funder, S., Gataullin, V., Henriksen, M., Hjort, C., Houmark-Nielsen, M., Hubberten, H. W., Ingolfsson, O., Jakobsson, M., Kjaer, K. H., Larsen, E., Lokrantz, H., Lunkka, J. P., Lysa, A., Mangerud, J., Matiouchkov, A., Murray, A., Moller, P., Niessen, F., Nikolskaya, O., Polyak, L., Saarnisto, M., Siegert, C., Siegert, M. J., Spielhagen, R. F. & Stein, R. 2004: Late Quaternary ice sheet history of northern Eurasia. *Quaternary Science Reviews 23*, 1229–1271.

Svendsen, J. I., Briner, J. P., Mangerud, J. & Young, N. E. 2015: Early break-up of the Norwegian Channel Ice Stream during the Last Glacial Maximum. *Quaternary Science Reviews 107*, 231–242.

Svendsen, J. I., Kruger, L. C., Mangerud, J., Astakhov, V. I., Paus, A., Nazarov, D. & Murray, A. 2014: Glacial and vegetation history of the Polar Ural Mountains in northern Russia during the Last Ice Age, Marine Isotope Stages 5–2. *Quaternary Science Reviews 92*, 409–428.

Svendsen, J. I., Mangerud, J., Elverhoi, A., Solheim, A. & Schuttenhelm, R. T. E. 1992: The Late Weichselian glacial maximum on western Spitsbergen inferred from offshore sediment cores. *Marine Geology 104*, 1–17.

Tarasov, L., Dyke, A. S., Neal, R. M. & Peltier, W. R. 2012: A data-calibrated distribution of deglacial chronologies for the North American ice complex from glaciological modeling. *Earth and Planetary Science Letters 315–316*, 30–40.

Telfer, M. W., Wilson, P., Lord, T. C. & Vincent, P. J. 2009: New constraints on the age of the last ice sheet glaciation in NW England using optically stimulated luminescence dating. *Journal of Quaternary Science 24*, 906–915.

Thoresen, M. & Bergersen, O. F. 1983: Sub-till sediments in Folldal, Hedmark, Southeast Norway. *Norges Geologiske Undersøkelse, Bulletin 389*, 37–55.

Thrasher, I. M., Mauz, B., Chiverrell, R. C., Lang, A. & Thomas, G. S. P. 2009: Testing an approach to OSL dating of Late Devensian glaciofluvial sediments of the British Isles. *Journal of Quaternary Science 24*, 785–801.

Tornivaara, A. 2007: *Stratigrafiset kohteet maaperän monimuotoisuuden suojelussa (Stratigraphic sites as references in geodiversity conservation)*. M.Sc. thesis, University of Helsinki.

Ukkonen, P., Aaris-Sørensen, K., Arppe, L., Clark, P. U., Daugnora, L., Lister, A. M., Lõugas, L., Seppä, H., Sommer, R. S., Stuart, A. J., Wojtal, P. & Zupiņš, I. 2011: Woolly mammoth (*Mammuthus*

primigenius Blum.) and its environment in northern Europe during the last glaciation. *Quaternary Science Reviews 30*, 693–712.
Ukkonen, P., Arppe, L., Houmark-Nielsen, M., Kjær, K. H. & Karhu, J. A. 2007: MIS 3 mammoth remains from Sweden—implications for faunal history, palaeoclimate and glaciation chronology. *Quaternary Science Reviews 26*, 3081–3098.
Ukkonen, P., Lunkka, J. P., Jungner, H. & Donner, J. 1999: New radiocarbon dates from Finnish mammoths indicating large ice-free areas in Fennoscandia during the Middle Weichselian. *Journal of Quaternary Science 14*, 711–714.
Uścinowicz, S. 1999: Southern Baltic area during the last deglaciation. *Geological Quarterly 43*, 137–148.
Valen, V., Larsen, E. & Mangerud, J. A. N. 1995: High-resolution paleomagnetic correlation of Middle Weichselian ice-dammed lake sediments in two coastal caves, western Norway. *Boreas 24*, 141–153.
Valen, V., Mangerud, J., Larsen, E. & Hufthammer, A. K. 1996: Sedimentology and stratigraphy in the cave Hamnsundhelleren, western Norway. *Journal of Quaternary Science 11*, 185–201.
Vasil'chuk, Y. K. & Vasil'chuk, Y. K. 1998: ^{14}C and ^{18}O in Siberian syngenetic ice-wedge complexes. *Radiocarbon 40*, 883–893.
Vorren, T. O. & Mangerud, J. 2008: Glaciations come and go. Pleistocene, 2.6 million-11,500 years ago. *In* Ramberg, I., Bryhni, I., Nøttvedt, A. & Rangnes, K. (eds.): *The Making of a Land - Geology of Norway*, 480–533. Norsk Geologisk Forening, Trondheim.
Vorren, T. O. & Plassen, L. 2002: Deglaciation and palaeoclimate of the Andfjord-Vagsfjord area, North Norway. *Boreas 31*, 97–125.
Vorren, T. O., Rydningen, T. A., Baeten, N. J. & Laberg, J. S. 2015: Chronology and extent of the Lofoten–Vesterålen sector of the Scandinavian Ice Sheet from 26 to 16 cal. ka BP. *Boreas 44*, 445–458.
Vorren, T. O., Vorren, K.-D., Aasheim, O., Dahlgren, K. I. T., Forwick, M. & Hassel, K. 2013: Palaeoenvironment in northern Norway between 22.2 and 14.5 cal. ka BP. *Boreas 42*, 875–895.
Vorren, T. O., Vorren, K.-D., Alm, T., Gulliksen, S. & Løvlie, R. 1988: The last deglaciation (20,000 to 11,000 B. P.) on Andoya, northern Norway. *Boreas 17*, 41–77.
Wilson, L. J., Austin, W. E. N. & Jansen, E. 2002: The last British Ice Sheet: growth, maximum extent and deglaciation. *Polar Research 21*, 243–250.
Winsborrow, M. C. M., Andreassen, K., Corner, G. D. & Laberg, J. S. 2010: Deglaciation of a marine-based ice sheet: late Weichselian palaeo-ice dynamics and retreat in the southern Barents Sea reconstructed from onshore and offshore glacial geomorphology. *Quaternary Science Reviews 29*, 424–442.
Wohlfarth, B. 2009: *Ice-free conditions in Fennoscandia during Marine Oxygen Isotope Stage 3?* Technical Report: TR-09-12. Swedish Nuclear Fuel and Waste Management Company, Stockholm.
Wohlfarth, B. 2010: Ice-free conditions in Sweden during Marine Oxygen Isotope Stage 3? *Boreas 39*, 377–398.
Wohlfarth, B., Bjorck, S. & Possnert, G. 1995: The Swedish Time Scale: a potential calibration tool for the radiocarbon time scale during the Late Weichselian. *Radiocarbon 37*, 347–359.
Wysota, W., Lankauf, K. R., Szmańda, J., Chruścińska, A., Oczkowski, H. L. & Przegiętka, K. R. 2002: Chronology of the Vistulian (Weichselian) glacial events in the Lower Vistula Region, Middle-North Poland. *Geochronometria 21*, 137–142.
Wysota, W., Molewski, P. & Sokołowski, R. J. 2009: Record of the Vistula ice lobe advances in the Late Weichselian glacial sequence in north-central Poland. *Quaternary International 207*, 26–41.
Young, N. E., Schaefer, J. M., Briner, J. P. & Goehring, B. M. 2013: A ^{10}Be production-rate calibration for the Arctic. *Journal of Quaternary Science 28*, 515–526.
Zeeberg, J. J., Lubinski, D. J. & Forman, S. L. 2001: Holocene relative sea-level history of Novaya Zemlya, Russia and implications for Late Weichselian ice sheet loading. *Quaternary Research 56*, 218–230.
Zelčs, V., Markots, A., Nartišs, M. & Saks, T. 2011: Pleistocene glaciations in Latvia. *In* Ehlers, J., Gibbard, P. & Hughes, P. D. (eds.): *Quaternary Glaciations – Extent and Chronology: A Closer Look*, 221–230. Elsevier, Amsterdam.

Supporting Information

Additional Supporting Information may be found in the online version of this article at http://www.boreas.dk.

Data S1. Document describing details of DATED-1 GIS .shp and .kmz files, including notes relating to their use, and reference list for citations contained within DATED-1 database.

Data S2. DATED-1 database and time-slice reconstruction maps in GIS .shp and .kmz format. Also available to download from PANGAEA: http://doi.pangaea.de/10.1594/PANGAEA.848117).

Table S1. DATED-1 database of dates related to the build-up and retreat of the last Eurasian ice sheets, separated by dating method: A. Radiocarbon dates, B. Terrestrial Cosmogenic Nuclide dates, C. Luminescence dates, D. Uranium Series dates.

Table S2. Additional data from radiocarbon calibration conducted on the DATED-1 database.

Table S3. Additional metadata required for calculation of terrestrial cosmogenic nuclide exposure ages (^{10}Be and ^{26}Al) contained within the DATED-1 database.

Table S4. Terrestrial cosmogenic nuclide exposure ages contained within DATED-1 calculated using different scaling schemes and global (Balco *et al*. 2008) and Arctic (Young et al. 2013) production rates.

Table S5. Area and volume of DATED-1 time-slices.

Fig. S1. ISO A3 versions of DATED-1 time-slice maps as shown in Fig. 5: Pre-25 ka DATED-1 time-slice reconstruction.

Fig. S2. ISO A3 versions of DATED-1 time-slice maps as shown in Fig. 6: DATED-1 time-slice reconstruction of the evolution of the extent of the Eurasian ice Sheets 25-10 ka.